Calculating Massive One-Loop Amplitudes in QCD

Ori Yudilevich

Master Thesis

Institute of Theoretical Physics, Utrecht University
Theory Group, Nikhef
Supervised by: prof. dr. E.L.M.P. Laenen

NIKHEF

24/08/2009

Abstract

Various methods of calculating one-loop level contributions to scattering amplitudes are reviewed. These include the unitarity method, color decomposition, spinor helicity, on-shell recursion relations, dimensional regularization and the Mellin-Barnes transformation. A special emphasis is placed on the case of massive external particles and massive particles propagating in the loop. The methods are applied in calculating the leading order one-loop contribution to the Higgs pair production process by the fusion of two gluons. An extensive introduction to traditional loop calculations is included.

Acknowledgments

Since most readers will end their reading of my thesis in this chapter, it makes sense to spend a considerable amount of time on it. Unfortunately, the writing of this chapter is traditionally put off to the very last moment, and so I apologize to any deserving reader who I fail to acknowledge. The past year of working on my master thesis has been a mixture of frustration, fun, anxiety and satisfaction. Fortunately, with a good ending. I would like to thank all the people that I have encountered in this process. A special gratitude to my supervisor, prof. Eric Laenen, who knew how to give the push in the right direction, improve my confidence in moments of frustration and provide aid when needed. To all my colleagues in the theory group in Nikhef, from whom I have learned and with whom I have enjoyed some fine moments. Specifically, Rob and Maciek, my fellow master students, and Reinier and Michele, my dear officemates. I would also like to thank Pierpaolo Mastrolia (CERN) and Thomas Reiter for useful discussions.

Although my thesis work was done in Nikhef, Amsterdam, my home base was the Minnaert building, which lies somewhere in the outskirts of the city of Utrecht. This thesis work is the final chapter of two marvelous years spent alongside both friendly and talented people, both Dutch of local produce and foreigners of faraway lands. I would like to thank my classmates for being good friends, and the full staff of the Institute for Theoretical Physics for creating such a ”gezellig” (look it up!) environment.

To my family and friends in Israel. I chose to continue my studies in faraway Europe (although the Dutch train service at times makes Israel seem relatively close), but ”in heart” I am back home with you. Thanks to my dear parents for a constant and loving support, to my sister (who is responsible for the beautiful cover art) and my brother, to my broader family and friends.

And to the wonderful Catherina, who had to suffer my constant physics babbling, but whom I caught off-guard explaining the Doppler effect to a friend. You have been a wonderful companion in the past year, making it all so much nicer.

Contents

CHAPTER 1

Introduction

The main aim of particle physics is to persistently search for increasingly accurate theories to describe the fundamental laws of nature which we believe underly all physical phenomena, ranging from an understanding of the structure of the nucleus and spanning to the dynamics of the universe as a whole. The status of our physical understanding is that two separate theories exist, Einstein's General Relativity to describe the upper extreme, and a quantum field theory dubbed the Standard Model to describe the microscopic and below. The former describes the gravitational force, while the latter describes the strong, electromagnetic and weak forces. The latter, in fact, is a merge of two separate theories: QCD (Quantum ChromoDynamics), a theory describing the strong force, the force responsible for the attraction between the protons and the neutrons in the nuclei of atoms; and the Electroweak theory, (unavoidably) intertwining the electromagnetic force, responsible for most day-to-day phenomena, with the weak force, responsible for some types of radioactive decays such as Beta radiation.

In order to test their theories, physicists often look for the simplest possible experiments that could isolate specific interesting features of the theory. Physicists would, ideally, like theory to be a step ahead of experiment, with the hope that the experiment could posteriorly confirm or invalidate their assertions. The most successful method up-to-date of testing the Standard Model theory is by colliding (or scattering) incoming particles against one another at extreme energies in machines called Particle Accelerators. Such events turn out to produce a myriad of outgoing particles, whose scattering patterns provide clues on the inner workings

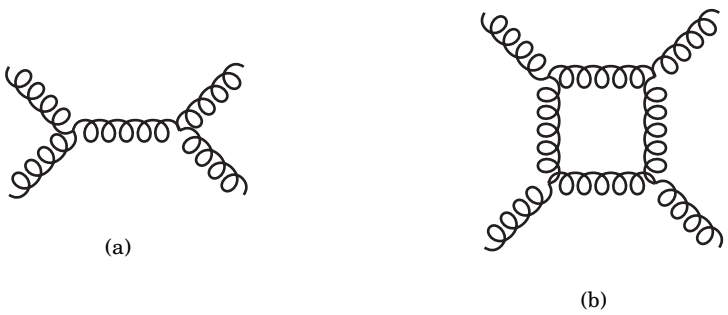

(a) (b)

Figure 1.1: A tree level (left) and a one-loop level (right) contribution to the 2 gluon to 2 gluon scattering process.

of the fundamental forces. In quantum field theories such as the Standard Model, we are interested in calculating a complex valued quantity called the S-matrix. This quantity is a measure of the probability that a certain scattering process will occur, and can be directly compared to experiment.

Usually an exact calculation of the S-matrix is not possible and we resort to perturbation theory, where we expand (approximate) the S-matrix in small parameters of our theories. To this end, we employ a method due to R.P. Feynman, in which diagrammatic entities known as Feynman diagrams are drawn and then evaluated. These diagrams correspond to the terms of our expansion. To obtain the lowest order (LO) contribution, it suffices to consider tree level diagrams which are relatively simple to calculate (figure 1.1(a) is an example of a tree diagram). Higher precision calculations are in need as higher precision experiments are devised. Such experiments are the Tevatron in Illinois, which collides protons against anti-protons at energies of 1 TeV, or the upcoming Large Hadron Collider (LHC) in Switzerland/France, planned to collide protons at energies of 14 TeV. To increase predictive accuracy, one must calculate next-to-leading order (NLO) contributions, i.e. one-loop Feynman diagrams such as in figure 1.1(b), which are notoriously difficult.

Consider, as an example, the scattering of 2 gluon particles into 2 gluon particles. Evaluating the loop diagram contribution in figure 1.1(b) would require multiplying four triple-gluon vertices (figure 1.2), each containing 6 terms. This single diagram would result in an expression containing 6^4 terms. The full NLO contribution would require summing over $\sim$220 such diagrams (the diagrams were generated by `FeynArts`[1]). We thus witness a general feature of amplitudes. As we either increase the number of loops or the number of external particles, the expressions grow rapidly and quickly become unmanageable. To make matters even worse, loop diagrams and the integrals accompanying them, often suffer from divergences in both the ultraviolet region and the infrared and collinear regions. Newer, more efficient methods are crucial if theory is to confront experiment.

The past couple of decades have seen a rising interest and great progress in this domain, as theorists are stimulated by the challenge of discovering the missing piece of the standard model, the Higgs boson, and possibly observing the springs of new "beyond the Standard Model" physics. For example, the main channel for the discovery of the Higgs particle is the fusion of two gluons[2], resulting in the production of a Higgs particle through a top quark loop. The LO contribution to this process is in itself a one-loop Feynman diagram, requiring already at this stage the use of one-loop methods to obtain a prediction. The NLO contribution[3, 4, 5], a QCD correction containing either an extra loop or a real emission of an extra particle, is relatively large, increasing the cross section by about 50%. This illustrates the importance of one-loop, and in this case higher loop calculation.

Many new devices have been invented to cope with ever growing complexity. We give a taste of some of the topics that will be discussed in this work. The spinor helicity and color decomposition methods [6, 7] have become a common feature in QCD calculations, providing an efficient way for working with external gluons and for taking advantage of the color content ($SU(3)$ group generators) of amplitudes to decompose them into smaller pieces. The unitarity property of the S-matrix [8], which is a consequence of its probabilistic interpretation, and the more general Cutkosky rules [9] based on Landau's [10] analysis of Feynman diagrams, have proved to be extremely powerful tools in calculating full amplitudes without the need to explicitly evaluate large numbers of Feynman diagrams. Bern, Dixon, Kosower [11, 12, 13] and others have made great process in producing large numbers of previously unattainable analytical results, e.g. all one-loop corrections to 5-point massless parton amplitudes [14, 15, 16] have been calculated by these methods. Recently, Ossola, Papadopoulos and Pittau have devised a new unitarity-like approach [17], dubbed the OPP method, which could prove yet more efficient, especially in the context of computerized implementations.

Progress has also been made in evaluating tree-level diagrams, which form building blocks in the above mentioned unitarity method. Following a discovery of Witten [18] on the relation between perturbative scattering amplitudes and twistor space, an on-shell method was proposed [19, 20] in which larger tree amplitudes are constructed recursively from smaller ones.

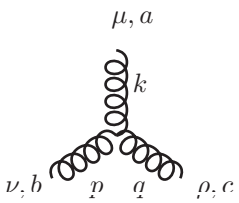

$$= \quad g f^{abc} \left(g^{\mu\nu}(k-p)^{\rho} + g^{\nu\rho}(p-q)^{\mu} + g^{\rho\mu}(q-k)^{\nu} \right)$$

Figure 1.2: Feynman rule of a triple-gluon vertex.

Yet another tool, different in character from those mentioned above, first put to use by Usyukina [21], makes use of a mathematical tool called the Mellin-Barnes transformation [22] to simplify loop integrals at different stages, either prior to the momentum integration [23] or prior to the Feynman parameter integration. Tausk [24] applied the latter approach in calculating a four point Feynman diagram with two loops and seven internal legs.

In this thesis we assume a knowledge of quantum field theory and the Standard Model [8, 25]. The goal of the thesis is to provide a coherent and detailed review of various one-loop calculational methods, and finally apply these methods on a non-trivial scattering process. All the topics discussed throughout the thesis are also illustrated in fully worked out examples. In chapter 2, we begin with an in-depth review of some of the traditional methods of calculating one-loop corrections to amplitudes, emphasizing the dimensional regularization scheme [26] and the Passarino-Veltman reduction scheme [27], which will form the basis of the subsequent chapters. Chapters 3-5 will introduce various modern methods to tackle loop-calculations, some of which discussed earlier in this introduction. Where relevant, our emphasis will be on amplitudes containing massive fermions, which often introduce new difficulties. In chapter 6, we will focus on a specific scattering process of special interest for the LHC experiment, namely the scattering of two gluons into two Higgs particles. This process provides a channel for testing the potential of the Higgs sector of the Standard Model. A detailed calculation of the process will be carried out, demonstrating a large number of the techniques reviewed throughout the thesis. A collection of appendices of useful formulae appears in the back.

CHAPTER 2

Basics of One-Loop Calculations

The difficulties that arise in the calculation of a scattering amplitudes by introducing loop corrections into the perturbation expansion lie in both the messy integral expressions and coping with their divergent nature. In this chapter we introduce the by now ubiquitous dimensional regularization scheme and discuss its application in treating the different types of divergences through two examples: the vacuum polarization and the Drell-Yan processes. We also introduce the Passarino-Veltman reduction scheme which is widely used in simplifying loop expression. These preliminary concepts form the basis of our later discussions.

2.1 Dimensional Regularization

Ultraviolet and infrared divergences

A well known feature of Quantum Field theories is the appearance of ultraviolet, infrared and collinear divergences in perturbation expansions of scattering amplitudes. It has been demonstrated for both Abelian and non-Abelian gauge theories that the ultraviolet divergences are in fact renormalizable, i.e. non-observable parameters in the theory such as coupling constants, masses and fields, can be redefined to absorb the infinities yielding finite values for observable quantities. This process of absorbing the behavior of the fields at high momenta reflects the theory's inability to explain this region of momentum space, but at the

same time shows that this information is not crucial for understanding behavior at lower momenta values.

In practice [25] renormalization is accomplished by expressing these "bare" infinite parameters as products of a renormalized finite quantity and an infinite factor Z_i (e.g. the QED coupling constant $e_0 = e_R Z_e$). The Z_i factor is expanded around the same expansion parameter used to expand the amplitude. The zeroth order term of the expansion is finite reflecting the fact that tree level diagrams are finite and do not require renormalization. The higher order terms of the expansion are defined such that they will cancel the infinities of higher order corrections to the amplitude. Put differently, infinities arising from divergent integrals cancel against infinite parameters and fields of the Lagrangian. Diagrammatically, this procedure can be understood as introducing new Feynman rules, since by expanding Z_i we are effectively adding new terms to the Lagrangian. The additional diagrams generated by the new rules are chosen such that they cancel the infinities of the original diagrams. In a renormalizable theory, Z_i factors can be defined universally, i.e. they will successfully render every observable finite.

Infrared and collinear divergences are different in character. These divergences are not a consequence of the limitation of the theory but rather of modifying an observable to be "more physical". For example, we will see that the first order correction in the scattering process of two quarks into two muons is infrared divergent. This is partially healed by a procedure known as factorization which modifies the observable to be the scattering of two protons instead of two quarks. Since quarks cannot be isolated this is naturally the more physical question, while protons which are bound states of three quarks are stable particles.

To fully rid the amplitude of divergences one has to further take into account the real emission of a gluon from one of the incoming quarks (i.e. a scattering amplitude of three outgoing particles). Low energy gluons could go undetected and should thus be taken into account when considering the scattering amplitude of two quarks into two electrons. Including real emissions is a procedure used originally in QED to treat infrared and collinear divergences. The emission of on-shell massless particles by massless particles (e.g. gluons emitted by high energy quarks assumed to be massless) is divergent in the region of phase space where the particles have zero energy or become collinear with the emitting particle. These divergences cancel against the loop correction of the $2 \to 2$ process. Both factorization and real emission will be discussed in greater in section 2.3.

Dimensional Regularization

A crucial ingredient of both the renormalization program and the treatment of infrared and collinear divergences is a regularization scheme. Different regularization schemes targeted at different applications have been devised. The various methods introduce some continuous

parameter into the divergent Feynman integral such that in some region of the parameter space the integral will be finite, with a pole at the physical value of the parameter. Examples of such schemes are:

- *Pauli-Villars regularization* - fictitious fields are introduced, the physical limit corresponds to sending the masses of these fields to infinity, causing the contribution of the fields to vanish.
- *Analytic regularization* - normal propagators $(p^2 + m^2)^{-1}$ are replaced by $(p^2 + m^2)^{\lambda}$, the physical limit is reached when taking the limit $\lambda \to -1$.
- *Dimensional regularization* - the dimension of space-time d is a variable, $d = 4$ is the physical limit.

The latter, *dimensional regularization*, is a scheme found to be extremely powerful in the calculation of loop diagrams. It was introduced by 't Hooft and Veltman [26] in 1972. One observes that integrals divergent at four dimensions become ultraviolet finite when the number of dimensions is reduced, and infrared finite when the number of dimensions is increased. In fact, if Feynman integrals are analytically continued in the dimensions d of space-time the integrals turn out to be analytical in d space with simple poles at some integer values. The physical result is defined as the limit $d \to 4$ after the removal of the divergences.

In addition to being convenient for calculations, as we shall see, dimensional regularization also preserves Ward identities which are crucial to the proof of the unitarity of the S-matrix. In this thesis we demonstrate the usefulness of the unitarity property as a calculational tool (see chapter 3), further justifying the use of this regularization method.

An obvious downside of this method is its failure in dealing with quantities that are dimension dependent. Such quantities are the γ_5 Dirac matrix, the projection matrices $w_{\pm} = \frac{1}{2}(1 \pm \gamma_5)$ and the antisymmetric tensor $\epsilon_{\alpha\beta\gamma\delta}$. If dimension dependent properties of these quantities are necessary for proving Ward identities then the method fails since these quantities cannot be generalized to d dimensions (see [26] for an example).

To deal with helicities of gauge bosons and massless fermions, quantities which typically introduce projection matrices into an amplitude expression, we will resort to the four-dimensional helicity scheme (FDH) [28]. This scheme dictates that all external quantities (external momenta, polarization vectors and spinors) are taken to be four dimensional, and only loop momenta are extended to d dimensions. Section 4.4 will discuss an elegant technique to deal with the extra dimensions of the loop momentum vector in the case of one loop diagrams. In actual calculations, we will see that projection matrices do in fact appear and they could in theory come into conflict with the dimensional regularization scheme. As

long as we are dealing with QCD and QED, theories that do not violate parity, using dimensional regularization is safe. This can be understood if we consider an alternative route for calculating an amplitude. The helicities of the particles could be left unspecified in the beginning of the calculation and only after reaching a finite renormalized result one could contract the amplitude with the helicity information. In other words, if the Feynman rules for vertices and propagators do not contain four-dimension-only quantities then dimensional regularization is a safe choice.

The remainder of this section will be dedicated to the derivation of essential dimensional regularization identities. These include general Feynman integral expressions in d dimensions and a generalization of the Dirac γ matrices to d dimensions. The section will be concluded with a detailed example.

2.1.1 Loop integrals

When a scattering amplitude is calculated in perturbation theory, all contributing Feynman diagrams up to a given order must be considered. A general expression of a one-loop Feynman diagram takes the following form,

$$\int \frac{d^d l}{(2\pi)^d} \frac{\mathcal{N}(l_i, m_i, k_j)}{(l_1^2 - m_1^2 + i\epsilon)(l_2^2 - m_2^2 + i\epsilon)...(l_n^2 - m_n^2 + i\epsilon)} \tag{2.1}$$

n is the number of internal lines in the loop and l_i is the momentum of the particle of mass m_i propagating through the i'th line. Because of momentum conservation at each vertex and in the overall graph, only one of the l_i momenta is independent and we denote it by l. $\{k_j\}$ is the set of external momenta and $\mathcal{N}$ is a function of the internal and external momenta determined by the details of the diagram and the corresponding Feynman rules. Higher loop diagrams would involve integrating over larger number of independent loop momenta. We will restrict our discussion to the one-loop case.

The common procedure for evaluating (2.1) involves first combining the propagator factors in the denominator using Feynman parameters,

$$\frac{1}{A_1 A_2 ... A_n} = \int_0^1 da_1 da_2 ... da_n \frac{(n-1)!\delta(\sum a_i - 1)}{(a_1 A_1 + a_2 A_2 + ... + a_n A_n)^n} \tag{2.2}$$

where $A_i = l_i^2 - m_i^2$. All l_i can be expressed in terms of the integration variable l and $\{k_j\}$. The sum appearing in the denominator is a second order polynomial of l. This allows a variable shift $l \to q = l + const$ with the constant chosen to rid the denominator of any linear terms in the integration variable. Ignoring for the moment the integrals over the Feynman parameters a_i, equation (2.1) reduces to,

$$\int \frac{d^d q}{(2\pi)^d} \frac{\mathcal{N}(q, k_j, a_i)}{[q^2 - M^2 + i\epsilon]^s} \tag{2.3}$$

We note that $\mathcal{N}$ is the same function as in (2.1) expressed in terms of the shifted variable.

We now seek to evaluate this integral, leaving the number of dimensions d unspecified. In the denominator, the integration variable appears only as q^2. The integral does not depend on any vectorial quantities and if even powers of q^μ appear in the numerator then they can be replaced by combinations of $q^2 g^{\mu\nu}$ (see appendix B). If odd powers of q^μ appear, these can be similarly replaced by factors of $q^2 g^{\mu\nu}$ multipled by a single factor of q^μ, leaving an odd integrand and consequently a vanishing integral. We are thus left with the simpler task of evaluating only integrals of the form,

$$\int \frac{d^d q}{(2\pi)^d} \frac{(q^2)^m}{[q^2 - M^2 + i\epsilon]^s} \tag{2.4}$$

In the following section we will discuss how the Passarino-Veltman reduction procedure can be used to remove any powers of the loop momentum l^μ from the numerator of (2.1). The reduced integrals are known as *scalar integrals* and form the basic building blocks of one-loop scattering amplitudes.

Having (2.4) depend only on q^2, it is natural to solve it using spherical coordinates in d dimensions. Since q lives in Minkowski space, a Wick rotation would allow us to work in the more familiar Eucledian space. We will carry out an explicit calculation of (2.4) for the case $m = 0$. The steps described can be retraced for the cases $m > 0$ (see appendix B for the case $m = 1$).

Wick Rotation

In the case $m = 0$, the scalar integral is,

$$\int \frac{d^d q}{(2\pi)^d} \frac{1}{[q^2 - M^2 + i\epsilon]^s} \tag{2.5}$$

Considering first the integration over the time component of q in the complex plane, there are poles in the bottom right and top left quadrants. The location of the poles is determined by the ϵ prescription of the propagators. According to the Feynman prescription (which we use throughout the thesis),

$$\begin{aligned} q^2 = M^2 - i\epsilon \;&\Rightarrow\; (q^0)^2 = \vec{q}^2 + M^2 - i\epsilon \\ &\Rightarrow\; q^0 = \pm\sqrt{\vec{q}^2 + M^2 - i\epsilon} \simeq \pm\sqrt{\vec{q}^2 + M^2}\,\left(1 - i\epsilon \frac{1}{\vec{q}^2 + M^2}\right) \end{aligned} \tag{2.6}$$

Since the top right and bottom left quadrants do not contain poles, and the integral vanishes in the limit $|q^0| \to \infty$ (when $s \geq 1$, which form the relevant cases of at least one propagator in the loop), then by Cauchy's theorem a line integral along the real axis ($-\infty < Re\ q^0 < \infty$) can be replaced by a line integral along the imaginary axis ($-\infty < Im\ q^0 < \infty$). This is known as a Wick rotation (see figure 2.1). For convenience, we define a new vector q_E such that $q^0 = iq_E^0$ and $\vec{q}_E = \vec{q}$. The time integration is then simply over the real axis $-\infty < l_E^0 < \infty$.

q_E has a Euclidean metric $q_E^2 = (q_E^0)^2 + \vec{q}_E^2$, where $\vec{q}_E$ is a $d-1$ dimensional vector. The Wick rotated integral contains no poles as long as $M^2 > 0$, and ϵ can be taken to zero.

$$\lim_{\epsilon \to 0} \int \frac{d^d q}{(2\pi)^d} \frac{1}{[q^2 - M^2 + i\epsilon]^s} = \int \frac{d^d q_E}{(2\pi)^d} \frac{i}{(-1)^s} \frac{1}{[q_E^2 + M^2]^s} \tag{2.7}$$

The i factor originates from the Jacobian, $d^d q^0 = i d^d q_E^0$, and the factor $(-1)^s$ from the fact that $q^2 = -q_E^2$. It is now safe to express q in polar coordinates,

$$\int \frac{d^d q_E}{(2\pi)^d} \frac{i}{(-1)^s} \frac{1}{[q_E^2 + M^2]^s} = \frac{i}{(-1)^s} \int_0^\infty \frac{dq_E}{(2\pi)^d} \frac{q_E^{d-1}}{[q_E^2 + M^2]^s} \int d\Omega^{d-1} \tag{2.8}$$

Angular integration

To calculate $\int d\Omega^{d-1}$, we first show that the integration measure transforms to spherical coordinates as follows,

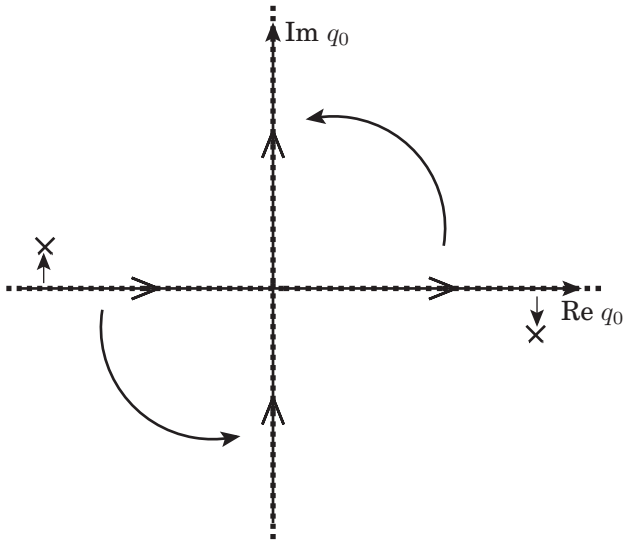

Figure 2.1: Wick rotation of the time component of q.

$$\int d^d q = \int_0^\infty dq q^{d-1} \int d\Omega^{d-1} = \int_0^\infty dq q^{d-1} \int_0^{2\pi} d\theta_1 \int_0^\pi d\theta_2 \sin\theta_2 ... \int_0^\pi d\theta_{d-1} \sin^{d-2}\theta_{d-1} \quad (2.9)$$

This is obviously true for $d = 2, 3$. Assuming by induction that it is true for d then in the case $d+1$ we have,

$$\begin{aligned} \int d^{d+1} q &= \int dq_{d+1} \int dq^d \\ &= \int dq_{d+1} \int_0^\infty dq' q'^{d-1} \int_0^{2\pi} d\theta_1 \int_0^\pi d\theta_2 \sin\theta_2 ... \int_0^\pi d\theta_{d-1} \sin^{d-2}\theta_{d-1} \end{aligned} \quad (2.10)$$

where q' is the magnitude of the d dimensional vector. Introduce a new angle $0 \leq \theta_d \leq \pi$,

$$\begin{aligned} q_{d+1} = q\cos\theta_d \;\Rightarrow\; dq_{d+1} = dq\cos\theta_d + q(-\sin\theta_d)d\theta_d \\ q' = q\sin\theta_d \;\Rightarrow\; dq' = dq\sin\theta_d + q\cos\theta_d d\theta_d \end{aligned} \quad (2.11)$$

The new measure is then,

$$dq_{d+1} dq' = q dq d\theta_d \quad (2.12)$$

Inserting this and the definition of q' into (2.10) reproduces (2.9) for the case $d+1$.

Since the integrand of (2.8) only depends on the magnitude of q, the angular part can be integrated out. To solve the angular part of (2.9) we first calculate the integral $\int_0^\pi d\theta \sin^k\theta$. Perform the substitution $y = \sin^2\theta$,

$$\int_0^\pi d\theta \sin^k\theta = 2\int_0^{\pi/2} d\theta (\sin^2\theta)^{k/2} = \int_0^1 dy y^{\frac{k-1}{2}} (1-y)^{-\frac{1}{2}} = \frac{\Gamma(\frac{k+1}{2})\Gamma(\frac{1}{2})}{\Gamma(\frac{k+2}{2})} \quad (2.13)$$

where in the last step the Beta function (B.9) was used.

Finally,

$$\begin{aligned} \int d\Omega^{d-1} &= \int_0^{2\pi} d\theta_1 \int_0^\pi d\theta_2 \sin\theta_2 ... \int_0^\pi d\theta_{d-1} \sin^{d-2}\theta_{d-1} \\ &= 2\pi \frac{\Gamma(\frac{1}{2})\Gamma(\frac{1}{2}+\frac{1}{2}\cdot 1)}{\cancel{\Gamma(1+\frac{1}{2}\cdot 1)}} \frac{\Gamma(\frac{1}{2})\cancel{\Gamma(\frac{1}{2}+\frac{1}{2}\cdot 2)}}{\cancel{\Gamma(1+\frac{1}{2}\cdot 2)}} ... \frac{\Gamma(\frac{1}{2})\cancel{\Gamma(\frac{1}{2}+\frac{1}{2}\cdot (d-2))}}{\Gamma(1+\frac{1}{2}\cdot(d-2))} \\ &= 2\pi \frac{(\Gamma(\frac{1}{2}))^{d-2}\Gamma(1)}{\Gamma(\frac{d}{2})} = 2\pi(\sqrt{\pi})^{d-2}\frac{1}{\Gamma(\frac{d}{2})} = \frac{2\pi^{\frac{d}{2}}}{\Gamma(\frac{d}{2})} \end{aligned} \quad (2.14)$$

Radial integration

To complete the evaluation of (2.8), the radial integration must be performed. We perform the following series of substitutions,

- $q_E = My \Rightarrow dq_E = Mdy$

$$\int_0^\infty dq_E \frac{q_E^{d-1}}{[q_E^2 + M^2]^s} = \frac{M^d}{M^{2s}} \int_0^\infty dy \frac{y^{d-1}}{[1+y^2]^s}$$

- $y = \sinh z \ (0 \leq y < \infty \rightarrow 0 \leq z < \infty) \Rightarrow dy = \cosh z dz$

$$1 + y^2 = 1 + \sinh^2 z = \cosh^2 z = (1 - \tanh^2 z)^{-1}$$
$$y^2 = (1 - \tanh^2 z)^{-1} - 1 = \tanh^2 z (1 - \tanh^2 z)^{-1}$$

- $u = \tanh^2 z \ (0 \leq z < \infty \rightarrow 0 \leq u \leq 1) \Rightarrow du = 2 \tanh z \cosh^{-2} z dz$

$$1 + y^2 = (1-u)^{-1} \ , \ y^2 = u(1-u)^{-1}$$

Applying these substitutions to the integral and using the Beta function again, the radial integral yields,

$$(M^2)^{\frac{d}{2}-s} \int_0^\infty dy \frac{y^{d-1}}{[1+y^2]^s} = (M^2)^{\frac{d}{2}-s} \int_0^1 du \frac{\cosh^3 z}{2 \tanh z} u^{\frac{d-1}{2}} (1-u)^{\frac{1-d}{2}} (1-u)^s \tag{2.15}$$

$$= \frac{(M^2)^{\frac{d}{2}-s}}{2} \int_0^1 du \frac{(1-u)^{\frac{3}{2}}}{u^{\frac{1}{2}}} u^{\frac{d-1}{2}} (1-u)^{\frac{1}{2}-\frac{d}{2}+s} \tag{2.16}$$

$$= \frac{(M^2)^{\frac{d}{2}-s}}{2} \int_0^1 du u^{\frac{d-2}{2}} (1-u)^{s-\frac{d}{2}-1} \tag{2.17}$$

$$= \frac{(M^2)^{\frac{d}{2}-s}}{2} \frac{\Gamma(\frac{d}{2})\Gamma(s-\frac{d}{2})}{\Gamma(s)} \tag{2.18}$$

Combining both radial and angular integrations, the scalar integral (2.8) reduces to,

$$\lim_{\epsilon \to 0} \int \frac{d^d q}{(2\pi)^d} \frac{1}{[q^2 - M^2 + i\epsilon]^s} = \frac{i}{(-1)^s} \frac{1}{\Gamma(\frac{d}{2}) 2^{d-1} \pi^{\frac{d}{2}}} \frac{(M^2)^{\frac{d}{2}-s}}{2} \frac{\Gamma(\frac{d}{2})\Gamma(s-\frac{d}{2})}{\Gamma(s)}$$
$$= \frac{(-1)^s i}{(4\pi)^{\frac{d}{2}}} \frac{\Gamma(s-\frac{d}{2})}{\Gamma(s)} (M^2)^{\frac{d}{2}-s} \tag{2.19}$$

This result demonstrates the power of dimensional regularization. The only potentially divergent factor in this expression is the Gamma function, $\Gamma(s - \frac{d}{2})$. The Gamma function, $\Gamma(z)$, has simple poles at $z \in \mathbb{Z}$, $z \leq 0$. Thus, if the number of propagators s is such that

$s - \frac{d}{2}$ is a negative integer or zero in the physical value $d = 4$, the integral is divergent. It is common to express the dimensions as a deviation from the physical dimensions, $d = 4 - 2\epsilon$. In terms of ϵ we have $\Gamma(s - 2 + \epsilon)$, and we can use identity (B.5) to extract the poles from the Gamma function and have it appear explicitly as a pole in the deviation ϵ,

$$\Gamma(s-2+\epsilon) = \frac{1}{s-2+\epsilon}\Gamma(s-1+\epsilon) = \frac{1}{s-2+\epsilon}\frac{1}{s-1+\epsilon}\Gamma(s+\epsilon) = ... \tag{2.20}$$

This can be repeated recursively until the argument of the Gamma function is positive definite. This representation makes more apparent the subtraction of infinities described above in the discussion of renormalization. The example at the end of this section will demonstrate this.

Finally, recall that the term M appearing in (2.19) is in fact a function of the Feynman parameters $\{a_i\}$ (see (2.2)), and these must be integrated over. As the number of legs grows and with it the number of parameters, the integrals tend to become more complicated as a consequence of the delta function constraining their sum to be 1. Moreover, after the variable shift discussed above, Feynman parameters appear also in the numerator. Chapter 3 will introduce a reduction formula expressing integrals with parameters in the numerator in terms of integrals stripped of such parameters.

2.1.2 Dirac matrices in d dimensions

When working in d dimensions, one must take special care of contractions and traces of Dirac gamma matrices which are abundant in loop calculations. First note that a trace of a space-time Kronecker delta is the number of space-time dimensions, $\delta^\mu_\mu = d$. This implies that contracting two metric tensors is also equal to the number of space-time dimensions,

$$g^{\mu\nu}g_{\mu\nu} = d \tag{2.21}$$

Keeping the normal definition of the gamma matrices, $\{\gamma^\mu, \gamma^\nu\} = 2g^{\mu\nu}$ let us see what happens when two matrices are contracted,

$$\gamma^\mu\gamma_\mu = g_{\mu\nu}\gamma^\mu\gamma^\nu = \frac{1}{2}g_{\mu\nu}(\gamma^\mu\gamma^\nu + \gamma^\nu\gamma^\mu) = g_{\mu\nu}g^{\mu\nu} = d \tag{2.22}$$

or in the case of three matrices,

$$\begin{aligned}\gamma^\mu\gamma^\nu\gamma_\mu = g_{\mu\rho}\gamma^\mu\gamma^\nu\gamma^\rho &= \frac{1}{2}g_{\mu\rho}(\gamma^\mu\gamma^\nu\gamma^\rho + \gamma^\rho\gamma^\nu\gamma^\mu) \\ &= \frac{1}{2}g_{\mu\rho}(\gamma^\mu\gamma^\nu\gamma^\rho - \gamma^\rho\gamma^\mu\gamma^\nu + 2g^{\mu\nu}\gamma^\rho) \\ &= ... = g_{\mu\rho}(\gamma^\mu g^{\nu\rho} - \gamma^\nu g^{\rho\mu} + \gamma^\rho g^{\mu\nu}) = (2-d)\gamma^\nu\end{aligned} \tag{2.23}$$

A list of contraction formulas in d dimensions appears in appendix B. When performing a trace of a product of gamma matrices, the result is typically a combination of metric tensors. These metric tensors are in turn contracted with either vectors or other metric tensors, in which case one must again make use of (2.21). Such manipulations introduce factors of ϵ (through $d = 4 - 2\epsilon$) which cancel against factors of $\frac{1}{\epsilon}$ appearing through (2.20). In this case only the divergent parts of the integrals contribute to the physical expression, while the finite parts vanish in the limit $\epsilon \to 0$.

2.1.3 Vacuum polarization - an example

As a pedagogical example we calculate the one-loop correction to the photon self-energy amplitude using the dimensional regularization scheme described in this section. This process is also known as the one-loop vacuum polarization diagram since virtual electron-positron pairs are created, polarizing the overall distribution of charge. We will return to this process in later chaptersas an example of unitarity and the Mellin-Barnes transformation as calculational techniques.

Figure 2.2 displays the only contributing diagram. This diagram is mostly incorporated as a correction to the photon propagator, and we therefore allow the photon to be off-shell with an invariant momentum $k^2 = s$. The mass of the fermion is m. We will calculate the tensor amplitude, stripping off the external polarization vectors which can later be contracted with the tensorial quantity. Application of the Feynman rules (appendix A) yields,

$$i\mathcal{M}^{\mu\nu} = -\int \frac{d^d p}{(2\pi)^d} tr\left[(-ie\gamma^\mu)\frac{i(\not{p} - \not{k} + m)}{(p-k)^2 - m^2}(-ie\gamma^\nu)\frac{i(\not{p} + m)}{p^2 - m^2}\right] \tag{2.24}$$

An extra minus sign appears because of the fermionic loop. Denote,

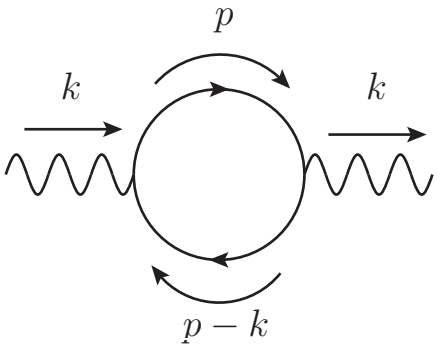

Figure 2.2: One-loop Feynman diagram contribution to the vacuum polarization amplitude

$$d_1 = p^2 - m^2 \quad d_2 = (p-k)^2 - m^2 \tag{2.25}$$

The trace appearing in the expression is over the spinor indices. This trace contains a maximum of four Dirac matrices and can be evaluated using the identities in appendix C or more conveniently using an algebraic program such as Form [29],

$$\begin{aligned} i\mathcal{M}^{\mu\nu} &= -4e^2 \int \frac{d^dp}{(2\pi)^d} \frac{2p^\mu p^\nu - k^\mu p^\nu - k^\nu p^\mu - g^{\mu\nu}(p^2 - m^2) + g^{\mu\nu} k \cdot p}{d_1 d_2} \\ &= -4e^2 (2B^{\mu\nu} - B^\mu p^\nu - B^\nu p^\mu - g^{\mu\nu} A^{(1)} + g^{\mu\nu} p \cdot B) \end{aligned} \tag{2.26}$$

where we defined the following tensorial integrals,

$$B^{\mu\nu} = \int \frac{d^dp}{(2\pi)^d} \frac{p^\mu p^\nu}{d_1 d_2} \; ; \; B^\mu = \int \frac{d^dp}{(2\pi)^d} \frac{p^\mu}{d_1 d_2} \; ; \; A^{(1)} = \int \frac{d^dp}{(2\pi)^d} \frac{1}{d_2} \tag{2.27}$$

The convention used here is that the letter refers to the number of propagators in the integral (e.g. A has one propagator and B has two) and a superscript refers to the missing propagators (e.g. $A^{(1)}$ means that d_1 is missing).

The next step will be to explicitly evaluate these three integrals.

$B^{\mu\nu}$ tensor integral

Apply the Feynman parameters formula to combine the factors in the denominator to one single factor,

$$\begin{aligned} B^{\mu\nu} &= \int \frac{d^dp}{(2\pi)^d} \frac{p^\mu p^\nu}{((p-k)^2 - m^2)(p^2 - m^2)} \\ &= \int_0^1 dx \int \frac{d^dp}{(2\pi)^d} \frac{p^\mu p^\nu}{[x((p-k)^2 - m^2) + (1-x)(p^2 - m^2)]^2} \end{aligned} \tag{2.28}$$

Denoting $s = k^2$, the denominator can be simplified to,

$$\begin{aligned} x((p-k)^2 - m^2) + (1-x)(p^2 - m^2) &= xp^2 + xk^2 - 2xp \cdot k - xm^2 + p^2 - xp^2 - m^2 + xm^2 \\ &= p^2 - 2xk \cdot p + xk^2 - m^2 \\ &= (p - xk)^2 - x^2 k^2 + xk^2 - m^2 \\ &= (p - xk)^2 + x(1-x)s - m^2 \end{aligned} \tag{2.29}$$

Performing the shift $q = p - xk$ and denoting $M = m^2 - x(1-x)s$,

$$
\begin{aligned}
B^{\mu\nu} &= \int_0^1 dx \int \frac{d^dq}{(2\pi)^d} \frac{(q^\mu + xk^\mu)(q^\nu + xk^\nu)}{[q^2 - M]^2} \\
&= \int_0^1 dx \int \frac{d^dq}{(2\pi)^d} \frac{q^\mu q^\nu}{[q^2 - M]^2} + \int_0^1 dx x^2 k^\mu k^\nu \int \frac{d^dq}{(2\pi)^d} \frac{1}{[q^2 - M]^2} \\
&+ \int_0^1 dx \underbrace{\int \frac{d^dq}{(2\pi)^d} \frac{\{q,p\}^{\mu\nu}}{[q^2 - M]^2}}_{=0,\ \text{odd function of } q^\mu}
\end{aligned}
\tag{2.30}
$$

The q part of the second term can be evaluated using (2.19) or (B.11),

$$
\int \frac{d^dq}{(2\pi)^d} \frac{1}{[q^2 - M]^2} = \frac{i}{(4\pi)^{\frac{d}{2}}} \frac{\Gamma(2 - \frac{d}{2})}{\Gamma(2)} \left(\frac{1}{M}\right)^{2-\frac{d}{2}} = \frac{i}{(4\pi)^{2-\epsilon}} \Gamma(\epsilon) M^{-\epsilon} \tag{2.31}
$$

where, as mentioned earlier, ϵ is defined by $d = 4 - 2\epsilon$.

Similarly for the first term, using (B.13),

$$
\int \frac{d^dq}{(2\pi)^d} \frac{q^\mu q^\nu}{[q^2 - M]^2} = \frac{-i}{(4\pi)^{\frac{d}{2}}} \frac{g^{\mu\nu}}{2} \frac{\Gamma(1 - \frac{d}{2})}{\Gamma(2)} \left(\frac{1}{M}\right)^{1-\frac{d}{2}} = -\frac{1}{2} \frac{i}{(4\pi)^{2-\epsilon}} g^{\mu\nu} \Gamma(-1 + \epsilon) M^{1-\epsilon} \tag{2.32}
$$

The result of the momentum tensor integral is,

$$
B^{\mu\nu} = \frac{i}{(4\pi)^{2-\epsilon}} \left[-\frac{g^{\mu\nu} \Gamma(-1 + \epsilon)}{2} \int_0^1 dx M^{1-\epsilon} + k^\mu k^\nu \Gamma(\epsilon) \int_0^1 dx x^2 M^{-\epsilon} \right] \tag{2.33}
$$

To perform the remaining x integral, M can be expanded up to order ϵ,

$$
M^{-\epsilon} = e^{\ln M^{-\epsilon}} = e^{-\epsilon \ln M} \simeq 1 - \epsilon \ln M = 1 - \epsilon \ln(m^2 - x(1-x)s) \tag{2.34}
$$

The solution of this integral is discussed below.

B^μ tensor integral

Using the same Feynman parameter shift as for $B^{\mu\nu}$ and again using (B.11),

$$
\begin{aligned}
B^\mu &= \int \frac{d^dp}{(2\pi)^d} \frac{p^\mu}{((p-k)^2-m^2)(p^2-m^2)} \\
&= \int_0^1 dx \int \frac{d^dp}{(2\pi)^d} \frac{p^\mu}{[x((p-k)^2-m^2)+(1-x)(p^2-m^2)]^2} \\
&= \int_0^1 dx \underbrace{\int \frac{d^dq}{(2\pi)^d} \frac{q^\mu}{[q^2-M]^2}}_{=0,\ \text{odd function of } q^\mu} + \int_0^1 dx x k^\mu \int \frac{d^dq}{(2\pi)^d} \frac{1}{[q^2-M]^2} \\
&= \frac{i}{(4\pi)^{2-\epsilon}} k^\mu \Gamma(\epsilon) \int_0^1 dx x M^{-\epsilon}
\end{aligned} \tag{2.35}
$$

$A^{(1)}$ scalar integral

Using (B.11) after performing the shift $q = p - k$,

$$
\begin{aligned}
A^{(1)} &= \int \frac{d^dp}{(2\pi)^d} \frac{1}{(p-k)^2-m^2} = \int \frac{d^dq}{(2\pi)^d} \frac{1}{q^2-m^2} = \frac{-i}{(4\pi)^{\frac{d}{2}}} \frac{\Gamma(1-\frac{d}{2})}{\Gamma(1)} (m^2)^{1-\epsilon} \\
&= -\frac{i}{(4\pi)^{2-\epsilon}} \Gamma(-1+\epsilon)(m^2)^{1-\epsilon}
\end{aligned} \tag{2.36}
$$

And expanding $(m^2)^{-\epsilon}$,

$$
(m^2)^{-\epsilon} \simeq 1 - \epsilon \ln m^2 \tag{2.37}
$$

Feynman parameter integration

The three integrals, $B^{\mu\nu}$, B^μ and A_1, all contain x integrals of the form $\int_0^1 x^n \ln M$, with $n = 0, 1, 2$. Denoting $\xi = \frac{s}{m^2}$ and using the definition of M, the integral is,

$$
\int_0^1 dx x^n \ln m^2 + \int_0^1 x^n \ln[1 - x(1-x)\xi] \tag{2.38}
$$

where the first term is equal to $\frac{1}{n} \ln m^2$ and is the result for the case $\xi = 0$. We will treat in detail the case $n = 0$ and quote the results for the other two cases which can be solved in a similar fashion. Consider,

$$
\int_0^1 dx \ln[1 - x(1-x)\xi] \tag{2.39}
$$

At $\xi < 4$ the integrand is definite real, whereas at $\xi \geq 4$ there are two poles (only one at $\xi = 4$) and a region where the integrand is complex between the two poles. To solve this for

all cases, we first solve the indefinite integral in the complex plane. The argument of the log can be factorized into,

$$1 - x(1-x)\xi = \xi(x - \frac{1}{2}(1+\beta))(x - \frac{1}{2}(1-\beta)) \tag{2.40}$$

where we define $\beta = \sqrt{1 - \frac{1}{r}}$, $r = \frac{\xi}{4}$. Splitting the log into a sum of three logs, the integral is straightforward,

$$\int_0^1 dx \ln[1-x(1-x)\xi] = x\ln[1-x(1-x)\xi] - 2x - \frac{1}{2}\ln(x^2 - x + \xi^{-1}) + \frac{1}{2}\beta \ln\left(\frac{2x-1+\beta}{2x-1-\beta}\right) \tag{2.41}$$

In the cases $0 < r < 1$ (where $\beta = ib$, $b > 1$, $b \in \Re$) and $r < 0$ (where $\beta > 1$, $\beta \in \Re$), there are no poles and we can simply solve the integral by plugging in the boundaries and taking the difference. Using the representations of the trigonometric and hyperbolic functions in terms of log functions: $\cot^{-1} x = \frac{i}{2}\ln\frac{ix+1}{ix-1}$, $\coth^{-1} x = \frac{1}{2}\ln\frac{y+1}{y-1}$, and using the relations: $\cot^{-1}\sqrt{\frac{1}{x^2}-1} = \sin^{-1} x$, $\coth^{-1}\sqrt{1+\frac{1}{x^2}} = \sinh^{-1} x$, we get,

$$\begin{aligned}
\int_0^1 dx \ln[1-x(1-x)\xi]\Big|_{0<r<1} &= -2 + 2\sqrt{\frac{1}{r}-1}\sin^{-1}\sqrt{r} \\
\int_0^1 dx \ln[1-x(1-x)\xi]\Big|_{r<0} &= -2 + 2\sqrt{1-\frac{1}{r}}\sinh^{-1}\sqrt{-r}
\end{aligned} \tag{2.42}$$

The third case is $r \geq 1$ (where $0 \leq \beta \leq 1$, $\beta \in \Re$). Here, there are poles and we use the Sokhatsky-Weierstrass theorem (see [30] p.112, note that in this source, as in many others, the theorem is not referred to by its name) which states,

$$\lim_{\epsilon\to 0^+}\int_a^b \frac{f(x)}{x \pm i\epsilon}dx = \mp i\pi\int_a^b f(x)\delta(x) + \mathcal{P}\int_a^b \frac{f(x)}{x}dx \tag{2.43}$$

where $\mathcal{P}$ stands for Cauchy's principal value of the integral, i.e. the integral evaluated with an excluded symmetric interval of radius ϵ around the poles. The principal value can be calculated the same way as for the other two cases. The difference is that in this case the integration range is split into three intervals by the excluded areas around the poles, so we must also evaluate (2.41) at $x' \pm \epsilon$ where x' is a pole of the integral. These contributions vanish in the limit $\epsilon \to 0$ and we are left with the contributions at 0 and 1,

$$\mathcal{P}\int_0^1 dx \ln[1-x(1-x)\xi] = -2 + 2\sqrt{1-\frac{1}{r}}\cosh^{-1}\sqrt{r} \tag{2.44}$$

To calculate the imaginary part we follow a trick used in [25]. First partial integrate (2.39), in which case the boundary term drops out. Then factorize the denominator,

$$\int_0^1 \ln[1-x(1-x)\xi] = \int_0^1 \frac{x-2x^2}{x^2-x+\xi^{-1}} \tag{2.45}$$
$$= \int_0^1 dx\beta^{-1}(x-2x^2)\left[\frac{1}{x-\frac{1}{2}(1+\beta)} - \frac{1}{x-\frac{1}{2}(1-\beta)}\right]$$

To perform the integration we must follow an $i\epsilon$ prescription (note the double use of ϵ, in this case as a prescription to remove the pole from the real axis and earlier in defining the principal value) to determine the sign. In fact, when evaluating the momentum integral of the Feynman integral we shifted $m^2 \to m^2 - i\epsilon$ which implies $\beta \to \beta + i\epsilon$. By the Sokhatsky-Weierstrass theorem each term will have an opposite sign and the imaginary term in (2.43) becomes $i\pi\sqrt{1-\frac{1}{r}}$. The final result for this case is,

$$\int_0^1 dx \ln[1-x(1-x)\xi]\Big|_{r>1} = -2 + 2\sqrt{1-\frac{1}{r}}(\cosh^{-1}\sqrt{r} + i\frac{\pi}{2}) \tag{2.46}$$

In fact, the last expression is simply an analytical continuation of the first two cases. This can be seen by writing $\sin^{-1}\sqrt{r}$ in the complex representation using the log functions, $\sin^{-1}x = -i\ln(iy+\sqrt{1-y^2})$. Comparing it with the representation $\cosh^{-1}x = \ln(y+\sqrt{y^2-1})$ one obtains the relation $i\sin^{-1}\sqrt{r} = \cosh^{-1}\sqrt{r} + i\frac{\pi}{2}$. Indeed, (2.42) and (2.46) are representations of one unique analytical function.

Similarly, (2.38) can be evaluated for the cases $n = 1, 2$. Here is a summary of all results,

$$\int_0^1 dx \ln[m^2 - x(1-x)s] = -2 + 2\sqrt{\frac{1}{r}-1}\sin^{-1}\sqrt{r} + \ln m^2 \tag{2.47}$$
$$\int_0^1 dx x \ln[m^2 - x(1-x)s] = -1 + \sqrt{\frac{1}{r}-1}\sin^{-1}\sqrt{r} + \frac{1}{2}\ln m^2 \tag{2.48}$$
$$\int_0^1 dx x^2 \ln[m^2 - x(1-x)s] = -\frac{13}{18} + \frac{1}{6r} + \frac{2}{3}\left(1-\frac{1}{4r}\right)\sqrt{\frac{1}{r}-1}\sin^{-1}\sqrt{r} + \frac{1}{3}\ln m^2 \tag{2.49}$$

Finally, combining all the results, the tensor amplitude is,

$$i\mathcal{M}(s) = -i(sg^{\mu\nu} - k^\mu k^\nu)\Pi(s) \tag{2.50}$$

where up to order $O(1)$,

$$\Pi(s) = \frac{\alpha}{3\pi}\left(\frac{1}{\epsilon} + \frac{5}{3} + \frac{1}{r} - \left(2+\frac{1}{r}\right)\sqrt{\frac{1}{r}-1}\sin^{-1}\sqrt{r} - \ln m^2\right) \tag{2.51}$$

Dimensional regularization makes the divergences evident. Only the term proportional to $\frac{1}{\epsilon}$ is UV divergent. As explained in the beginning of this section, some non-physical parameter in the Lagrangian can be renormalized to absorb this divergence. In this case, since

we are evaluating a correction to the photon propagator, the bare photon field $A_{0,\mu}$ should be renormalized by a proper definition of the Z_A factor (where $A_{0,\mu} = Z_A A_{R,\mu}$, $A_{R,\mu}$ is the renormalized field). This will add a Feynman rule that will generate a divergent tree diagram (a photon propagator) proportional to $\frac{1}{\epsilon}$. Of course since we can always add finite terms, there is an ambiguity in the choice of Z_A. In this case we choose Z_A such that the amplitude will receive a contribution $-\Pi(0) = -\frac{\alpha}{3\pi}\left(\frac{1}{\epsilon} - \ln m^2\right)$, successfully canceling the divergence. The renormalized, denoted $\Pi(s)$ by a hat is,

$$\hat{\Pi}(s) = \frac{\alpha}{3\pi}\left(\frac{5}{3} + \frac{1}{r} - \left(2 + \frac{1}{r}\right)\sqrt{\frac{1}{r} - 1}\arcsin\sqrt{r}\right) \tag{2.52}$$

2.2 Passarino-Veltman Reduction

The Passarino-Veltman [27] reduction scheme has become a basic tool in the evaluation of one-loop integrals, making possible the calculation of countless amplitudes since its inception. [31] provides a systematic presentation of the scheme and [32] includes various worked out examples. In this section we will give a description of the method through an example with a brief discussion of the more general case. In the next section, the Drell-Yan process will be calculated using a slight variation of this approach.

In the previous section, we discussed the general expression corresponding to a one-loop Feynman diagram and saw explicitly how to evaluate the case where the loop momentum does not appear in the numerator. (2.1) with $\mathcal{N} = 1$ is called a scalar integral since it does not have any tensorial indices. We saw that, in principal, tensor integrals could be evaluated using the same techniques. The Passarino-Veltman scheme is a much more efficient scheme allowing one to express any Feynman diagram as a sum of scalar integrals only, with each integral multiplied by some coefficient depending only on external kinematical quantities.

Stripping any external kinematics from the numerator, a one-loop integral has the following general form,

$$I^n_{\mu_1\ldots\mu_r}(l_1, ..., l_{n-1}, m_0, m_1, ...m_{n-1}) = \int \frac{d^d p}{(2\pi)^d} \frac{p_{\mu_1}\cdots p_{\mu_r}}{d_0 d_1 \cdots d_{n-1}} \tag{2.53}$$

where the inverse scalar propagators are,

$$d_0 = p^2 - m_0^2, \qquad d_i = (p + l_i)^2 - m_i^2, \qquad i = 1, ..., r \tag{2.54}$$

n is the number of propagators and r the rank of the tensor integral. It is common to use the n-th letter in the alphabet to denote an n-point integral (e.g. $C_\mu = I^3_\mu$). A zero subscript denotes a scalar integral (e.g. C_0).

Let us consider the case C_μ. Since the integrals is a Lorentz vector depending only on the quantities l_1 and l_2, its most general form is,

$$C_\mu = \bar{C}_1 l_{1\mu} + \bar{C}_2 l_{2\mu} \tag{2.55}$$

where $\bar{C}_i$ are scalar coefficients that are functions of scalar integrals, kinematical variables and the dimensions d of space-time. To find these coefficients, we contract this expression with both external vectors,

$$\begin{aligned} l_1^\mu C_\mu &= \bar{C}_1 l_1^2 + \bar{C}_2 l_1 \cdot l_2 \\ l_2^\mu C_\mu &= \bar{C}_1 l_1 \cdot l_2 + \bar{C}_2 l_2^2 \end{aligned} \tag{2.56}$$

On the left hand side we obtain the combinations $l_i \cdot p$ in the numerator of the 3-point integral. These combinations can be expressed in terms of propagators,

$$l_i \cdot p = d_i - d_0 - l_i^2 + m_i^2 - m_0^2 \tag{2.57}$$

By plugging this into (2.56), the left hand side can be reduced to integrals of one rank lower,

$$l_i^\mu C_\mu = B_0^{(i)} - B_0^{(0)} - (l_i^2 - m_i^2 + m_0^2) C_0 \tag{2.58}$$

where $B_0^{(i)}$ refers to the scalar integral obtained from C_0 by removing d_i. We obtain a set of two linear equations for two unknowns,

$$\underbrace{\begin{pmatrix} l_1^2 & l_1 \cdot l_2 \\ l_2 \cdot l_1 & l_2^2 \end{pmatrix}}_{\Delta_{ij}} \begin{pmatrix} \bar{C}_1 \\ \bar{C}_2 \end{pmatrix} = \begin{pmatrix} B_0^{(1)} - B_0^{(0)} - (l_1^2 - m_1^2 + m_0^2) C_0 \\ B_0^{(2)} - B_0^{(0)} - (l_2^2 - m_2^2 + m_0^2) C_0 \end{pmatrix} \tag{2.59}$$

The matrix Δ_{ij} on the left hand side is known as the Gram matrix. If it can be inverted, the system of equations has a solution. The solution in this case is,

$$\begin{pmatrix} \bar{C}_1 \\ \bar{C}_2 \end{pmatrix} = \frac{1}{l_1^2 l_2^2 - (l_1 \cdot l_2)^2} \begin{pmatrix} l_2^2 & -l_1 \cdot l_2 \\ -l_2 \cdot l_1 & l_1^2 \end{pmatrix} \begin{pmatrix} B_0^{(1)} - B_0^{(0)} - (l_1^2 - m_1^2 + m_0^2) C_0 \\ B_0^{(2)} - B_0^{(0)} - (l_2^2 - m_2^2 + m_0^2) C_0 \end{pmatrix} \tag{2.60}$$

We have successfully reduced the problem to the problem of solving scalar integrals. A complete set of up to 4-point scalar integrals (originally derived in [33]) is listed in [31], while [34] lists all UV divergent scalar integrals. [35] (see an alternative derivation in [31]) provides a recursive relation relating 5-point scalar integrals to 4-point scalar integrals.

To evaluate tensor integrals of higher ranks, one follows the same set of steps. First expand the integral in a basis of external momenta. For $r \geq 2$, one must also include the metric tensor in the basis. Since the tensor integral is symmetric, it is enough to take only completely symmetric tensors constructed out of external momenta and the metric tensor. For example,

$$C_{\mu\nu} = \bar{C}_{00} g_{\mu\nu} + \bar{C}_{11} l_{1\mu} l_{1\nu} + \bar{C}_{12} \{l_1, l_2\}_{\mu\nu} + \bar{C}_{22} l_{2\mu} l_{2\nu} \tag{2.61}$$

where $\{l_1, l_2\}_{\mu\nu} = l_{1\mu} l_{2\nu} + l_{2\mu} l_{1\nu}$. If $n \geq 5$, one chooses four linearly independent l_i vectors for the expansion, since in four space-time dimensions any other vector can be written as a linear combination of this base. In this case, one also drops the $g_{\mu\nu}$ term since it is also linearly dependent on the four chosen vectors.

Next, contract this expansion with each of the basis vectors (or all vectors if $n < 5$) and perform the reduction of type (2.57). This will reduce the rank of all tensor integrals by one. Finally, solve the set of equations, expressing the expansion coefficients in terms of lower rank tensor integrals. The loop momentum of the reduced tensors with the inverse propagator d_0 removed (e.g. $B_0^{(0)}$) must be shifted by $-l_i$ (for some i) so that these integrals will take on the form (2.53), i.e. will contain one d_0 factor in the denominator. One can repeat this process r times to obtain an expansion in terms of scalar integrals only.

Note that the Gram determinant could vanish for some expansions, in which case the set of linear equations cannot be solved by inverting the matrix. If $n \geq 5$, it is possible that the four l_i vectors chosen as a base are linearly dependent, and an attempt at another set of vectors should be made. If this is not the case or if $n < 5$, the Passarino-Veltman scheme breaks down. In [31], a method is described which takes advantage of the vanishing of the Gram matrix to perform the reduction in an alternative way.

To control divergences, we have performed this reduction in d dimensions. This has the effect that terms such as $g^{\mu\nu} g_{\mu\nu} = d$ could introduce ϵ terms into the coefficients of the scalar integral expansion. In terms such as ϵB_0, only the divergent parts of B_0 will contribute to the final result after ϵ is taken to zero. We will see in the calculation performed in chapter 6 that this could hinder our attempt at calculating the full amplitude using the method of unitarity (see chapter 3). In chapter 4 we will introduce extended reduction methods in which coefficients of the scalar integral expansion are ϵ-free.

2.3 The Drell-Yan Process

The scattering process of a quark-antiquark pair into a muon-antimuon pair (or any other charged leptonic pair), also known as the Drell-Yan process [36], is a suitable example at this stage of our review of one-loop methods. To demonstrate the tools of dimensional regulariza-

tion and Passarino-Veltman reduction, we will perform an explicit calculation of the virtual one-loop correction to the tree level process in the limit of massless quarks and muons. We will then discuss how factorization and the inclusion of the real gluon emission process are applied to treat infrared and collinear divergences in QCD processes. In the discussion of the Born cross section and of the divergences, we follow the presentation in [37].

Born cross section

The process under investigation is the following,

$$q(p_1) + \bar{q}(p_2) \to \mu^+(k_1) + \mu^-(k_2) \tag{2.62}$$

We begin with the leading order (LO) contribution, the tree level process involving one intermediary virtual of-shell photon of momentum $q = k_1 + k_2 = p_1 + p_2$ and mass $Q^2 = q^2$. The LO differential cross section for the $2 \to 2$ scattering process, the Born cross section, can be obtained from the amplitude as follows [38],

$$d\sigma^b = \frac{1}{36}\frac{1}{2s}|\mathcal{M}_b|^2 dPS^{(2)} \tag{2.63}$$

The $\frac{1}{36}$ factor originates from the averaging out all unobserved degrees of freedom of the incoming particles. In this case these are the three colors and two spins of each quark. The $\frac{1}{2s}$ flux normalization factor follows from the defintion that the cross section is the probability that some initial state will evolve to some final state per unit flux of incoming particles.

The two particle phase space factor should be calculated in d dimensions for consistency with the loop calculations to be carried out next (the Born cross section itself is finite). The integration over the phase space can be fully performed since the matrix element (we will see) depends only on the center of mass energy s and not on the angle between the outgoing particles (see [37] for derivation),

$$\begin{aligned}\int dPS^{(2)} &= \int \frac{1}{(2\pi)^{n-2}}\frac{d^{n-1}k_1}{2k_{10}}\frac{d^{n-1}k_2}{2k_{20}}\delta^n(p_1 + p_2 - k_1 - k_2) \\ &= \frac{1}{8\pi}\left(\frac{4\pi}{Q^2}\right)^{\epsilon}\frac{\Gamma(1-\epsilon)}{\Gamma(2-2\epsilon)}\end{aligned} \tag{2.64}$$

In order to express the differential cross section as a function of the photon invariant mass Q^2 we insert the identity,

$$1 = \int dQ^2\delta(s - Q^2) = \int dQ^2\delta(1 - Q^2/s) \tag{2.65}$$

and obtain,

$$\begin{aligned}\frac{dPS^{(2)}}{dQ^2} &= \frac{1}{8\pi s}\left(\frac{4\pi}{s}\right)^{\epsilon}\frac{\Gamma(1-\epsilon)}{\Gamma(2-2\epsilon)}\delta(1-\frac{Q^2}{s}) \\ &= \frac{1}{8\pi s}D(\epsilon)\frac{1}{1-2\epsilon}\delta(1-\frac{Q^2}{s})\end{aligned} \tag{2.66}$$

where $D(\epsilon)$ is defined in (2.104).

To calculate the squared amplitude we adopt the cut diagram method which in a single diagram takes into account the squaring of the amplitude and the summation over spins which leads to a traces over gamma matrices. Consider figure 2.3 where a single tree level diagram was connected through a cut to the reversed version of the same diagram, which corresponds to the complex conjugate of the diagram. Lines crossing through the cut are external and on-shell. A particle crossing the cut gives a factor $\not{p} \pm m$ ($+$ for fermion and $-$ for anti-fermion). We imagine that the external particles on the left and right edges are also connected through a separate cut. Following this prescription, the following expression is directly obtained,

$$|\mathcal{M}_b|^2 = Q_f^2 e^4 tr[\not{k}_1\gamma_\mu\not{k}_2\gamma_\nu]\frac{1}{(q^2)^2}tr[\not{p}_1\gamma^\mu\not{p}_2\gamma^\nu] \tag{2.67}$$

The squared matrix element divides into two tensorial parts contracted against one another through the two photon propagators, a leptonic part to which we attach the phase space factor and the photon propagators,

$$L_{\mu\nu} = \frac{e^2}{q^4}tr[\not{k}_1\gamma_\mu\not{k}_2\gamma_\nu]dPS^{(2)} \tag{2.68}$$

and a hadronic part,

$$H^{\mu\nu} = e^2 Q_f^2 tr[\not{p}_1\gamma^\mu\not{p}_2\gamma^\nu] \tag{2.69}$$

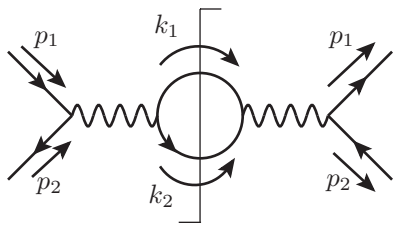

Figure 2.3: Cut diagram of the Born cross section.

When evaluating the Feynman diagram we have used the 't Hooft-Feynman gauge photon propagator. Gauge invariance (Ward identities) implies the following current conservation expression,

$$q^\mu L_{\mu\nu} = 0, \qquad q^\mu H_{\mu\nu} = 0 \tag{2.70}$$

If one considers the photon propagator before gauge fixing, these identities would make sure that the end result will not depend on the gauge parameter.

The first relation places a constraint on the form of the leptonic part, which must take the form $L_{\mu\nu} = (q^2 g_{\mu\nu} - q_\mu q_\nu) L(q^2)$. Performing the trace over $L^{\mu\nu}$ explicitly yields,

$$L(q^2) = -\frac{2}{3}\frac{\alpha}{q^4} D(\epsilon) \frac{1-\epsilon}{1-2\epsilon} \delta(1 - \frac{Q^2}{s}) \tag{2.71}$$

where $4\pi\alpha = e^2$. As a result of the second Ward identity relation, contraction of the leptonic and hadronic tensors give $L_{\mu\nu} H^{\mu\nu} = q^2 g_{\mu\nu} H^{\mu\nu} L(q^2)$ where the hadronic tensor trace is,

$$H^\mu_\mu = -16\pi\alpha Q_f^2 (1-\epsilon) \tag{2.72}$$

Finally we can plug our results into the cross section,

$$\frac{d\sigma^b}{dQ^2} = \frac{4\pi\alpha^2}{27 Q^4 s} Q_f^2 D(\epsilon) \frac{(1-\epsilon)^2}{1-2\epsilon} \delta(1 - Q^2/s) = \sigma^b(s)\delta(1 - Q^2/s) \tag{2.73}$$

the total Born cross section is obtained by integrating over Q^2/s,

$$\sigma^b(s) = \frac{4\pi\alpha^2}{27 Q^2 s} Q_f^2 D(\epsilon) \frac{(1-\epsilon)^2}{1-2\epsilon} \tag{2.74}$$

2.3.1 Virtual gluon exchange

We now move on to the next-to-leading order (NLO) contribution of order $\mathcal{O}(\alpha^2\alpha_s)$. This will correspond to an amplitude of order $\mathcal{O}(\alpha\alpha_s)$, containing an exchange of one virtual gluon, multiplied against a tree level amplitude. Figure 2.4 shows the three relevant cut diagrams.

In terms of the separate amplitudes, the cross section of the virtual gluon exchange process is given by,

$$d\sigma^v = \frac{1}{72s} \left(\mathcal{M}_v \cdot \mathcal{M}_b^* + \mathcal{M}_b \cdot \mathcal{M}_v^*\right) dPS^{(2)} = \frac{1}{72s}\, 2Re\left(\mathcal{M}_v \cdot \mathcal{M}_b^*\right) dPS^{(2)} \tag{2.75}$$

where the virtual amplitude $\mathcal{M}_v$ is a sum of the three diagrams in figure 2.4 with a combinatorial factor of 2 for diagram 2.4(c),

$$\mathcal{M}_v = \mathcal{M}_v^{(a)} + \mathcal{M}_v^{(b)} + 2\mathcal{M}_v^{(c)} \tag{2.76}$$

There are only two outgoing leptons since the gluon is virtual, hence the phase space measure is the same as is the Born cross section,

$$\frac{dPS^{(2)}}{dQ^2} = \frac{1}{8\pi s} D(\epsilon) \frac{1}{1-2\epsilon} \delta(1 - \frac{Q^2}{s}) \tag{2.77}$$

The two propagator correction diagrams (2.4(a) and 2.4(b)) give a zero contribution. This can be understood by considering a virtual $O(\alpha_s)$ correction to a quark propagator (see figure 2.5). Such a diagram gives rise to an integral of the form,

$$\int \frac{d^d k}{(2\pi)^d} \frac{1}{k^2 (p-k)^2} \tag{2.78}$$

The integral is a Lorentz scalar, and can only depend on the quantity p^2, but since the quarks are massless, the integral must give a vanishing contribution. Let us show this explicitly using the dimensional regularization scheme. Introducing Feynman parameters, the integral

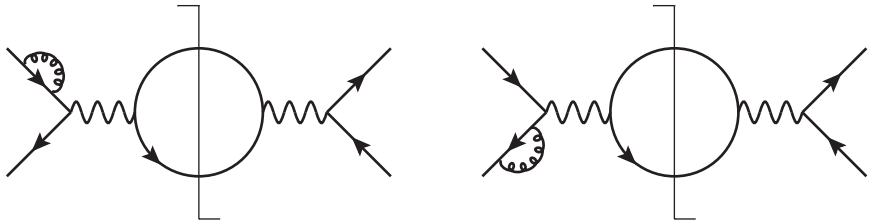

(a) quark propagator correction

(b) anti-quark propagator correction

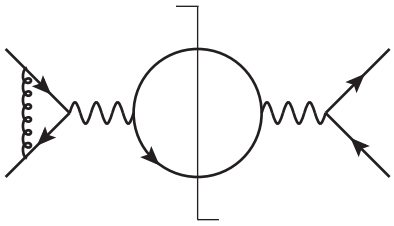

(c) vertex correction

Figure 2.4: Virtual contributions to the Drell-Yan cross section up to $O(\alpha\alpha_s)$. External kinematics are the same as in figure 2.3.

can be brought to the following form,

$$\int \frac{d^dk}{(2\pi)^d}\int_0^1 dx \frac{1}{[xk^2+(1-x)(p-k)^2]^2} = \int_0^1 dx \int \frac{d^dk}{(2\pi)^d}\frac{1}{[(k-(1-x)p)^2]^2} = \int_0^1 dx \int \frac{d^dk'}{(2\pi)^d}\frac{1}{(k'^2)^2} \tag{2.79}$$

This last integral is both UV and IR divergent when $d = 4$. Dimensional regularization softens these divergences. The UV divergence disappears when $d < 4$ and the IR divergence disappears when $d > 4$. By analytically continuing d to cover both these regions, both divergences disappear and the integral can be explicitly calculated. One way to do this is by adding a temporary mass to the quark, thus regularizing separately the IR divergence. In the region where d is less than 4 our integral is finite. We perform the integration using (B.11). This results in an expression which is finite both above and below $d = 4$. We can then analytically continue the expression to the region $d > 4$ and take the temporary mass term to zero,

$$\int_0^1 dx \int \frac{d^dk'}{(2\pi)^d}\frac{1}{(k'^2-M^2)^2} = \frac{i(M^2)^{d/2-2}}{(4\pi)^{d/2}}\frac{\Gamma(2-d/2)}{\Gamma(2)} \to 0 \tag{2.80}$$

Taking the limit $d \to 4$ is of course trivial, and our integral vanishes at the physical value of d.

We now turn to the non-zero contribution of the vertex correction diagram, 2.4(a). Reading off the cut diagram, the expression to be evaluated is,

$$\begin{aligned}\mathcal{M}_v^{(c)}\cdot\mathcal{M}_b^* = \int \frac{d^dk}{(2\pi)^d}\, tr\Big[&(-ieQ_F\gamma^\mu)\not{p}_2(-ig_s\gamma^\rho T^a)\frac{-ig_{\rho\sigma}\delta_{ab}}{k^2} \\ &\times \frac{i(\not{p}_2+\not{k})}{(p_2+k)^2}(-ieQ_F\gamma^\nu)\frac{i(\not{p}_1-\not{k})}{(p_1-k)^2}(-ig_s\gamma^\sigma T^b)\not{p}_1\Big] \\ &\times \frac{-ig_{\mu\alpha}}{q^2}\,\frac{-ig_{\nu\beta}}{q^2}\, tr[(-ie\gamma^\alpha)\not{k}_1(-ie\gamma^\beta)\not{k}_2]\end{aligned} \tag{2.81}$$

After application of the Lorentz contractions, the expression can be broken up into a hadronic and a leptonic trace mediated by the photon which can be absorbed in the leptonic trace,

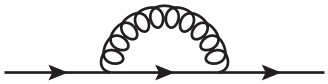

Figure 2.5: virtual $O(\alpha_s)$ correction to a quark propagator

$$L^{\mu\nu} = \frac{e^2}{q^4} tr[\gamma^\mu \not{k}_1 \gamma^\nu \not{k}_2] \tag{2.82}$$

$$H^{\mu\nu} = ie^2 Q_F^2 g_s^2 \int \frac{d^d k}{(2\pi)^d} \frac{1}{k^2 (p_1 - k)^2 (p_2 + k)^2} \times tr\left[\gamma^\mu \not{p}_2 \gamma^\rho (\not{p}_2 + \not{k}) \gamma^\nu (\not{p}_1 - \not{k}) \gamma_\rho \not{p}_1\right] tr[T^a T^a] \tag{2.83}$$

Leptonic Part

As in the Born case, gauge invariance implies that $q_\mu L^{\mu\nu} = 0$ which in turn implies that $L^{\mu\nu}$ must have the following form,

$$L^{\mu\nu} = (q^2 g^{\mu\nu} - q^\mu q^\nu) L(q^2) \;\Rightarrow\; L^\mu_\mu = 3q^2 L(q^2) \tag{2.84}$$

Performing the trace is straightforward, yielding,

$$L^\mu_\mu = \frac{e^2}{q^4} Tr\{\gamma^\mu \not{k}_1 \gamma_\mu \not{k}_2\} = \frac{e^2}{q^4} k_1 \cdot k_2 (8 - 4d) = -\frac{4e^2}{Q^2}(1 - \epsilon) \tag{2.85}$$

where $Q^2 = q^2 = (k_1 + k_2)^2 = 2k_1 \cdot k_2$.

Hadronic Part

The hadronic part must also obey $q_\mu H^{\mu\nu} = 0$,

$$L^{\mu\nu} H_{\mu\nu} = (q^2 g^{\mu\nu} - q^\mu q^\nu) L(q^2) H_{\mu\nu} = q^2 L(q^2) H^\mu_\mu = \frac{1}{3} L^\mu_\mu H^\nu_\nu \tag{2.86}$$

A trace over $SU(N_C)$ generators gives,

$$Tr[T^a T^a] = Tr[C_F I] = N_C C_F \tag{2.87}$$

and setting $N_C = 3$ and $C_F = 4/3$ [8],

$$Tr[T^a T^a] = 3C_F = 4 \tag{2.88}$$

The trace over eight γ matrices can be performed using Form,

$$\begin{aligned} &Tr\{\gamma^\mu \not{p}_2 \gamma^\rho (\not{p}_2 + \not{k}) \gamma_\mu (\not{p}_1 - \not{k}) \gamma_\rho \not{p}_1\} \\ &= -8((\epsilon - \epsilon^2) s k^2 + 2(1 - \epsilon) s (p_1 \cdot k - p_2 \cdot k) + (1 - \epsilon) s^2 - 4(1 - \epsilon) p_1 \cdot k p_2 \cdot k) \end{aligned} \tag{2.89}$$

Denoting $d_1 = k^2$, $d_2 = (p_1 - k)^2$, $d_3 = (p_2 + k)^2$ and $A = -8ie^2 Q_F^2 g_s^2$,

$$H_\mu^\mu = A\int \frac{d^dk}{(2\pi)^d}\Big\{(\epsilon-\epsilon^2)s\frac{1}{d_2d_3} + 2(1-\epsilon)s\frac{p_1\cdot k - p_2\cdot k}{d_1d_2d_3} + (1-\epsilon)s^2\frac{1}{d_1d_2d_3} - 4(1-\epsilon)\frac{p_1\cdot kp_2\cdot k}{d_1d_2d_3}\Big\} \tag{2.90}$$

Passarino-Veltman type reduction can be used to remove as many p factors as possible from the numerator,

$$\begin{aligned}
\frac{p_1\cdot k}{d_1d_2} &= \frac{1}{2}\frac{d_1-d_2}{d_1d_2} = \frac{1}{2}\left(\frac{1}{d_2}-\frac{1}{d_1}\right)\\
\frac{p_2\cdot k}{d_1d_3} &= \frac{1}{2}\frac{d_3-d_1}{d_1d_3} = \frac{1}{2}\left(\frac{1}{d_1}-\frac{1}{d_3}\right)\\
\frac{p_1\cdot kp_2\cdot k}{d_1d_2d_3} &= \frac{1}{2}\left(\frac{p_2\cdot k}{d_2d_3}-\frac{p_2\cdot k}{d_1d_3}\right) = \frac{1}{2}\left(\frac{p_2\cdot k}{d_2d_3}-\frac{1}{2}\frac{1}{d_1}+\frac{1}{2}\frac{1}{d_3}\right)
\end{aligned} \tag{2.91}$$

All integrals containing only one external momentum vanish for the same reason that the self energy diagrams vanished,

$$\int\frac{d^dk}{(2\pi)^d}\frac{1}{d_1d_2} = \int\frac{d^dk}{(2\pi)^d}\frac{1}{d_1d_3} = \int\frac{d^dk}{(2\pi)^d}\frac{1}{D_i} = 0\ \ (i=1,2,3) \tag{2.92}$$

The trace of the hadronic part is now reduced to,

$$\begin{aligned}
H_\mu^\mu &= A\int\frac{d^dk}{(2\pi)^d}\Big\{(\epsilon-\epsilon^2)s\frac{1}{d_2d_3} + 2(1-\epsilon)s\frac{1}{d_2d_3} + (1-\epsilon)s^2\frac{1}{d_1d_2d_3} - 2(1-\epsilon)\frac{p_2\cdot k}{d_2d_3}\Big\}\\
&= A\int\frac{d^dk}{(2\pi)^d}\Big\{(2-\epsilon-\epsilon^2)s\frac{1}{d_2d_3} + (1-\epsilon)s^2\frac{1}{d_1d_2d_3} - 2(1-\epsilon)\frac{p_2\cdot k}{d_2d_3}\Big\}
\end{aligned} \tag{2.93}$$

The last term can be further simplified if we note that on one hand (shifting the k variable under the integral),

$$\frac{1}{d_2d_3} = \frac{1}{(p_1-k)^2(p_2+k)^2} = \frac{1}{k'^2(k'+p_1+p_2)^2} \tag{2.94}$$

The last term in (2.93) can now be expressed in terms of the first term as follows,

$$\begin{aligned}
\frac{p_2\cdot k}{d_2d_3} &= \frac{p_2\cdot k}{(p_1-k)^2(p_2+k)^2} = \frac{p_2\cdot k'+p_1\cdot p_2}{k'^2(k'+p_1+p_2)^2} = \frac{p_2\cdot k'}{k'^2(k'-p_1-p_2)^2}\\
&= \frac{-p_2\cdot k'}{k'^2(k'+p_1+p_2)^2} = \frac{\frac{1}{2}p_1\cdot p_2}{k'^2(k'+p_1+p_2)^2} = \frac{s}{4}\frac{1}{d_2d_3}
\end{aligned} \tag{2.95}$$

where the result of the second and fourth equality were used to re-express $p_2\cdot k'$ in terms of

$p_1 \cdot p_2$. In the second equality the substitution $p_1 - k = k'$ was made, whereas in the third equality the substitution $p_2 + k = k'$ was made.

The trace of the hadronic part takes now the following more simplified form,

$$H^{\mu}_{\mu} = A\{(\frac{3}{2} - \frac{1}{2}\epsilon - \epsilon^2)sB_0^{(1)} + (1-\epsilon)s^2 C_0\} \tag{2.96}$$

In the following, we explicitly evaluate these integrals.

$B_0^{(1)}$ integral

$$B_0^{(1)} = \int \frac{d^dk}{(2\pi)^d}\frac{1}{d_2 d_3} = \int \frac{d^dk}{(2\pi)^d}\frac{1}{(p_1-k)^2(p_2+k)^2} \tag{2.97}$$

Introducing Feynman parameters,

$$\int \frac{d^dk}{(2\pi)^d}\frac{1}{(p_1-k)^2(p_2+k)^2} = \int \frac{d^dk}{(2\pi)^d}\int_0^1 dx \frac{1}{[x(p_1-k)^2 + (1-x)(p_2+k)^2]^2} \tag{2.98}$$

Working out the denominator, taking the particles to be massless ($p_1^2 = p_2^2 = 0$) and replacing $s = 2p_1 \cdot p_2$,

$$\begin{aligned} x(p_1-k)^2 + (1-x)(p_2+k)^2 &= xk^2 - 2xp_1\cdot k + k^2 - xk^2 + 2(1-x)p_2\cdot k \\ &= k^2 - 2xp_1\cdot k + 2(1-x)p_2\cdot k \\ &= (k - (xp_1 - (1-x)p_2))^2 - (xp_1 - (1-x)p_2)^2 \\ &= (k - (xp_1 - (1-x)p_2))^2 + 2x(1-x)p_1\cdot p_2 \\ &= (k - (xp_1 - (1-x)p_2))^2 + x(1-x)s \end{aligned} \tag{2.99}$$

Shift the integration variable $k' = k - (xp_1 - (1-x)p_2)$ and evaluate the integral using (B.11),

$$\begin{aligned} \int_0^1 dx \int \frac{d^dk}{(2\pi)^d}\frac{1}{[x(p_1-k)^2 + (1-x)(p_2+k)^2]^2} &= \int_0^1 dx \int \frac{d^dk'}{(2\pi)^d}\frac{1}{(k'^2 + x(1-x)s)^2} \\ &= \int_0^1 dx \frac{i}{(4\pi)^{\frac{d}{2}}}\frac{\Gamma(2-\frac{d}{2})}{\Gamma(2)}\frac{1}{(-sx(1-x))^{2-\frac{d}{2}}} \end{aligned} \tag{2.100}$$

Extract the poles in ϵ using the identity $\Gamma(1+\epsilon) = \epsilon\Gamma(\epsilon)$,

$$\int_0^1 dx \frac{i}{(4\pi)^{\frac{d}{2}}} \frac{\Gamma(2-\frac{d}{2})}{\Gamma(2)} \frac{1}{(-sx(1-x))^{2-\frac{d}{2}}} = \frac{i}{(4\pi)^{2-\epsilon}} \Gamma(\epsilon) \int_0^1 \frac{dx}{(-sx(1-x))^{\epsilon}}$$
$$= \frac{i}{(4\pi)^2} \left(\frac{4\pi}{-s}\right)^{\epsilon} \frac{\Gamma(1+\epsilon)}{\epsilon} \int_0^1 dx x^{-\epsilon}(1-x)^{-\epsilon}$$
$$= \frac{i}{(4\pi)^2} \left(\frac{4\pi}{-s}\right)^{\epsilon} \frac{1}{\epsilon} \frac{\Gamma(1+\epsilon)\Gamma(1-\epsilon)^2}{\Gamma(2-2\epsilon)} \tag{2.101}$$

The Γ function can be expanded,

$$\Gamma(1 \pm \epsilon) = 1 \mp \epsilon\gamma_E + \frac{1}{2}\epsilon^2(\gamma_E^2 + \frac{\pi}{6}) + O(\epsilon^3) \tag{2.102}$$

In addition, we can the minus sign raised to the power of ϵ. Since in the end we are only interested in the real part of B_0, the imaginary parts do not contribute,

$$(-1)^{\epsilon} = (e^{i\pi})^{\epsilon} = e^{i\pi\epsilon} = 1 + i\pi\epsilon + \frac{1}{2}(i\pi\epsilon)^2 + O(\epsilon^3) \tag{2.103}$$

And denoting,

$$D(\epsilon) = \left(\frac{4\pi}{s}\right)^{\epsilon} \frac{\Gamma(1-\epsilon)}{\Gamma(1-2\epsilon)} \tag{2.104}$$

We finally get,

$$Re\ B_0^{(1)} = \frac{i}{(4\pi)^2} \left(\frac{4\pi}{s}\right)^{\epsilon} Re\ (-1)^{\epsilon} \frac{1}{\epsilon} \frac{\Gamma(1+\epsilon)\Gamma(1-\epsilon)^2}{\Gamma(2-2\epsilon)}$$
$$= \frac{i}{(4\pi)^2} D(\epsilon) \frac{1}{\epsilon} \Gamma(1+\epsilon)\Gamma(1-\epsilon) \frac{1}{1-2\epsilon}$$
$$= \frac{i}{(4\pi)^2} D(\epsilon) \left(\frac{1}{\epsilon} + 2\right) + O(\epsilon) \tag{2.105}$$

Evaluating C_0

$$C_0 = \int \frac{d^dk}{(2\pi)^d} \frac{1}{d_1 d_2 d_3} = \int \frac{d^dk}{(2\pi)^d} \frac{1}{k^2(p_1-k)^2(p_2+k)^2} \tag{2.106}$$

First use Feynman parameters twice (this way we avoid taking special care of the boundaries of the feynman parameter integrals),

$$\int \frac{d^dk}{(2\pi)^d} \frac{1}{k^2(p_1-k)^2(p_2+k)^2} = \int \frac{d^dk}{(2\pi)^d} \int_0^1 dx \frac{1}{[xk^2 + (1-x)(p_1-k)^2]^2(p_2+k)^2}$$
$$= \int \frac{d^dk}{(2\pi)^d} \int_0^1 dx \int_0^1 dy \frac{2y}{[(1-y)(p_2+k)^2 + y[xk^2 + (1-x)(p_1-k)^2]]^3} \tag{2.107}$$

Again completing the square for k in the denominator,

$$\begin{aligned}(1-y)(p_2+k)^2+y[xk^2+(1-x)(p_1-k)^2] \\ &= (1-y)(2p_2\cdot k+k^2)+xyk^2+y(1-x)(-2p_1\cdot k+k^2)\\ &= k^2-yk^2+(1-y)2p_2\cdot k+xyk^2+yk^2-xyk^2-y(1-x)2p_1\cdot k\\ &= k^2-2[y(1-x)p_1-(1-y)p_2]\cdot k\\ &= (k-(y(1-x)p_1-(1-y)p_2))^2-(y(1-x)p_1-(1-y)p_2)^2\\ &= (k-(y(1-x)p_1-(1-y)p_2))^2+y(1-y)(1-x)s\end{aligned} \tag{2.108}$$

We shift the integration variable, $k'=k-(y(1-x)p_1-(1-y)p_2)$, and evaluate the integral using (B.11). We then use the expansions (2.102) and (2.103) (omitting again the imaginary part) and the definition (2.104),

$$\begin{aligned}Re\ C_0 &= \int\frac{d^dk}{(2\pi)^d}\int_0^1dx\int_0^1dy\frac{2y}{[k'^2+y(1-y)(1-x)s]^3}\\ &= \int_0^1dx\int_0^1dy\frac{i}{-1}y\frac{(-sy(1-y)(1-x))^{2-\epsilon-3}}{(4\pi)^{2-\epsilon}}\frac{\Gamma(1+\epsilon)}{\Gamma(3)}\\ &= -\frac{i}{(4\pi)^2}\left(\frac{4\pi}{-s}\right)^\epsilon\frac{1}{-s}\Gamma(1+\epsilon)\int_0^1dx(1-x)^{-1-\epsilon}\int_0^1dyy^{-\epsilon}(1-y)^{-1-\epsilon}\\ &= \frac{i}{(4\pi)^2}\left(\frac{4\pi}{-s}\right)^\epsilon\frac{1}{s}\Gamma(1+\epsilon)\frac{\Gamma(1)\Gamma(-\epsilon)}{\Gamma(1-\epsilon)}\frac{\Gamma(1-\epsilon)\Gamma(-\epsilon)}{\Gamma(1-2\epsilon)}\\ &= \frac{i}{(4\pi)^2}\left(\frac{4\pi}{-s}\right)^\epsilon\frac{1}{s}\frac{1}{\epsilon^2}\frac{\Gamma(1+\epsilon)\Gamma(1-\epsilon)^2}{\Gamma(1-2\epsilon)}\\ &= \frac{i}{(4\pi)^2}D(\epsilon)\frac{1}{s}\frac{(-1)^\epsilon}{\epsilon^2}\Gamma(1+\epsilon)\Gamma(1-\epsilon)\\ &= \frac{i}{(4\pi)^2}D(\epsilon)\frac{1}{s}\frac{1}{\epsilon^2}(1+\cancel{i\pi\epsilon}-\frac{\pi^2}{2}\epsilon^2)(1-\epsilon\gamma_E+\frac{\epsilon^2}{2}\gamma_E^2+\epsilon^2\frac{\pi^2}{12})(1+\epsilon\gamma_E+\frac{\epsilon^2}{2}\gamma_E^2+\epsilon^2\frac{\pi^2}{12})+O(\epsilon)\\ &= \frac{i}{(4\pi)^2}D(\epsilon)\frac{1}{s}\left(\frac{1}{\epsilon^2}-\frac{\pi^2}{3}\right)+O(\epsilon)\end{aligned} \tag{2.109}$$

The hadronic trace is,

$$\begin{aligned}H_\mu^\mu &= AD(\epsilon)s\frac{i}{(4\pi)^2}\{(\frac{3}{2}-\frac{1}{2}\epsilon-\epsilon^2)(\frac{1}{\epsilon}+2)+(1-\epsilon)(\frac{1}{\epsilon^2}-\frac{\pi^2}{3})\}+O(\epsilon)\\ &= AD(\epsilon)s\frac{i}{(4\pi)^2}\{\frac{1}{\epsilon^2}+\frac{1}{2}\frac{1}{\epsilon}+\frac{5}{2}-\frac{\pi^2}{3}\}+O(\epsilon)\end{aligned} \tag{2.110}$$

Final result

Combining the leptonic and hadronic parts and inserting those into the total cross section,

$$\begin{aligned}\frac{d\sigma^v}{dQ^2} &= \left[\frac{1}{72s}\right] \times 2 \cdot 2 \left[\frac{1}{3}\left(-\frac{4e^2}{Q^2}\right)(1-\epsilon)\right] \\ &\times \left[(-8ie^2Q_F^2g_s^2)D(\epsilon)s\frac{i}{(4\pi)^2}\left(\frac{1}{\epsilon^2}+\frac{1}{2}\frac{1}{\epsilon}+\frac{5}{2}-\frac{\pi^2}{3}\right)3C_F\right] \\ &\times \left[\frac{1}{8\pi s}D(\epsilon)\frac{1}{1-2\epsilon}\delta(1-\frac{Q^2}{s})\right] + O(\epsilon)\end{aligned} \tag{2.111}$$

We use the definitions $e^2 = 4\pi\alpha$ and $g_s^2 = 4\pi\alpha_s$, and the expression for the total Born cross section (2.74). The virtual exchange contribution to the differential cross section is,

$$\frac{d\sigma^v}{dQ^2} = \frac{\alpha_s\sigma_B C_F}{\pi}D(\epsilon)^2\left(-\frac{2}{\epsilon^2}-\frac{3}{\epsilon}-10+\frac{2\pi^2}{3}\right)\delta(1-z)+O(\epsilon) \tag{2.112}$$

where $z \equiv \frac{Q^2}{s}$.

2.3.2 Infrared and collinear divergences

The Born cross section (2.73) calculated in the beginning of the section gave a finite result, one that could be compared to experiment. Once we attempted to add a loop correction, divergences of the form $\frac{1}{\epsilon}$ and $\frac{1}{\epsilon^2}$ appeared. What is the origin of these divergences? These divergences originate from the triangular loop in figure 2.4(c). One could suspect that they are UV in nature and should thus be absorbed by counter terms. This is implausible in this case, because that would imply that the QED counter term (of a fermion-antifermion-photon vertex) must contain the QCD coupling constant α_s, contradicting the fact that QED is a self consistent renormalizable theory.

The divergences must then all be infrared and collinear in nature. When a massless virtual particle is present, the following propagators typically occur,

$$\frac{1}{(p_1-k)^2} \tag{2.113}$$

the denominator can be rewritten as,

$$(p_1-k)^2 = -2p_1\cdot k = -2|\vec{p}_1||\vec{k}|(1-\cos\theta) \tag{2.114}$$

where θ is the angle between the two spatial vectors. The denominator can vanish if either $|k| = 0$ (infrared or *soft divergence*, energy of the particle vanishes) or $\cos\theta = 1$ (*collinear*

divergence, particles are parallel). Of course if $p_1 = 0$ an infrared divergence can also occur. Powers of the loop momentum in the numerator (also arising from the integration measure) could prevent such divergences and every case must be carefully examined.

Real gluon emission

The first step towards the resolution of such divergences, also used in pure QED processes, would be to add to the cross section the contribution of a process where a real gluon is emitted from one of the incoming massless quarks. With low energy gluons being emitted, such a process with three outgoing particles cannot be experimentally distinguished from the two outgoing particle processes discussed so far. In fact, as we will see shortly, in QCD a gluon emission of any energy cannot be distinguished. The amplitude of this process is of order $\mathcal{O}(\alpha g_s)$ and when squared against the same amplitude gives the desired order of $\mathcal{O}(\alpha^2\alpha_s)$ which could potentially cancel against the virtual exchange divergences. One of the three possible cut diagrams is shown in figure 2.6. Such a diagram contains a quark propagator of the type discussed above, and could thus suffer from infrared or collinear divergence when the emitted gluon is either soft or collinear to the quark emitting it.

The contribution of these diagrams to the differential cross section is (see [37] for a full derivation),

$$\frac{d\sigma^r}{dQ^2} = \sigma_B \frac{\alpha_s}{\pi} C_F D(\epsilon) \left[\frac{2}{\epsilon^2}\delta(1-z) - \frac{2}{\epsilon}\frac{(1+z)^2}{(1-z)_+} + 4(1+z^2)\left(\frac{\ln(1-z)}{1-z}\right)_+ - 2\left(\frac{1+z^2}{1-z}\right)\ln z \right] \tag{2.115}$$

The plus function $F_+(x)$ is defined in [37]. Similar to the Dirac delta function, it is a distribution giving a finite result when integrated over. Only the term proportional to $\frac{1}{\epsilon^2}$ is divergent and is multiplied by a desired $\delta(1-z)$. This term indeed cancels exactly the $\frac{1}{\epsilon^2}$ divergence of the virtual exchange contribution.

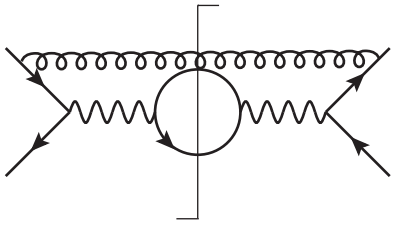

Figure 2.6: Cut diagram for real gluon emission. Two more diagrams exist, a gluon emitted from the anti-quark on both sides, or a gluon emitted from the quark on one side and from the anti-quark on the other.

Factorization

The remaining divergence is specific to QCD and requires a novel tool, namely *factorization*. In QED we are able to treat all scattering processes perturbatively because the coupling constant, which under the renormalization scheme is dependent on the energy scale of the problem, is small enough to expand around. In QCD this is not the case. At high energies or short distances, the coupling constant is indeed small, whereas at low energies, or equivalently at larger distances, the coupling constant becomes very large and the perturbative approach we took by calculating Feynman diagrams breaks down. This gives rise to the phenomenon of *asymptotic freedom*, i.e. quarks barely interact by the strong force at short distances, and *confinement*, i.e. quarks cannot be isolated and are always found in bound states containing pairs or triples. Therefore, our question of what happens when quarks scatter off each other is in fact not a physical one. A more appropriate formulation of the Drell-Yan process would be to ask what happens when two protons, bound states of quarks, scatter of each other. The process is as follows,

$$A(P_1) + B(P_2) \to \mu^+(k_1) + \mu^-(k_2) + X \tag{2.116}$$

A and B are protons with momentum P_1 and P_2 and X contains any other asymptotic state created by the scattering interaction in addition to the muons.

The structure of the proton is still an open question in physics, and cannot be calculated from basic principles of QCD. To perform calculations in QCD such as the one above, one uses a model first proposed by Feynman known as the parton model. Consider two protons approaching each other as viewed from their center of mass frame. In high energies, these protons are Lorentz contracted along the axis of their collision and we can view them as two pancake-like structures passing through each other. The moment of interaction is extremely short with respect to the typical time scale of the strong interaction, which is strong only at low energies or long time scales by the uncertainty principle. Therefore, during this moment of collision the proton consists of some number of *partons* (quarks and gluons), some of which could be virtual but are stable in this time scale. Each parton carries a fraction $p_i = x_i P$ of the total momentum P of the proton. As the two protons pass each other, a parton of one proton will scatter off a parton of the other proton with some probability. After the collision, at a strong interaction time scale, the partons not participating in the scattering process (or those being produced in the scattering process) will undergo a process of hadronization. This is a process in which new stable bound states of partons are produced via the strong interaction. These states are what we denoted by X. The real emitted gluon discussed above cannot be distinguished from X, which is the reason that we integrate over all of its phase space.

In essence what we have done is separate the high energy process (i.e. the scattering) from the low energy process (i.e. the confinement of the partons before the scattering and the

hadronization that follows). This trick is captured in the following formula of factorization,

$$d\sigma_{AB}^{H}(S) = \sum_{i,j} \int_0^1 dx_1 dx_2 f_{iA}(x_1) d\sigma_{ij}(s) f_{jB}(x_2) \tag{2.117}$$

where S is the hadronic center of mass energy and is related to the partonic center of mass energy by $S = x_1 x_2 s$.

Put in words, the formula states that the differential cross section of the scattering of the protons is given by summing over all partons in A and all partons in B. For each combination of partons we multiply the partonic differential cross section (e.g. scattering of two quarks) by the probability of finding parton i in proton A having momentum fraction x_i. Similarly for parton j. We have seen in the above calculation of the Drell-Yan process that the partonic cross section $d\sigma_{ij}$ is divergent. This means that to obtain a finite quantity for the hadronic cross section we must demand that the probability functions f_{iA} will be divergent in such a way that they exactly cancel the divergence of the cross section. In this sense, this resembles the renormalization procedure where divergences in cross sections are cancelled by adding divergent counter terms to the Lagrangian. The functions f_{iA} are called the *parton density functions* (PDF) and at this point in time can be only measured experimentally. They are extremely powerful in that they are process independent, depending only on the parton type and the hadron type. Once found experimentally through measuring one scattering event, they can be used to predict other scattering events.

Let us now see how this factorization equation is used in practice to remove divergences. First define a renormalized partonic cross section as follows,

$$d\sigma_{ij} = \int dz_1 dz_2 \Gamma_{ik}(z_1) d\bar{\sigma}_{kl}(z_1 z_2 s) \Gamma_{jl}(z_2) \tag{2.118}$$

$d\bar{\sigma}$ is a finite renormalized differential cross section and $\Gamma_{ik}(z_i)$ is called the transition function. Similar to the PDF, it tells us what the probability is of a quark with momentum q_i emanates with a fraction z_i of its original momentum p_i. For example, in the real gluon emission process in figure 2.6, p_i is the momentum of the quark before emitting the gluon and q_i its momentum after. Similarly for the virtual gluon exchange process. The transition function absorbs the infinities of the non-renormalized partonic cross section, and we can now define the renormalized PDF as follows,

$$\bar{f}\eta = \int_0^1 \int_0^1 dx dz f(x) \Gamma(z) \delta(\eta - xz) = \int_\eta^1 \frac{dz}{z} f\left(\frac{\eta}{z}\right) \Gamma(z) = f(\eta) \otimes \Gamma(\eta) \tag{2.119}$$

The factorization formula (2.117) can now be rewritten in terms of finite quantities only,

$$d\sigma_{AB}^{H}(s) = \int d\eta_1 d\eta_2 \bar{f}_{kA}(\eta_1) d\bar{\sigma}_{kl}(\eta_1 \eta_2 s) \bar{f}_{lB}(\eta_2) \tag{2.120}$$

It is straightforward to check that both formulas are identical.

Having defined all the necessary ingredients, the process of factorization is as follows. The bare partonic cross section $d\sigma_{ij}$ is calculated up to some order and is found to be divergent. The transition function Γ_{ik} is defined using (2.118) in such a way that the renormalized partonic cross section $d\bar{\sigma}_{kl}$ is finite. Now one performs an experiment, measures the hadronic cross section $d\sigma^H_{AB}$, and according to (2.120) measures the renormalized PDFs $\bar{f}_{kA}$ for each parton and hadron type. By (2.119) one could calculate the non-renormalized PDFs f_{iA}, but this is not a necessary step. One must take care that when the experimental renormalized PDF is used, the corresponding transition function must be used to renormalize the partonic cross section.

Let us calculate what the transition function must be in our case according to the above prescription. First expand all the quantities in (2.118) in the strong coupling constant,

$$\begin{aligned} d\bar{\sigma}(s) &= \sum_{n=0}^{\infty} \left(\frac{\alpha_s}{2\pi}\right)^n d\bar{\sigma}^{(n)}(s) \\ d\sigma(s) &= \sum_{n=0}^{\infty} \left(\frac{\alpha_s}{2\pi}\right)^n d\sigma^{(n)}(s) \\ \Gamma_{ij}(z) &= \delta_{ij}\delta(1-z) + \sum_{n=1}^{\infty} \left(\frac{\alpha_s}{2\pi}\right)^n \Gamma^{(n)}_{ij}(z) \end{aligned} \tag{2.121}$$

Then plug the expansion into (2.118) and keep only terms up to first order, since we calculated the cross section up to first order in α_s,

$$\begin{aligned} d\sigma^{(0)}_{ij}(s) + \frac{\alpha_s}{2\pi} d\sigma^{(1)}_{ij}(s) = d\bar{\sigma}^{(0)}_{ij}(s)\frac{\alpha_s}{2\pi}\Bigg[& d\bar{\sigma}^{(1)}_{ij}(s) + \int dz_1 \Gamma^{(1)}_{ik}(z_1) d\bar{\sigma}^{(0)}_{kj}(z_1 s) \\ & + \int dz_2 d\bar{\sigma}^{(0)}_{kj}(z_2 s)\Gamma^{(1)}_{ik}(z_2)\Bigg] \end{aligned} \tag{2.122}$$

Matching the terms on both sides per order, we see that the renormalized Born cross section is just equal to the non-renormalized one (since it was finite in the first place). The first order renormalized cross section is given by,

$$d\bar{\sigma}^{(1)}_{ij}(s) = d\sigma^{(1)}_{ij}(s) - \int dz_1 \Gamma^{(1)}_{ik}(z_1) d\bar{\sigma}^{(0)}_{kj}(z_1 s) - \int dz_2 d\bar{\sigma}^{(0)}_{kj}(z_2 s)\Gamma^{(1)}_{ik}(z_2) \tag{2.123}$$

We must choose the transition function such that it cancels the $\frac{1}{\epsilon}$ terms in the cross section. The overall cross section, given by the sum of the virtual gluon exchange and the real gluon exchange, is,

$$\frac{d\sigma^{(1)}}{dQ^2} = \frac{d\sigma^r}{dQ^2} + \frac{d\sigma^v}{dQ^2} = \sigma_B D(\epsilon)\left(-\frac{2}{\epsilon}P_{qq}(z) + R(z)\right) \tag{2.124}$$

where the two following functions were defined,

$$P_{qq}(z) = C_F \left[\frac{(1+z)^2}{(1-z)_+} + \frac{3}{2}\delta(1-z) \right] \tag{2.125}$$

$$R(z) = C_F \left[\delta(1-z)\left(\frac{2\pi^2}{3} - 8\right) + 4(1+z^2)\left(\frac{\ln(1-z)}{1-z}\right)_+ - 2\left(\frac{1+z^2}{1-z}\right)\ln z \right] \tag{2.126}$$

Inserting the Born cross section wherever $d\bar{\sigma}_{kj}^{(0)}$ appears, the choice of the transition function is obvious, yielding also the following renormalized cross section,

$$\Gamma^{(1)}(z) = -\frac{1}{\epsilon} D(\epsilon) P_{qq}(z) \tag{2.127}$$

$$\frac{d\bar{\sigma}^{(1)}}{dQ^2} = \sigma_B R(z) \tag{2.128}$$

Note that the choice of transition function has an ambiguity of finite terms. This ambiguity will not appear in the physical observable result, the hadronic cross section, as long as we are consistent. As explained above, we choose a transition function and then measure the PDF. When using this PDF to make predictions, we must use the same transition function to renormalize our partonic cross section.

CHAPTER 3

Unitarity and Cutkosky Rules

In perturbation theory, one can calculate an amplitude to increasing accuracy by evaluating Feynman diagrams with growing number of loops. Higher order calculations in general imply many complications, e.g. large number of diagrams and large number of integration variables per diagram. In this chapter we will show that one can take advantage of the analytical properties of an amplitude to simplify the expression into smaller more manageable pieces. The unitarity property of the S-matrix can be used to derive the imaginary part of an amplitude. This result turns out to be a special case of the Cutkosky rules [9], which allow one to exploit the analytical properties of an amplitude to calculate the discontinuity along branch cuts. The locations of these branch cuts can be detected using the Landau equations [10]. Dispersion relations, in turn, can be used to extract the full amplitude. These techniques have already been known in the earlier years of Quantum Field Theory, and were a common approach in the problem of the strong interactions [39] before the advent of QCD. A serious disadvantage of this method is its incapacity to reproduce rational terms free of branch cuts. In a modern application of the Cutkosky rules, the amplitude is first expanded in a base of scalar integrals and the coefficients are obtained by projecting the amplitude using the Cutkosky rules. This method spares us of the need for the rather cumbersome dispersion relations and solves the problem of ambiguities in rational terms for certain cases.

3.1 Unitarity

We recall that it is common to split the S-matrix into an interacting part, the T-matrix, and a forward scattering part (see for example [8] for a discussion of unitarity),

$$S = \mathbb{1} + iT \tag{3.1}$$

The scattering amplitude is then defined as a matrix element of the T-matrix after stripping off an overall momentum conserving delta function,

$$\langle \Psi_f | T | \Psi_i \rangle = (2\pi)^4 \delta^{(4)}(\sum_{m \in I} k_m - \sum_{m \in F} p_m) \cdot \mathcal{M}(\{k_m\} \to \{p_m\}) \tag{3.2}$$

where I (F) is the set of all particles in the initial (final) state i (f) with momenta $\{k_m\}$ ($\{p_m\}$).

The S-matrix is a unitary operator, i.e. $S^\dagger S = \mathbb{1}$. Since this relation imposes a strong constraint on amplitudes, let us briefly review its origin. Consider a system which at time t is at some state $|\Psi\rangle$. For example, in a system of n particles each in a momentum eigenstate, $|\Psi\rangle$ would be $|k_1, ..., k_n\rangle$. To this we could add spin, flavor, color, charge, etc. In the Heisenberg picture, where states are time-independent, this state would be given by $|\Psi^H\rangle_t = e^{iHt}|\Psi\rangle$. The S-matrix element is defined as an inner product of two Heisenberg states,

$$\lim_{\tau \to \infty} {}_\tau\langle \Psi_f^H | \Psi_i^H \rangle_{-\tau} = \lim_{\tau \to \infty} \langle \Psi_f | e^{-iH(2\tau)} | \Psi_i \rangle \equiv \langle \Psi_f | S | \Psi_i \rangle \tag{3.3}$$

The S-matrix is in practice a time evolution operator, advancing a state from time negative infinity to time positive infinity. The initial state $|\Psi_i\rangle$ describes a state of n-particles infinitely separated from each other, each with some well defined quantum numbers (or some superposition of such states). The S-matrix acts on this state, advancing it by the time interval "2∞" defined by the limiting procedure. All the interactions between the particles are encoded in the S-matrix. The resulting state is then projected onto the final state $|\Psi_f\rangle$. The squared absolute value of this inner product is precisely the probability that the system will be at this final state at time ∞. For this probability to be normalized, the S-matrix must be a unitary operator. This is evidently so if the Hamiltonian H is a Hermitian operator.

Using (3.1), the unitarity of the S-matrix implies the following constraint on the T-matrix,

$$-i(T - T^\dagger) = T^\dagger T \tag{3.4}$$

If we contract this equation with some initial and final state and insert a complete set of states between the two operators on the right hand side, we obtain,

$$-i(\langle\Psi_f|T|\Psi_i\rangle - \langle\Psi_i|T|\Psi_f\rangle^*) = \sum_k \langle\Psi_k|T|\Psi_f\rangle^* \langle\Psi_k|T|\Psi_i\rangle \tag{3.5}$$

The sum over k should be understood in the broad sense as a sum over all possible final states, i.e. a sum over all possible numbers of final particles and all possible spins/flavors/ colors/charges (taking care of conservation laws), and an integration over all of phase space.

Using (3.2) this can be rewritten in terms of the amplitude,

$$\begin{aligned} -i\Big(\mathcal{M}(\{k_m\} \ \to \{p_m\}) - \mathcal{M}^*(\{p_m\} \to \{k_m\})\Big) = \\ \sum_k \mathcal{M}(\{p_n\} \to \{q_n\})\mathcal{M}^*(\{k_m\} \to \{q_m\})(2\pi)^4\delta^{(4)}(\sum_{m\in I} k_m - \sum_{m\in Q} q_m) \end{aligned} \tag{3.6}$$

where Q is the set of all particles in the final state k with momenta $\{q_m\}$. This expression is further multiplied on both sides by an overall momentum conserving delta function, $(2\pi)^4\delta^{(4)}(\sum_{m\in I} k_m - \sum_{m\in F} p_m)$.

If we now assume that the amplitude is invariant with respect to time reversal and adopt a short hand notation, we obtain the following simple unitarity identity,

$$2Im\mathcal{M}_{i\to f} = \sum_k \mathcal{M}^*_{f\to k}\mathcal{M}_{i\to k}(2\pi)^4\delta^{(4)}(i-k) \tag{3.7}$$

This identity becomes especially useful in perturbation theory where we can apply this equation order by order. We obtain a relation between lower order terms of amplitudes and the imaginary parts of higher order terms. Furthermore, the fact that we are dealing with amplitudes and not individual Feynman diagrams means that we do not have to consider the actual Feynman diagrams that make up the higher order term of the amplitude we are calculating. We simply need to identify the channel we are dealing with, i.e. the initial and final states, and then construct all the lower order amplitudes that could potentially contribute to the higher order term we seek to evaluate. To clarify this procedure, we will apply it to the one-loop (first order) contribution to the vacuum polarization amplitude.

3.1.1 Vacuum polarization - alternative approach

Let us calculate the Imaginary part of the first order correction to the vacuum polarization amplitude in QED using the prescription above [40]. The process is depicted in figure 3.1. According to (3.7), we should first identify the incoming and outgoing states i and f. In this simple case, those states are identical,

$$|i\rangle = |f\rangle = |p^\mu\rangle \tag{3.8}$$

We denote the single invariant in this process by $s \equiv p^2$. For a physical photon, $s = 0$. The next step would be to identify all possible states $|k\rangle$ such that the product of the amplitudes $\mathcal{M}(i \to k)$ and $\mathcal{M}(f \to k)$ would give a first order contribution in the fine structure constant $\alpha = \frac{e^2}{4\pi}$. The only possibility is a state of an outgoing fermion and anti-fermion, $|k\rangle = |k^\mu, \bar{k}^\mu\rangle$. Only the zeroth order Feynman diagram of these amplitudes will contribute, see figure 3.2.

Using the Feynman rules for QED, the contribution of this diagram to the amplitudes is:

$$\begin{aligned} i\mathcal{M}_{i\to k} &= \bar{u}(k)(-ie\gamma^\mu)v(\bar{k}) \\ i\mathcal{M}_{f\to k} &= \bar{u}(k)(-ie\gamma^\mu)v(\bar{k}) \Rightarrow i\mathcal{M}^*_{f\to k} = \bar{v}(\bar{k})(-ie\gamma^\mu)u(k) \end{aligned} \tag{3.9}$$

Finally, we sum over all possible states $|k\rangle$. This includes a sum over the spins of the fermions an a phase space integration under the constraint $\delta^{(4)}(i-k)$. First summing over spins using the completeness relations we obtain a trace of γ^μ matrices,

$$\begin{aligned} \sum_{spins} \mathcal{M}^*_{f\to k}\mathcal{M}_{i\to k} &= \sum_{spins} (-\bar{u}(k)e\gamma^\nu v(\bar{k}))(-\bar{v}(\bar{k})e\gamma^\mu u(k)) \\ &= e^2 tr[(\not{k}+m)\gamma^\nu(\not{\bar{k}}-m)\gamma^\mu] \\ &= 4e^2[k^\nu\bar{k}^\mu + k^\mu\bar{k}^\nu - k\cdot\bar{k}g^{\mu\nu} - m^2 g^{\mu\nu}] \end{aligned} \tag{3.10}$$

Applying the momentum conserving delta ($k+\bar{k}=p$) and the on-shellness of the momenta k and $\bar{k}$ yields the relation $p^2 = s = (k+\bar{k})^2 = 2(m^2 + k\cdot\bar{k})$. The sum over the spins reduces to,

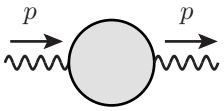

Figure 3.1: First order correction to the vacuum polarization amplitude.

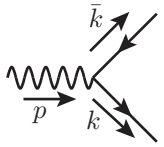

Figure 3.2: Feynman diagram contributing to the first order correction of the vacuum polarization amplitude in the unitarity method.

$$\sum_{spins} \mathcal{M}^*_{f\to k}\mathcal{M}_{i\to k} = 4e^2[k^\nu \bar{k}^\mu + k^\mu \bar{k}^\nu - \frac{s}{2}g^{\mu\nu}] \tag{3.11}$$

The phase space integral will produce the desired imaginary part of the vacuum polarization amplitude,

$$2Im\mathcal{M}_{i\to f} = \int \frac{d^3k}{(2\pi)^3 2k^0}\int \frac{d^3\bar{k}}{(2\pi)^3 2\bar{k}^0}(2\pi)^4\delta^{(4)}(p-k-\bar{k})4e^2[k^\nu \bar{k}^\mu + k^\mu \bar{k}^\nu - \frac{s}{2}g^{\mu\nu}] \tag{3.12}$$

To perform the integral over $\bar{k}$, it is more convenient to switch to a four dimensional integral,

$$\int \frac{d^3\bar{k}}{(2\pi)^3 2\bar{k}^0} \to \int \frac{d^4\bar{k}}{(2\pi)^4} 2\pi\delta(\bar{k}^2 - m^2)\theta(\bar{k}^0) \tag{3.13}$$

Applying $\delta^{(4)}(p-k-\bar{k})$ simply means removing the integral over $\bar{k}$ and replacing $\bar{k} \to p-k$. We do this implicitly.

Next, we perform the spatial k integral which is better done in spherical coordinates. As a first step we rewrite $\delta(\bar{k}^2 - m^2)$ in terms of the magnitude of the spatial momentum,

$$\begin{aligned}\delta(\bar{k}^2 - m^2) &= \delta((\bar{k}^0)^2 - \vec{\bar{k}} - m^2) = \delta((p^0-k^0)^2 - (\vec{p}-\vec{k}) - m^2) \\ &= \delta((p^0-k^0)^2 - \vec{p}^2 - \vec{k}^2 + 2|\vec{p}||\vec{k}|\cos\theta - m^2) \\ &= \frac{1}{|(-2|\vec{k}| + 2|\vec{p}|\cos\theta)|}\,\delta(|\vec{k}| - |\vec{k}|')\end{aligned} \tag{3.14}$$

where $|\vec{k}|'$ solves the equation $\bar{k}^2 - m^2 = 0$ for $\bar{k}^0 > 0$. In spherical coordinates, the measure changes according to $d^3k \to |\vec{k}|^2 d|\vec{k}|d\Omega$. So far we have,

$$2Im\mathcal{M}_{i\to f} = \frac{e^2}{8\pi^3}\int d|\vec{k}|d\Omega \frac{|\vec{k}|^2}{k^0|(-|\vec{k}| + |\vec{p}|\cos\theta)|}\delta(|\vec{k}| - |\vec{k}|')[k^\nu \bar{k}^\mu + k^\mu \bar{k}^\nu - \frac{s}{2}g^{\mu\nu}] \tag{3.15}$$

The first factor of the integrand is a constant since all quantities have been constrained by the delta functions used so far. To see this, it is best to choose the center of mass frame and re-express this quantity in terms of Lorentz invariant quantities, namely s and m. Since the photon is off shell, i.e. "massive" with mass $\sqrt{s}$, we can boost the system to its rest frame, i.e. $p = (\sqrt{s}, 0, 0, 0)$. It then follows that $k = (\frac{\sqrt{s}}{2}, \sqrt{\frac{s}{4} - m^2}, 0, 0)$ and $\bar{k} = (\frac{\sqrt{s}}{2}, -\sqrt{\frac{s}{4} - m^2}, 0, 0)$ in a properly rotated frame of reference. We obtain the Lorentz invariant quantity which is independent of the remaining integration variables,

$$\frac{|\vec{k}|^2}{k^0(|-|\vec{k}| + |\vec{p}|\cos\theta|)} = \frac{\frac{s}{4} - m^2}{\frac{\sqrt{s}}{2}\sqrt{\frac{s}{4} - m^2}} = \sqrt{1 - \frac{4m^2}{s}} \tag{3.16}$$

We are left with only an angular integration,

$$\begin{aligned} 2Im\mathcal{M}_{t\to t} &= 2\alpha\sqrt{1-\frac{4m^2}{s}}\int\frac{d\Omega}{4\pi^2}[k^\nu\bar{k}^\mu+k^\mu\bar{k}^\nu-\frac{s}{2}g^{\mu\nu}] \\ &= 2\alpha\sqrt{1-\frac{4m^2}{s}}T^{\mu\nu} \end{aligned} \tag{3.17}$$

where $\alpha=\frac{e^2}{4\pi}$ and $T^{\mu\nu}=\int\frac{d\Omega}{4\pi}[k^\nu\bar{k}^\mu+k^\mu\bar{k}^\nu-\frac{s}{2}g^{\mu\nu}]$ is a Lorentz tensor which can only depend on p^μ and on the metric. Its most general form is,

$$T^{\mu\nu}=Ap^\mu p^\nu+Bg^{\mu\nu} \tag{3.18}$$

We can contract $T^{\mu\nu}$ in both representations,

$$\begin{aligned} p_\mu p_\nu T^{\mu\nu} &= As^2+Bs=\int\frac{d\Omega}{4\pi}(2p\cdot kp\cdot\bar{k}-\frac{s^2}{2})=0 \\ g_{\mu\nu}T^{\mu\nu} &= As+4B=\int\frac{d\Omega}{4\pi}(2k\cdot\bar{k}-2s)=(-s-2m^2)\int\frac{d\Omega}{4\pi}=-s-2m^2 \end{aligned} \tag{3.19}$$

where we used the following kinematic relations,

$$\begin{aligned} k^2=m^2=(p-\bar{k})^2=s+m^2-2p\cdot\bar{k}\to p\cdot\bar{k}=\frac{1}{2}s \\ \bar{k}^2=m^2=(p-k)^2=s+m^2-2p\cdot k\to p\cdot k=\frac{1}{2}s \\ s=p^2=(k+\bar{k})^2=2m^2+2k\cdot\bar{k}\to k\cdot\bar{k}=\frac{s}{2}-m^2 \end{aligned} \tag{3.20}$$

The coefficients A and B can be easily solved,

$$A=-\frac{B}{s}=-1-\frac{2m^2}{s}-4\frac{B}{s}\quad\to\quad B=-\frac{s}{3}(1+\frac{2m^2}{s}),\quad A=\frac{1}{3}(1+\frac{2m^2}{s}) \tag{3.21}$$

Yielding,

$$T^{\mu\nu}=\frac{1}{3}(1+\frac{2m^2}{s})(p^\mu p^\nu-sg^{\mu\nu}) \tag{3.22}$$

The imaginary part of the first order correction to the vacuum polarization amplitude is,

$$Im\mathcal{M}_{i\to f}=\underbrace{\alpha\sqrt{1-\frac{4m^2}{s}}\frac{1}{3}(1+\frac{2m^2}{s})}_{\equiv Im\,\Pi(s)}(p^\mu p^\nu-sg^{\mu\nu})=Im\Pi(s)(p^\mu p^\nu-sg^{\mu\nu}) \tag{3.23}$$

This agrees with the straightforward calculation (2.52). To show this, we write the $\arccos$ function as a real and imaginary part [41],

$$\sin^{-1} z = k\pi + (-1)^k \sin^{-1} \beta_- + (-1)^k i \ln[\alpha_+ + \sqrt{\alpha_+^2 - 1}] \tag{3.24}$$
$$\text{with } \; k \in \mathbb{Z}, \quad \alpha_\pm = \frac{1}{2}\sqrt{(x+1)^2 + y^2} \pm \frac{1}{2}\sqrt{(x-1)^2 + y^2}, \quad z = x + iy$$

Taking z to be real and along the branch cut of (2.52) (at $z > 1$), (3.23) is recovered.

This example illustrates the procedure of obtaining higher order corrections by "gluing" lower order terms, the gluing being a summation over intermediate states and a phase space integration. In this example, the unitary method does not reduce the amount of work since there is only one Feynman diagram contributing to the first order correction of the amplitude, namely the bubble diagram with a fermion propagating in the loop. As the number of external legs of amplitudes grows, the number of Feynman diagrams increases drastically, and the unitarity method proves to be very powerful. Such an example will be treated in detail in chapter 6.

3.2 Dispersion Relations

Before the advent of QCD, dispersion relations constituted a main tool in tackling strong interaction processes which could not be treated perturbatively [39]. By studying the analytical properties of arbitrary order Feynman diagrams, one could extract information about the imaginary parts of decay and scattering amplitudes. Dispersion relations were then used to deduce the full amplitude from its imaginary part. We will first review this method and then apply it to the result of the previous section to obtain the full amplitude of the vacuum polarization amplitude.

Consider a function $F(z)$ which is analytic in the entire complex plane, except for a branch cut along the real axis starting at a point M. We can draw a contour circumventing the branch cut as depicted in figure 3.3. By Cauchy's theorem, the following holds,

$$F(z) = \frac{1}{2\pi i} \int_C dz' \frac{F(z')}{z' - z} \tag{3.25}$$

where z is some point located away from the branch cut.

By Schwarz's reflection principle [42], since $F(z)$ is analytic in the upper half complex plane and real on the real line in the interval $Re z < M$, then $F(z)$ can be analytically continued to the lower half plane with $F(z) = \overline{F(\overline{z})}$ for $Im\ z < 0$. Let y be a point along the branch cut of $F(z)$. Above and below the branch cut,

$$F(y+i\epsilon) = ReF(y+i\epsilon) + iImF(y+i\epsilon)$$
$$F(y-i\epsilon) = ReF(y+i\epsilon) - iImF(y+i\epsilon) \tag{3.26}$$

The imaginary part along the branch cut is given by the limit,

$$2iImF(y) = \lim_{\epsilon\to 0}(F(y+i\epsilon) - F(y-i\epsilon)) \tag{3.27}$$

Performing the Cauchy integral, one obtains,

$$\begin{aligned} F(z) &= \frac{1}{2\pi i}\int_M^\infty dz' \frac{F(z'+i\epsilon) - F(z'-i\epsilon)}{z'-z} + C_\infty \\ &= \frac{1}{\pi}\int_M^\infty dz' \frac{ImF(z')}{z'-z-i\epsilon} + \frac{1}{2\pi i}\int_{|z'|=\infty} dz' \frac{F(z')}{z'-z} \end{aligned} \tag{3.28}$$

This formula holds as long as the integral along the infinite circle, C_∞, vanishes. If the integrand does not decay fast enough, one can subtract the value of the integral at some point z_0 in the analytical region [40],

$$F(z) - F(z_0) = \frac{z-z+0}{\pi}\int_M^\infty \frac{dz'}{z'-z_0}\frac{ImF(z')}{z'-z-i\epsilon} + \frac{z-z_0}{2\pi i}\int_{|z'|=\infty} dz' \frac{F(z')}{(z'-z)(z'-z_0)} \tag{3.29}$$

We will see that this subtraction scheme is analogous to the renormalization subtraction

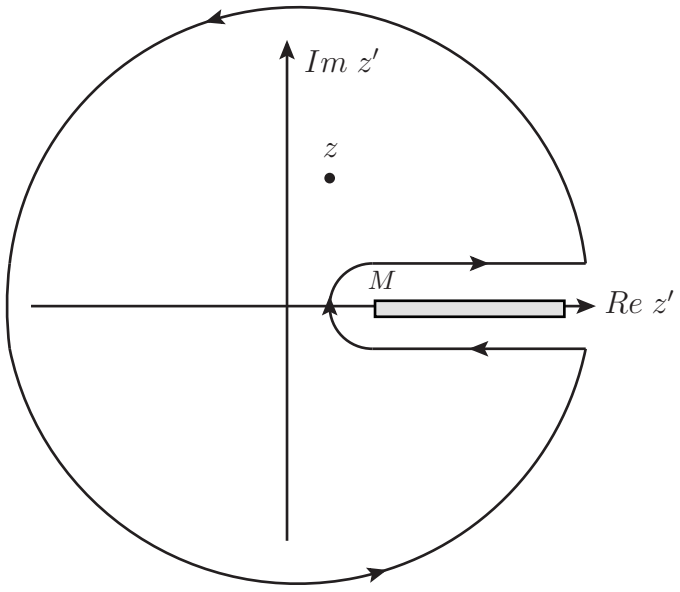

Figure 3.3: The complex function $F(z)$ has a branch cut along the real axis starting at M. Cauchy's therem can be used to calculate the value of the function at every point from the knowledge of the imaginary part along the branch cut

scheme in the following example. If C_∞ converges, the integral is finite and does not require working in dimensional regularization.

3.2.1 Vacuum polarization - extracting the full amplitude

We use the once subtracted dispersion relation (3.29) to complete the calculation of the vacuum polarization amplitude, i.e. extract the full expression for Π from it's imaginary part. Our starting point is,

$$\hat{\Pi}(s) = \Pi(s) - \Pi(0) = \frac{s}{\pi}\int_{4m^2}^{\infty}\frac{ds'}{s'}\frac{Im\Pi(s)}{s'-s-i\epsilon} \tag{3.30}$$

This integral can be solved by a series of substitutions. The initial integral is,

$$\int_{4m^2}^{\infty} ds'(1+\frac{2m^2}{s'})\sqrt{1-\frac{4m^2}{s'}}\frac{1}{s'}\frac{1}{s'-s} \tag{3.31}$$

Substitute $x = \frac{s'}{4m^2}$ and denote $r = \frac{s}{4m^2}$,

$$\frac{1}{4m^2}\int_1^{\infty}\frac{dx}{x}\frac{1}{x-r}\left(1+\frac{1}{2x}\right)\sqrt{1-\frac{1}{x}} \tag{3.32}$$

Next substitute $z = 1-\frac{1}{x}$, so $x = \frac{1}{1-z}$ and $dx = \frac{dz}{(1-z)^2}$,

$$\begin{aligned}\frac{1}{4m^2}\int_0^1\frac{dz}{1-z}\frac{1}{\frac{1}{1-z}-r}(1+\frac{1}{2}(1-z))\sqrt{z} &= \frac{1}{4m^2}\int_0^1 dz\frac{\cancel{(1-z)}(\frac{3}{2}-\frac{1}{2}z)\sqrt{z}}{\cancel{(1-z)}((1-r)+rz)} \\ &= \frac{1}{8m^2}\frac{1}{1-r}\int_0^1 dz\frac{3\sqrt{z}-z^{3/2}}{1+\frac{r}{1-r}z}\end{aligned} \tag{3.33}$$

Then substitute $y = \frac{r}{1-r}z$,

$$\frac{1}{8m^2 r}\int_0^{\frac{r}{1-r}} dy\left[3\left(\frac{1-r}{r}\right)^{1/2}\frac{\sqrt{y}}{1+y} - \left(\frac{1-r}{r}\right)^{3/2}\frac{y^{3/2}}{1+y}\right] \tag{3.34}$$

Substitute $1+y=t$, so the upper boundary becomes $\frac{1}{1-r}$,

$$\frac{1}{8m^2 r}\int_1^{\frac{1}{1-r}} dt\left[3\left(\frac{1-r}{r}\right)^{1/2}\frac{\sqrt{t-1}}{t} - \left(\frac{1-r}{r}\right)^{3/2}\frac{(t-1)^{3/2}}{t}\right] \tag{3.35}$$

The second term can be written in terms of the first term as follows,

$$\int dt\frac{(t-1)^{3/2}}{t}=\int dt\frac{\sqrt{t-1}(t-1)}{t}=\int dt\sqrt{t-1}-\int dt\frac{\sqrt{t-1}}{t}=\frac{2}{3}(t-1)^{3/2}-\int dt\frac{\sqrt{t-1}}{t} \tag{3.36}$$

The integral reduces to,

$$\frac{1}{8m^2r}\left\{\int_1^{\frac{1}{1-r}}dt\left[3\left(\frac{1-r}{r}\right)^{1/2}+\left(\frac{1-r}{r}\right)^{3/2}\right]\frac{\sqrt{t-1}}{t}-\underbrace{\frac{2}{3}\left(\frac{1-r}{r}\right)^{3/2}(t-1)^{3/2}/_1^{\frac{1}{1-r}}}_{=\frac{2}{3}}\right\} \tag{3.37}$$

The remaining integral can then be evaluated by making the substitution $u=\sqrt{t-1}$ and $du=\frac{1}{2}\frac{dt}{\sqrt{t-1}}$, so $t=1+u^2$,

$$\begin{aligned}\int dt\frac{\sqrt{t-1}}{t}&=\int dt\frac{t-1}{t\sqrt{t-1}}=\int\frac{dt}{\sqrt{t-1}}-\int dt\frac{1}{t\sqrt{t-1}}=2\sqrt{t-1}-\int dt\frac{1}{t\sqrt{t-1}}\\&=2\sqrt{t-1}-2\int\frac{2du}{1+u^2}=2\sqrt{t-1}-2\arctan\sqrt{t-1}\end{aligned} \tag{3.38}$$

And the integral is,

$$\begin{aligned}&\frac{1}{8m^2r}\left\{\left[3\left(\frac{1-r}{r}\right)^{1/2}+\left(\frac{1-r}{r}\right)^{3/2}\right](2\sqrt{t-1}-2\arctan\sqrt{t-1})/_1^{\frac{1}{1-r}}-\frac{2}{3}\right\}\\&=\frac{1}{8m^2r}\left\{\sqrt{\frac{1}{r}-1}\left(2+\frac{1}{r}\right)\left(2\sqrt{\frac{r}{1-r}}-2\arctan\sqrt{\frac{r}{1-r}}\right)-\frac{2}{3}\right\}\\&=\frac{1}{8m^2r}\left\{4+\frac{2}{r}-\frac{2}{3}-2\left(2+\frac{1}{r}\right)\sqrt{\frac{1}{r}-1}\arctan\sqrt{\frac{r}{1-r}}\right\}\\&=\frac{1}{s}\left\{\frac{5}{3}+\frac{1}{r}-\left(2+\frac{1}{r}\right)\sqrt{\frac{1}{r}-1}\arcsin\sqrt{r}\right\}\end{aligned} \tag{3.39}$$

where in the last step we used that $\arctan\sqrt{\frac{r}{1-r}}=\arcsin\sqrt{r}$. Inserting the integral into 3.30, the final renormalized Π is,

$$\hat{\Pi}(s)=\frac{\alpha}{3\pi}\left(\frac{5}{3}+\frac{1}{r}-\left(2+\frac{1}{r}\right)\sqrt{\frac{1}{r}-1}\arcsin\sqrt{r}\right) \tag{3.40}$$

Both methods yield an identical renormalized answer, where in the unitarity method it was not necessary to use any regularization recipe since our prescription leads us directly to the renormalized answer. There is one subtlety we must remark on, namely the ambiguity embedded in the unitarity method. Terms in the amplitude that do not contain branch cuts will not appear in the unitarity cut, and consequently will not be recovered by the dispersion relation. In our original calculation of the vacuum polarization amplitude (2.52), we had an

additional term $\ln m^2$. At that point, we decided to take advantage of the freedom in choosing our renormalization subtraction term and absorb it, but we could have chosen otherwise. The unitarity method, on the other hand, is blind to this term, a fact which obstructed this method from becoming a main calculational tool. In section 3.4 an alternative approach to unitarity is presented, one which manages to avoid this ambiguity in many cases.

3.3 Landau Equations and Cutkosky Rules

We have seen in the previous example that branch cuts could appear in an amplitude in physical values of the kinematic variables. These branch cuts could show up in the form of a log function, a square root or any other multi-valued complex function. This feature is in fact a general property of Feynman integrals. Landau [10] has put forth a set of equations allowing us to determine the location of such branch points, from which branch cuts extend. Subsequently, Cutkosky [9] has proposed a more general formulation of the unitarity method to determine the discontinuity along these branch cuts.

Consider an arbitrary n-loop Feynman integral with v-internal legs, after the introduction of Feynman parameters as in (2.2). Leaving out the loop momenta integrations, the integral takes the form,

$$(v-1)!\int_0^1 da_1...da_v\delta(1-\sum_i a_i)\frac{\mathcal{N}(l_i,m_i)}{J^v}, \qquad J=a_1d_1+...+a_vd_v, \qquad d_i=l_i^2-m_i^2 \quad (3.41)$$

To determine the singularities (see the original paper [10] or a slightly modified proof in [39]), one considers the diagram corresponding to this integral and then separately all reduced diagrams. By reduced diagrams, we refer to diagrams in which one or more of the internal legs are absent (which is equivalent to setting the corresponding a_is to zero). In each case, all internal legs are set to be on shell, i.e. all particles circulating in the loop are taken to be physical,

$$d_i=l_i^2-m_i^2=0, \qquad \forall\ i \text{ in the (reduced) diagram} \quad (3.42)$$

Under these conditions, one has to solve the equation,

$$\sum_i a_i l_i=0 \quad \text{(summing over lines in the diagram in consideration)} \quad (3.43)$$

taking into account that the a_i's are real and positive (the condition that $\sum_i a_i=1$ is not necessary). Landau has made the following analogy. If the direction of each vector l_i is the direction of a force i and $a_i|l_i|$ is the magnitude of this force, then one must find the point

of equilibrium. (3.42) and (3.43) are known as the Landau equations. Their solutions will produce points or surfaces in the space of external kinematic variables where singularities will occur. This takes place at the edge of the subspace of external variables in which J is positive. When J is positive definite for all positive values of the a_i's, the integral is analytic and no branch cuts occur. When the kinematic variables reach values that allow J to vanish at some values of the Feynman parameters, the integral will be singular yielding the branch point. This singularity cannot be avoided by shifting the integration contour because the singularity either occurs at the end points of the integration contour or it pinches the contour from both sides (see [39]). In the subspace where J can become negative, singularities can be avoided by such a shift of the contour. In this last case, the integral develops an imaginary part and branch cuts appear.

Cutkosky Rules

Based on the above analysis of Landau, Cutkosky has proved that the discontinuity along the branch cut can be calculated by replacing a subset of propagators with on-shell delta functions,

$$\text{Disc } I\big|_{m\ cut} = (2\pi i)^m \int \prod_{i=1}^{L} \left(\frac{d^4 k_i}{(2\pi)^4}\right) \delta_+(l_1^2 - m_1^2) \cdots \delta_+(l_m^2 - m_m^2) \frac{\mathcal{N}}{d_{m+1} \cdots d_v} \tag{3.44}$$

where the Integral I has L loops and v internal lines. The m cut refers to choosing m internal lines which will be cut, i.e. their propagators will be replaced by delta functions placing those particles on shell. This formula will reproduce the discontinuity along branch cuts of certain external invariants, namely invariants constructed out of the total momenta between two cut propagators. By δ_+ we mean that only the proper root must be considered, i.e. one chooses a certain flow of momentum through the diagram representing the integral, and only the root corresponding to this choice is applied.

For example consider the integral in figure 3.4. Three propagators have been cut, i.e. placed on shell. Assume all external momenta are outgoing. Between cut 1 and 2 flows momentum k_1+k_2 from which we construct the invariant $s_{12} = (k_1+k_2)^2$. Any discontinuities of branch cuts in the space of these invariants (e.g. the imaginary part of $\ln s_{12}$) will be found by applying (3.44) to this set of cuts. Similarly, the same formula will isolate branch cuts of k_3^2 and $s_{45} = (k_4 + k_5)^2$.

The same rules can be applied at the amplitude level. In this case a cut is performed on the sum of all contributing diagrams, each diagram consisting of one or more integrals. In this case, to determine which branch cuts are being isolated and which not, one must perform the same analysis illustrated in the example above on each integral. An example of a double cut on a 4-point amplitude is worked out in detail in chapter 6.

Cutkosky demonstrated that this formula is in fact a generalization of the unitarity formula described in the beginning of this chapter. Removing two propagators in the sum of all diagrams contributing to an amplitude reproduces the unitarity formula. A larger number of cuts, such as in figure 3.4, can be viewed as a "generalized unitarity" condition. In the case of three cuts for example, we glue three lower order amplitudes to reproduce a higher order one. The application of generalized unitarity is discussed in [13].

3.4 Modern Approach to Unitarity

Using a different approach in the application of unitarity, it is possible to reconstruct both real (dispersive) and imaginary (absorptive) parts at once, thus circumventing the need for dispersion relations. This approach involves expanding the amplitude in a basis of integrals, and then making use of unitarity [13] to determine the expansion coefficients.

Given a 1-loop amplitude, the Passarino-Veltman procedure can be used to reduce any tensor integral to a sum of scalar integrals with tensorial coefficients. These coefficients will depend only on external momenta, masses, coupling constants and the metric. The scalar integrals will correspond to either the integral containing one propagator for each line in the loop or to reduced integrals with any number of these legs missing (put differently, the missing legs are contracted to a point). For example, in a four point process we could encounter one box integral, four triangle integrals corresponding to four possible contractions, six bubble integral and four tadpoles.

Let I_i be such a set of scalar integrals. A 1-loop amplitude can be expanded as follows,

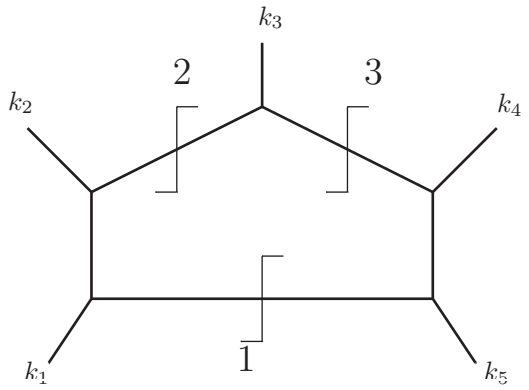

Figure 3.4: Example of three cuts in a 5-point one-loop integral.

$$A_n^{1-loop} = \sum_i c_i I_i \tag{3.45}$$

Our goal is to calculate the coefficients c_i. Once completed, the desired amplitude is fully known. We have seen that using unitarity, the imaginary part of this amplitude can be calculated as follows,

$$2ImA_n^{1-loop} = \sum_{helicity} \int \frac{d^d l_1}{(2\pi)^d} 2\pi\delta^{(+)}(l_1^2 - m^2) A_{n-j+2}^{tree}(left) 2\pi\delta^{(+)}(l_2^2 - m^2) A_{j+2}^{tree}(right) \tag{3.46}$$

where j is the number of lines to the right of the cut, l_1 and l_2 are the momenta flowing through the cut lines (only one of them is independent), and *right* / *left* refer to the tree amplitudes to the right / left of the cut. The $+$ sign in the delta function means that only momenta corresponding to a physical scattering process must be considered.

This expression, or alternatively the discussion of the Cutkosky rules earlier in the chapter, demonstrates that cutting means replacing propagators with delta functions thus imposing on-shellness,

$$\frac{i}{p^2 - m^2 + i\epsilon} \to 2\pi\delta^{(+)}(p^2 - m^2) \tag{3.47}$$

In order to extract the sought after coefficients c_i, we perform such a cut of two propagators on both sides of (3.45). When performed on the right hand side of the equation, the cut amounts to removing all integrals that do not contain the two cut legs, and in the remaining integrals, replacing the two propagators with appropriate delta functions.

When performing the cut on the left hand side, equation (3.46) is obtained. In this case, the relevant tree amplitudes must be explicitly calculated. This will result in a sum of tensor integrals that can be subsequently reduced using the Passarino-Veltman reduction. This reduction involves re-expressing powers of the loop momentum (contracted with external momenta) with sums over inverse propagators and masses. These inverse propagators, in turn, cancel out with the actual propagators, with one exception. If the inverse propagator corresponds to one of the cut lines, it does not cancel with any propagator but is set to zero by the delta function appearing in (3.46).

A more elegant way (mathematically less sound, but justified by the above procedure) of performing the cut of the left hand side is to upgrade the delta functions to propagators,

$$2\pi\delta^{(+)}(p^2 - m^2) \to \frac{i}{p^2 - m^2 + i\epsilon} \tag{3.48}$$

perform the Passarino-Veltman reduction in the normal way, and then identify the basis integrals in the resulting expression. If an integral appears that does not contain the cut

propagators, this integral must be disregarded (corresponding to setting inverse propagators to zero, as described above). In this case, (3.46) takes the form,

$$A_n^{1-loop}\big|_{cut} = \sum_{helicity} \int \frac{d^d l_1}{(2\pi)^d} \frac{i}{l_1^2 - m^2} A^{tree}_{n-j+2}(left) \frac{i}{l_2^2 - m^2} A^{tree}_{j+2}(right)\big|_{cut} \tag{3.49}$$

Once the cut has been performed, the coefficients of all the integrals on the right hand side of 3.45 that survive the cut are uniquely determined. This procedure is then repeated with as many cuts necessary to determine all the coefficients. Note that coefficients of integrals that do not contain any cuts cannot be determined by this method. These are referred to as rational functions, or the rational part of the amplitude. For example, in the above example of a four point amplitude, the bubble integral corresponding to a contraction of two adjacent legs can only depend on the square of a single momentum (the mass of the external leg caught between the two non contracted lines). If this momentum is massless, the integral does not contain any cuts. To determine these coefficients, other methods such as known IR or UV behavior of the amplitude [43] must be applied.

CHAPTER 4

QCD and One-Loop Methods

Brute force calculations of amplitudes in quantum field theory tend to become less and less manageable as we either increase the number of external legs or increase the order in perturbation theory. In both cases the number of Feynman diagrams grows drastically for each external leg or loop added. Working with a non-Abelian gauge theory, such as QCD, enhances the problem considerably. Two new types of vertices appear that do not exist in Abelian theories such as QED, namely the three- and four-boson vertices. These vertices contain six terms (see appendix A), and thus expressions will typically contain 6^v terms, where v is the number of boson vertices in the diagram.

This chapter introduces two methods commonly used to simplify QCD amplitudes. *Color decomposition* is used to factorize the amplitude into color content and "the rest". The color content appears in the form of group generators and group structure constants, while "the rest" includes all kinematic and spin/helicity information. The amplitude becomes, in practice, a sum of products of color matrices (i.e. group generators) with coefficients which are referred to as *partial amplitudes*. These color-stripped amplitudes are gauge invariant (or a sum of gauge invariant pieces) and generally more compact than the full amplitude.

When calculating a QCD amplitude involving external gluons, we must in general specify the color (in the adjoint representation), helicity and momentum of the gluon, and this is accomplished by contracting the amplitude with polarization vectors. Specifying color and helicity is in general just an intermediate step toward a calculation of some final observable.

These are then summed over since they are experimentally inaccessible. Color is "stripped off" the amplitude by applying the color decomposition described above. To deal with helicity, one uses the *Spinor helicity* method of representing (colorless) polarization vectors in terms of spinor products. This unifies the formalism of helicity with that of other spinor quantities (e.g. Dirac gamma matrices, external fermions), and various spinor product identities can be used to manipulate and simplify the amplitude in a relatively straightforward way.

4.1 Color Decomposition

4.1.1 Partial and primitive amplitudes

In QCD we define a multiplet of massive spin-half quark fields (Dirac spinors) that transform under the fundamental representation of the group $SU(3)$. To upgrade global invariance to local invariance, we define gauge fields that transform under the adjoint representation of the same group. From these we construct a covariant derivative from which we can then freely build gauge invariant terms in the theory's action. This construction gives rise to the QCD Feynman rules (see appendix A): three- and four- gluon vertex, quark-antiquark-gluon vertex and propagators for both types of particles.

In the following discussion we will consider the more general case of $SU(N_c)$. This will make the dependence on the number of colors (i.e. N_c) more apparent. We will follow the conventions of reviews [7, 44, 6]. The generators of the fundamental representation will be normalized as follows,

$$(ab) := Tr(T^a T^b) = \delta^{ab} \tag{4.1}$$

where this shorthand notation for a trace over *color matrices* (i.e. fundamental representation generators) will be used throughout the chapter. Note that this normalization differs from the conventional normalization by a factor of $\frac{1}{\sqrt{2}}$. The dimension of the group $SU(N_c)$ is $N_c^2 - 1$, while the dimension of the fundamental representation is N_c.

The generators of $SU(N_c)$ satisfy the commutation relations,

$$[T^a, T^b] = i\sqrt{2} f^{abc} T^c \tag{4.2}$$

f^{abc} are the structure constants of $SU(N_c)$ and define the group. In addition, they themselves satisfy the above group relation when viewed as a set of $N_c^2 - 1$ matrices of dimension $N_c^2 - 1$. These matrices form the adjoint representation.

Quark-antiquark-gluon vertices contain a factor $(T^a)_i^{\bar{j}}$, where a is an adjoint index and contracts with the gluon, while i and $\bar{j}$ are fundamental indices and contract with the quark

and antiquark, respectively. Three-gluon vertices contain a factor f^{abc}, where all three indices are adjoint and contract with the three gluons. Similarly, a four gluon vertex contains a factor $f^{abe}f^{cde}$. For each External gluon or quark, one of these indices remains free, all other indices are contracted.

The color decomposition, in essence, involves applying the following two identities,

$$f^{abc} = -\frac{i}{\sqrt{2}}\left(Tr(T^aT^bT^c) - Tr(T^aT^cT^b)\right) \tag{4.3}$$

$$(T^a)^{\bar{j}}_i(T^a)^{\bar{l}}_k = \delta^{\bar{l}}_i\delta^{\bar{j}}_k - \frac{1}{N_c}\delta^{\bar{j}}_i\delta^{\bar{l}}_k \tag{4.4}$$

The first identity is just 4.2 rewritten. The second identity, known as Fierz rearrangement, follows from the fact that the generators of the fundamental representation form a complete set of traceless hermitian $N_c \times N_c$ matrices. The term proportional to $\frac{1}{N_c}$ enforces the tracelesness.

A useful trick when dealing with diagrams that contain only particles that transform under the adjoint representation is to substitute the group $SU(N_c)$ with $U(N_c)$. In this case, the term proportional to $\frac{1}{N_c}$ drops, since the set of generators of this group includes a generator proportional to the unit matrix in addition to the generators of $SU(N_c)$. This is in fact the generator of the subgroup $U(1)$ representing a "photon" particle (with a different coupling constant than the QED photon). Since this matrix commutes with all others, all structure constants containing it will be zero, and it effectively decouples from $SU(N_c)$. This reflects the fact that photons do not self interact nor do they interact with other gauge bosons. To summarize, given a gluon only diagram, we can effectively work with the group $U(N_c)$ and ignore the term proportional to $\frac{1}{N_c}$ in the Fierz rearrangement identity.

It is often easier to visualize the Fierz rearrangement in the following form, where X,Y,Z and W are strings of color matrices and a is some single color matrix,

$$..XaY..\ \ ..ZaW.. = ..XW..\ \ ..ZY.. - \frac{1}{N_c}..XY..\ \ ..ZW.. \tag{4.5}$$

Identities (4.3) and (4.4) can be used to remove all structure constants and contractions of color matrices from the initial expression obtained from a Feynman diagram. The color content of a diagram will be reduced to traces over color matrices, strings of color matrices terminating with fundamental indices (e.g. $(T^aT^bT^c)^{\bar{j}}_i$ or products of such. To clarify the procedure, let us take a look at an example of a tree amplitude.

Four gluon tree amplitude - example

Consider a scattering process involving four gluons, and consider the Feynman diagram of the 1-4-channel depicted in figure 4.1. Let us color decompose it using (4.3) and (4.4).

The contribution of this channel to the amplitude is,

$$\begin{aligned} A_4^{tree}|_{14} &= g^2 \tilde{A}_4^{part}|_{14} f^{145} f^{532} \\ &= g^2 \tilde{A}_4^{part}|_{14} \left(-\frac{i}{\sqrt{2}}\right)^2 [(145)-(154)][(532)-(523)] \\ &= g^2 \tilde{A}_4^{part}|_{14} \left(-\frac{i}{\sqrt{2}}\right)^2 [(1234)+(4321)-(1324)-(4231)] \end{aligned} \tag{4.6}$$

where the numbers appearing in the trace and in the structure constants are the color indices of gluons as numbered in figure 4.1, and,

$$\begin{aligned} \tilde{A}_4^{part}|_{14} = & \left(-\frac{i}{k_5^2+i\epsilon}\right) \left(g^{14}(k_1-k_4)^5 + g^{45}(k_4+k_5)^1 + g^{51}(-k_5-k_1)^4\right) \\ & \times \left(g^{53}(k_5-k_3)^2 + g^{32}(k_3-k_2)^5 + g^{25}(k_2-k_5)^3\right) \epsilon_1\epsilon_2\epsilon_3\epsilon_4 \end{aligned} \tag{4.7}$$

Note that the terms proportional to $\frac{1}{N_c}$ drop out explicitly. This was expected since this diagram contains only adjoint particles and we could have simply used the Fierz rearrangement for $U(N_c)$ as explained above. (4.6) is the color decomposition of the diagram in figure 4.1. It is a sum of four terms, each term being a product of a color factor containing only color matrices and a *partial amplitude* containing all the kinematic and helicity information.

Only specific color traces appear in this expression, namely those that match the clockwise order of the external legs of the diagram when the diagram is restricted to be planar. For example, the trace (1324) corresponds to rotating the two legs on the right which results in an identical diagram. The trace (3124), on the other hand, does not appear since this diagram cannot be brought to the proper ordering and be kept planar at the same time. Note

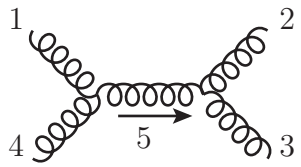

Figure 4.1: One of the three Feynman diagrams contributing to the full tree amplitude of the four gluon scattering process. All external momenta are taken to be incoming. For brevity, the gluon number is used as both the color and Lorentz index of the gluon. We will denote by k_i the momentum of gluon line i.

that two of the traces have a relative minus sign. These originate from the sensitivity of the Feynman rule of three gluons to the ordering of the legs once we strip off the color factor f^{abc}. We will absorb these minus signs and the factor of $\frac{i}{\sqrt{2}}$ in the partial amplitude. We must then have a separate partial amplitude corresponding to each trace. The amplitude takes the form,

$$\begin{aligned} A_4^{tree}|_{14} = \; & g^2\Big[(1234)A_4^{part}|_{14}(1,2,3,4) + (4321)A_4^{part}|_{14}(4,3,2,1) \\ & +(1324)A_4^{part}|_{14}(1,3,2,4) + (4231)A_4^{part}|_{14}(4,2,3,1)\Big] \end{aligned} \tag{4.8}$$

The modified partial amplitudes are calculated using the *color ordered Feynman rule* in figure 4.2, where the color factor has been stripped off. In each case, the legs are ordered clockwise according to the arguments of the partial amplitude. This generates the proper sign. The partial amplitudes (with the contribution of the 1-4-channel only) are,

$$\begin{aligned} A_4^{part}|_{14}(1,2,3,4) = & \left(\frac{i}{\sqrt{2}}\right)^2\left(-\frac{i}{k_5^2+i\epsilon}\right)(g^{15}(k_1+k_5)^4 + g^{54}(-k_5-k_1)^1 + g^{41}(k_4-k_1)^5) \\ & \times(g^{52}(k_5-k_2)^3 + g^{23}(k_2-k_3)^5 + g^{35}(k_3-k_5)^2)\epsilon_1\epsilon_2\epsilon_3\epsilon_4 \\ A_4^{part}|_{14}(4,3,2,1) = & -A_4^{part}|_{14}(1,3,2,4) = -A_4^{part}|_{14}(4,2,3,1) = A_4^{part}|_{14}(1,2,3,4) \end{aligned} \tag{4.9}$$

In this example, a single Feynman diagram was color decomposed into traces of color matrices and partial amplitude coefficients. This result can be obtained for all three channels of the four gluon process by a simple relabeling of the legs. The trace (1234), for example, will appear in the 1-2-channel but not in the 1-3 channel. This means that the full $A_4^{part}(1,2,3,4)$ partial amplitude will only take contributions from the 1-4-channel and the 1-2-channel.

The above result was a specific decomposition of a four gluon scattering amplitude. It is rather straightforward to show that this result can be generalized to the n-gluon tree amplitude [6],

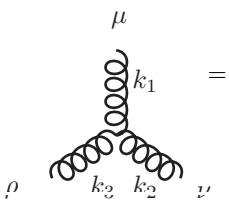

$$= \frac{i}{\sqrt{2}}(g^{\mu\nu}(k_1-k_2)^\rho + g^{\rho\mu}(k_3-k_1)^\nu + g^{\nu\rho}(k_2-k_3)^\mu)$$

Figure 4.2: Color ordered feynman rule for a 3-gluon vertex.

$$A_4^{tree} = g^{n-2} \sum_{\sigma \in S_n/Z_n} (\sigma(1) \cdots \sigma(n))\, A_n^{part}\, (\sigma(1) \cdots \sigma(n)) \tag{4.10}$$

where S_n/Z_n is the group of all permutations of n elements such that cyclically related elements are identified, or put differently, the sum over all distinct traces of n distinct matrices.

4.1.2 Loop amplitudes

We have seen that the partial amplitudes have a very useful property, they receive contributions only from Feynman diagrams that match a given order of the external legs. We will refer to diagrams with this property as *primitive amplitudes*. Primitive amplitudes will be the basic building blocks from which full amplitudes will be constructed. In the case of tree amplitudes, partial amplitudes are primitive amplitudes. In loop amplitudes, on the other hand, this will not generally be the case and we will seek to find a set of primitive amplitudes from which partial amplitudes can be constructed. To see this, let us consider the four gluon one-loop amplitude .

Four gluon one-loop amplitude - example

Let us proceed in a similar fashion to what was done above in the case of the four gluon tree amplitude. For brevity, we write the Feynman rule for a three gluon vertex as $f^{abc}v_{abc}$, where $v_{abc} = g^{ab}(k_a - k_b)^c + g^{bc}(k_b - k_c)^a + g^{ca}(k_c - k_a)^b$ contains all kinematic information and will be finally absorbed in the partial amplitude. As an example, we consider the box diagram appearing in figure 4.3. The contribution of this diagram (denoted by "14box" for 1-4-channel box diagram) to the amplitude is,

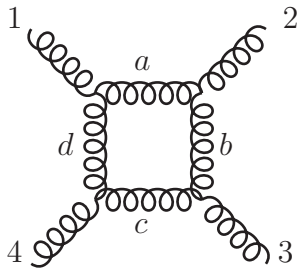

Figure 4.3: A box diagram contributing to the one-loop amplitude of the four gluon scattering process. The numbers refer to external gluons and the lower-case letters to internal gluon lines.

$$
\begin{aligned}
&A_4^{1-loop}|_{14box} \\
&= g^4 \prod_{i=1}^{4} \left(-\frac{i}{q_i^2 + i\epsilon} \right) f^{1ad} f^{4dc} f^{3cb} f^{2ba} v_{1ad} v_{4dc} v_{3cb} v_{2ba} \\
&= g^4 \tilde{A}_4^{part}|_{14box} \left(-\frac{i}{\sqrt{2}} \right)^4 \big((1ad) - (1da)\big)\big((4dc) - (4cd)\big)\big((3cb) - (3bc)\big)\big((2ba) - (2ab)\big) \\
&= g^4 A_4^{part}|_{14box} \big(N_c(1234) + N_c(1432) + 2(12)(34) + 2(13)(24) + 2(14)(23) \big) \qquad (4.11)
\end{aligned}
$$

This calculation involved taking products of four traces over three color matrices and simplifying them using the Fierz rearrangement identity. The N_c factors arise from traces over identity matrices, for example,

$$
(1ad)(4dc)(3cb)(2ba) = (1ac4)(3ca2) = (c41)(23c) = (1234)(1) = N_c(1234) \qquad (4.12)
$$

Similarly the other combinations of traces can be simplified to yield the result in equation (4.12). A similar calculation for the 1-4-channel triangle diagram yields,

$$
A_4^{1-loop}|_{14triangle} = g^4 A_4^{part}|_{14triangle} \big(N_c(1234) + N_c(1432) - N_c(1423) - N_c(1324) \big) \qquad (4.13)
$$

where four terms of the form $(14)(23)$ appear in the calculation but cancel against each other leaving only single trace terms.

In the case of one-loop, the Feynman diagrams decompose into single traces over four color matrices and double traces over two color matrices each. Traces over one color matrices also appear but do not contribute since all external matrices are taken to be in the group $SU(N_c)$ and are thus traceless. By relabeling the external legs, the above two diagrams can be used to calculate all Feynman diagrams with a gluon circulating in the loop. The full contribution of these diagrams to the total amplitude is,

$$
\begin{aligned}
A_4^{1-loop}|_{gluon} = g^4 &\sum_{\sigma \in S_4/Z_4} N_c(\sigma(1)\sigma(2)\sigma(3)\sigma(4)) A_{4;1}(\sigma(1)\sigma(2)\sigma(3)\sigma(4)) \\
&+ \sum_{\sigma \in S_4/S_{4;3}} (\sigma(1)\sigma(2))(\sigma(3)\sigma(4)) A_{4;3}(\sigma(1)\sigma(2)\sigma(3)\sigma(4)) \qquad (4.14)
\end{aligned}
$$

where σ belongs to the group of permutations of four elements up to a cyclic permutation leaving the single trace (Z_4) or the double trace ($S_{4;3}$) invariant. The partial amplitudes $A_{4;1}$ is a primitive amplitude, i.e. the sum over all color ordered diagrams with a leg ordering corresponding to its arguments. The partial amplitude $A_{4;3}$, on the other hand, is no longer a primitive amplitude since it receives contributions from diagrams with different leg orderings. For example, (4.12) shows us that $A_{4;3}(1324)$ receives a contribution from a diagram with a leg ordering of 1234. We see, though, that in this case these partial amplitudes can be expressed as a sum of primitive amplitudes,

$$A_{4;3} = \sum_{\sigma \in S_4/Z_4} A_{4;1}(\sigma(1)\sigma(2)\sigma(3)\sigma(4)) \tag{4.15}$$

The above example demonstrated that one loop amplitudes, similar to tree amplitudes, can be color decomposed, but also double trace color coefficients must be taken into account. The loop case becomes much more complicated, since partial amplitudes are no longer primitive amplitudes in the general case. Luckily, we were able to identify a subset of the partial amplitudes as being primitive amplitudes, while the remaining partial amplitudes could be expressed in terms of those same primitive amplitudes. This result turns out to be generally true. In [45], string theory methods are used to color decompose an n-point amplitude with external gluons, and the decoupling of $U(1)$ from $SU(N)$ is used to express partial amplitudes in terms of primitive amplitudes. [15] performs a similar task for an n-point amplitude with two external quarks and $n-2$ external gluons using a pure field theoretical approach. In this case, the $A_{n;1}$ partial amplitudes are not fine enough to be used as primitive amplitude building blocks, and further constraints are placed on the diagrams contributing to the primitive amplitudes. In addition to being color ordered, the primitive amplitudes receive contributions from diagrams with a specific orientation of the fermion line. These finer building blocks can be then used to construct all partial amplitudes.

4.1.3 Color sums

To calculate a cross section, the amplitude must be squared for a fixed configuration of colors. Since color is an unobservable quantity, one must then sum over outgoing particle colors and average over the incoming ones. Since we have separated the color factors from the rest of the amplitude, we can perform the color sum independently. If there are only two external gluons, the color sum will simply be,

$$(T^a T^b)(T^a T^b) = (T^a T^a) - \frac{1}{N_c}(T^a)(T^a) = N_c^2 - 1 \tag{4.16}$$

where the sum over double indices is implied. In the first equality, the Fierz rearrangement was applied. In the second equality, the tracelessness of the generators implies that $(T^a) = 0$ and the second term vanishes. The first term is evaluated by first applying the normalization (4.1) of the $SU(N_c)$ generators and then summing over the number of generators, i.e. $N_c^2 - 1$. Finally, we divide by a factor of $N_c^2 - 1$ per incoming gluon.

For a larger number of gluons, we repeat this process for all possible contractions of partial amplitudes. For example, in the case of three external gluons there are two possible color factors, $(T^a T^b T^c)$ and $(T^a T^c T^b)$. The two possible contractions of partial amplitudes will yield two color sums,

$$(T^aT^bT^c)(T^aT^bT^c) = -2\frac{N_c^2-1}{N_c}$$
$$(T^aT^bT^c)(T^aT^cT^b) = (N_c^2-1)(N_c - \frac{2}{N_c}) \tag{4.17}$$

[6] demonstrates a graphical technique to perform these color sums. In gluon only diagrams, one can ignore the $\frac{1}{N_c}$ in the Fierz rearrangement identity and the color sums become significantly simpler. For example, the above three-gluon color sums simplify to N_c and N_c^3 respectively.

4.2 Spinor Helicity

When calculating amplitudes involving massless gauge bosons, it is useful to represent the polarization vectors by spinor products, particularly if massless fermions are present. This method goes under the name of the *spinor helicity method*, and is widely used in QCD calculations. We begin by a review of massless spinor solutions to the Dirac equation and then introduce the representation of polarization vectors. Appendix D contains a list of useful identities. The section will conclude with an example of a tree amplitude calculation. [6, 7] provide good reviews of the spinor helicity method.

When considering plane-wave solutions with momentum k^μ to the Dirac equation, two independent solutions exist (see [8]). These are further divided into two classes of solutions, those with positive energy, $k^0 > 0$, and those with negative energy, $k^0 < 0$. The former is identified with fermions, $u_s(k)$, while the latter with anti-fermions, $v_s(k)$. The two independent solutions in each class, $s \in \{1, 2\}$, correspond to two possible spin states.

In the massless limit, since a boost cannot flip the spatial direction of the momentum, the solutions can be chosen to have a well defined helicity, i.e. they will be eigenvectors of the helicity operator,

$$h \equiv \hat{p} \cdot \vec{S} = \frac{1}{2}\hat{p}_i \begin{pmatrix} \sigma^i & 0 \\ 0 & \sigma^i \end{pmatrix} \tag{4.18}$$

which measures the spin of the particle along the momentum axis. We can therefore denote the particles by $u_\pm(k)$ and $v_\pm(k)$, corresponding to $\pm\frac{1}{2}$ eigenvalues of the helicity operator. In this limit, the two classes of particles degenerate into one class, because the phase can be chosen such that $u_\pm(k) = v_\mp(k)$.

Using the light-cone coordinates, defined as $k^\pm = k^0 \pm k^3$, and choosing the Dirac representation of the gamma matrices,

$$\gamma^0 = \begin{pmatrix} 1 & 0 \\ 0 & -1 \end{pmatrix}, \qquad \gamma^i = \begin{pmatrix} 0 & \sigma^i \\ -\sigma^i & 0 \end{pmatrix}, \qquad \gamma_5 = \begin{pmatrix} 0 & 1 \\ 1 & 0 \end{pmatrix} \tag{4.19}$$

the spinor solutions are,

$$u_+(k) = v_-(k) = \frac{1}{\sqrt{2}} \begin{pmatrix} \sqrt{k^+} \\ \sqrt{k^-}e^{i\psi_k} \\ \sqrt{k^+} \\ \sqrt{k^-}e^{i\psi_k} \end{pmatrix}, \qquad u_-(k) = v_+(k) = \frac{1}{\sqrt{2}} \begin{pmatrix} \sqrt{k^-}e^{-i\psi_k} \\ -\sqrt{k^+} \\ -\sqrt{k^-}e^{-i\psi_k} \\ \sqrt{k^+} \end{pmatrix} \tag{4.20}$$

and the row spinors corresponding to this representation of the gamma matrices, defined by $\overline{u_\pm} \equiv u^\dagger \gamma^0$, are,

$$\begin{aligned} \overline{u_+(k)} = \overline{v_-(k)} &= \frac{1}{\sqrt{2}} \left(\sqrt{k^+}, \ \sqrt{k^-}e^{-i\psi_k}, \ -\sqrt{k^+}, \ -\sqrt{k^-}e^{-i\psi_k} \right) \\ \overline{u_-(k)} = \overline{v_+(k)} &= \frac{1}{\sqrt{2}} \left(\sqrt{k^-}e^{i\psi_k}, \ -\sqrt{k^+}, \ \sqrt{k^-}e^{i\psi_k}, \ -\sqrt{k^+} \right) \end{aligned} \tag{4.21}$$

where

$$e^{\pm i\psi_k} \equiv \frac{k^1 \pm ik^2}{\sqrt{k^+k^-}} \tag{4.22}$$

We can verify that these solutions satisfy the Dirac equation in momentum space. For example, the positive helicity fermion satisfies,

$$\begin{aligned} \not{k} u_+(k) &= (\frac{1}{2}k^+\gamma^- + \frac{1}{2}k^-\gamma^+ - k^1\gamma^1 - k^2\gamma^2)u_+(k) \\ &= \frac{1}{\sqrt{2}} \begin{pmatrix} \frac{1}{2}(k^+ + k^-) & & -\frac{1}{2}(k^+ - k^-) & -(k^1 - ik^2) \\ 0 & \frac{1}{2}(k^+ + k^-) & -(k^1 + ik^2) & \frac{1}{2}(k^+ - k^-) \\ \frac{1}{2}(k^+ - k^-) & (k^1 - ik^2) & -\frac{1}{2}(k^+ + k^-) & 0 \\ (k^1 + ik^2) & -\frac{1}{2}(k^+ - k^-) & 0 & -\frac{1}{2}(k^+ + k^-) \end{pmatrix} \begin{pmatrix} \sqrt{k^+} \\ \sqrt{k^-}e^{i\psi_k} \\ \sqrt{k^+} \\ \sqrt{k^-}e^{i\psi_k} \end{pmatrix} = 0 \end{aligned} \tag{4.23}$$

where the fact that k is massless implies that $k^+k^- - (k^1)^2 - (k^2)^2 = 0$. The positive helicity spinor is an eigenstate of the helicity operator with helicity $+\frac{1}{2}$ (here preferably working with the Minkowski coordinates),

$$hu_+(k) = \frac{1}{2\sqrt{2}p_0}\begin{pmatrix} k^3 & k^1 - ik^2 & 0 & 0 \\ k^1 + ik^2 & -k^3 & 0 & 0 \\ 0 & 0 & k^3 & k^1 - ik^2 \\ 0 & 0 & k^1 + ik^2 & -k^3 \end{pmatrix}\begin{pmatrix} \sqrt{k^0+k^3} \\ \frac{k^1+ik^2}{\sqrt{k^0+k^3}} \\ \sqrt{k^0+k^3} \\ \frac{k^1+ik^2}{\sqrt{k^0+k^3}} \end{pmatrix}$$
$$= \frac{1}{2\sqrt{2}}\begin{pmatrix} \sqrt{k^0+k^3} \\ \frac{k^1+ik^2}{\sqrt{k^0+k^3}} \\ \sqrt{k^0+k^3} \\ \frac{k^1+ik^2}{\sqrt{k^0+k^3}} \end{pmatrix} = \frac{1}{2}u_+(k) \tag{4.24}$$

Similarly, the negative helicity spinor can be shown to have the desired properties. Having constructed a basis for the massless spinors, spinor products can be explicitly calculated. We use the following shorthand notation for spinors,

$$|i^\pm\rangle \equiv |k_i^\pm\rangle \equiv u_\pm(k_i) = v_\mp(k_i), \qquad \langle i^\pm| \equiv \langle k_i^\pm| \equiv \overline{u_\pm(k_i)} = \overline{v_\mp(k_i)} \tag{4.25}$$

and spinor products,

$$\langle ij\rangle \equiv \langle i^-|j^+\rangle = \overline{u_-(k_i)}u_+(k_j), \qquad [ij] \equiv \langle i^+|j^-\rangle = \overline{u_+(k_i)}u_-(k_j) \tag{4.26}$$

These quantities prove to have a rather compact form, where for positive energy momenta $k_i^0 > 0$ and $k_j^0 > 0$,

$$\langle ij\rangle = \sqrt{|s_{ij}|}e^{i\phi_{ij}}, \qquad [ij] = \sqrt{|s_{ij}|}e^{-i(\phi_{ij}+\pi)} \tag{4.27}$$

with,

$$\cos\phi_{ij} = \frac{k_i^1 k_j^+ - k_j^1 k_i^+}{\sqrt{|s_{ij}|k_i^+ k_j^+}}, \qquad \sin\phi_{ij} = \frac{k_i^2 k_j^+ - k_j^2 k_i^+}{\sqrt{|s_{ij}|k_i^+ k_j^+}}, \qquad s_{ij} = 2k_i k_j \tag{4.28}$$

The product of these two spinor products is simply the invariant formed by the sum of the momenta,

$$\langle ij\rangle[ji] = (k_i + k_j)^2 = s_{ij} \tag{4.29}$$

From (4.27), we see that the two types of spinor products are related by complex conjugation,

$$\langle ij\rangle^* = [ji] \tag{4.30}$$

To allow the definition of the spinor products to encompass negative energy momenta as well, which is important for taking full advantage of the cross symmetry property of

amplitudes, we first analytically continue the spinor product $\langle ij\rangle$ in (4.27) by replacing k_i by $-k_i$ if $k_i^0 < 0$ and similarly for k_j. We then define the second spinor product $[ij]$ through (4.29).

A summary of the above properties together with an extensive collection of identities appears in appendix D.

A spinor product representation for polarization vectors

Thanks to the compact notation and wide range of identities, spinor products are powerful in evaluating amplitudes containing massless fermions. Their main virtue, though, lies in the ability to express polarization vectors of massless gauge bosons through them, thus achieving a uniform algebraic tool for all external particles. We conform to the representation of Xu, Zhang and Chang [46],

$$\epsilon_\mu^+(k;q) = \frac{\langle q^-|\gamma_\mu|k^-\rangle}{\sqrt{2}\langle qk\rangle}, \qquad \epsilon_\mu^-(k;q) = -\frac{\langle q^+|\gamma_\mu|k^+\rangle}{\sqrt{2}[qk]} \tag{4.31}$$

q is a reference momentum which captures the gauge invariance inherent to the polarization vectors. For every polarization vector in an amplitude, an arbitrary massless reference momentum can be chosen. The choice must be consistent within every gauge invariant piece, such as a partial amplitude. The two polarization vectors are related by complex conjugation,

$$(\epsilon_\mu^+(k;q))^* = \epsilon_\mu^-(k;q) \tag{4.32}$$

To check that this representation is plausible, one can confirm that it satisfies all identities obeyed by the standard polarization vectors. This suggests that its role in scattering amplitudes will be equivalent. Applying the spinor helicity identities in D, it is straightforward to show that the standard normalization and orthogonality conditions (D.13) hold. We will demonstrate here explicitly two other properties of the polarization vectors: gauge invariance and the completeness relation.

In coordinate space, a gauge transformation is achieved by adding a derivative of a function to the solution of the equations of motion. In momentum space, this implies that the solution is defined up to a vector proportional to the momentum vector. We will now show that a change in the reference momentum q has exactly this effect,

$$\begin{aligned}\epsilon_\mu^+(k;q') - \epsilon_\mu^+(k;q) &= \frac{\langle q'^-|\gamma_\mu|k^-\rangle}{\sqrt{2}\langle q'k\rangle} - \frac{\langle q^-|\gamma_\mu|k^-\rangle}{\sqrt{2}\langle qk\rangle} \\ &= \frac{\langle q^-|k^+\rangle\langle k^+|\gamma_\mu|q'^+\rangle + \langle q^-|\gamma_\mu|k^-\rangle\langle k^-|q'^+\rangle}{\sqrt{2}\langle q'k\rangle\langle qk\rangle} \\ &= \frac{\langle q^-|w_+\not{k}\gamma_\mu + \gamma_\mu w_-\not{k}|q'^+\rangle}{\sqrt{2}\langle q'k\rangle\langle qk\rangle} \\ &= \frac{\sqrt{2}\langle q^-|q'^+\rangle}{\langle q'k\rangle\langle qk\rangle}k_\mu \end{aligned} \tag{4.33}$$

where $w_\pm = \frac{1}{2}(1+\gamma_5)$ is the projection matrix which obeys $w_\pm\gamma_\mu = \gamma_\mu w_\mp$. We also used that positive (negaitve) helicity spinors are eigenvectors of the positive (negative) projection matrix with eigenvalue 1.

The spinor polarization vectors obey the standard completeness relation,

$$\begin{aligned}\sum_{\lambda=\pm}\epsilon_\mu^\lambda(k;q)(\epsilon_\nu^\lambda(k;q))^* &= \frac{\langle q^-|\gamma_\mu|k^-\rangle\langle q^-|\gamma_\nu|k^-\rangle^*}{2\langle qk\rangle\langle qk\rangle^*} + \frac{\langle q^+|\gamma_\mu|k^+\rangle\langle q^+|\gamma_\nu|k^+\rangle^*}{2[qk][qk]^*} \\ &= \frac{1}{4k\cdot q}\left(\langle q^-|\gamma_\mu|k^-\rangle\langle k^-|\gamma_\nu|q^-\rangle + \langle q^+|\gamma_\mu|k^+\rangle\langle k^+|\gamma_\nu|q^+\rangle\right) \\ &= \frac{1}{4k\cdot q}tr[\not{q}\gamma_\mu\not{k}\gamma_\nu] = -g_{\mu\nu} + \frac{k_\mu q_\nu + k_\nu q_\mu}{k\cdot q} \end{aligned} \tag{4.34}$$

(D.7), (D.4) and (D.6) were used.

Appendix D contains a collection of useful identities involving the spinor representation of the polarization vectors. One should try to take advantage of gauge invariance to simplify calculations. A proper choice of the reference momenta can cause many terms in an initial amplitude expression to vanish, vastly simplifying intermediate expressions.

4.2.1 Example - $gg \to ss$ tree amplitude

We calculate here the color ordered tree amplitude for the scattering of two massive scalars and two positive helicity gluons, $A_4^{tree}(-l_1, 1^+, 2^+, l_2)$. Three different diagrams contribute to this amplitude, these appear in figure 4.4.

The momenta were chosen such that the gluons are outgoing, and the scalars flow against the direction of the charge flow. From momentum conservation we have that $l_1 = l_2 + k_1 + k_2$. In addition, since the external particles are on shell, we have that $k_1^2 = k_2^2 = 0$ and $l_1^2 = l_2^2 = m^2$. From these relations we can derive the following useful relations:

$$\left.\begin{aligned} m^2 &= l_1\cdot l_2 + l_1\cdot k_1 + l_1\cdot k_2 \\ m^2 &= l_2\cdot l_1 - l_2\cdot k_1 - l_2\cdot k_2 \end{aligned}\right\} \Rightarrow l_1\cdot(k_1+k_2) = -l_2\cdot(k_1+k_2)$$

$$\left.\begin{aligned} 0 &= k_1 \cdot l_1 - k_1 \cdot l_2 - k_1 \cdot k_2 \\ 0 &= k_2 \cdot l_1 - k_2 \cdot l_2 - k_2 \cdot k_1 \end{aligned}\right\} \Rightarrow k_1 \cdot (l_1 - l_2) = k_2 \cdot (l_1 - l_2)$$

$$\Rightarrow l_1 \cdot k_2 = -l_2 \cdot k_1, \;\; l_1 \cdot k_1 = -l_2 \cdot k_2 \tag{4.35}$$

We can now calculate the three diagrams. The amplitude of diagram 4.4(a) is:

$$\begin{aligned} A^{(a)} &= \frac{\langle 2-|\gamma_\mu|1-\rangle}{\sqrt{2}\langle 21\rangle} \frac{\langle 1-|\gamma_\nu|2-\rangle}{\sqrt{2}\langle 12\rangle} \frac{i}{\sqrt{2}} \left(g^{\mu\nu}(k_2-k_1)^\rho + g^{\rho\mu}(k_1-p)^\nu + g^{\nu\rho}(p-k_2)^\mu\right) \\ &\quad \times \frac{-i}{p^2} \frac{i}{\sqrt{2}} (l_1+l_2)^\rho \\ &= i \frac{2\langle 21\rangle[21]}{4\langle 21\rangle\langle 12\rangle} \frac{1}{2k_1\cdot k_2} 2(-k_1\cdot l_1 + k_2\cdot l_2 - k_1\cdot l_2 + k_2\cdot l_1) \\ &= i \frac{-4k_1\cdot k_2}{-4\langle 21\rangle^2} \frac{1}{2k_1\cdot k_2} (-4)(k_1\cdot l_1 + k_1\cdot l_2) \\ &= -i \frac{k_1\cdot l_1 + k_1\cdot l_2}{\langle 21\rangle^2} \end{aligned} \tag{4.36}$$

As reference momenta we chose $q_1 = k_2$ and $q_2 = k_1$. As a result of this choice, the last two metric terms in the 3-gluon vertex drop out when contracted with one of the polarization

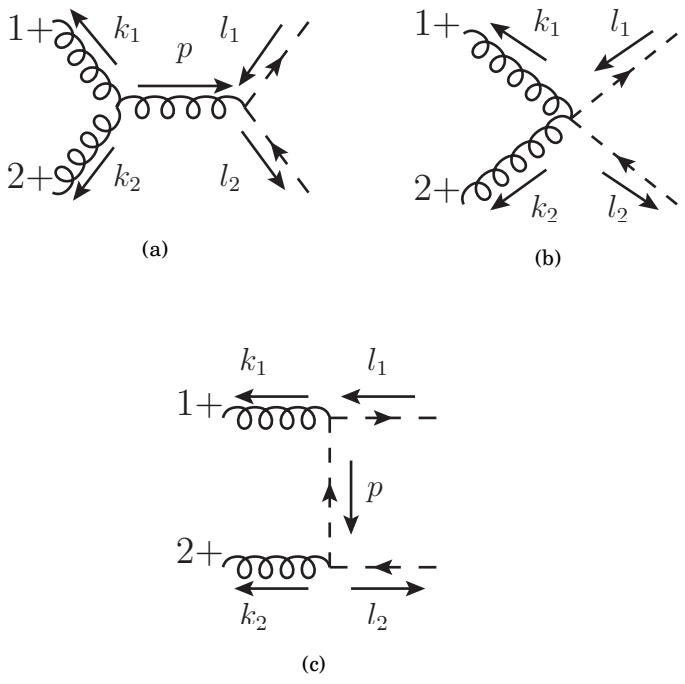

Figure 4.4: Contributions to the 2 scalar → 2 gluon tree amplitude

vectors. We also used that $p = -k_1 - k_2$ in the first equality, and (4.35) in the second equality.

Moving on to diagram 4.4(b):

$$A^{(b)} = \frac{\langle 2-|\gamma_\mu|1-\rangle}{\sqrt{2}\langle 21\rangle}\frac{\langle 1-|\gamma^\mu|2-\rangle}{\sqrt{2}\langle 12\rangle}\left(\frac{i}{2}\right) = -\frac{i}{2}\frac{2\langle 21\rangle[21]}{2\langle 21\rangle^2} = i\frac{k_1\cdot k_2}{\langle 21\rangle^2} \tag{4.37}$$

And the scalar exchange diagram, 4.4(c):

$$\begin{aligned} A^{(c)} &= \frac{\langle 2-|\gamma_\mu|1-\rangle}{\sqrt{2}\langle 21\rangle}\frac{\langle 1-|\gamma_\nu|2-\rangle}{\sqrt{2}\langle 12\rangle}\frac{i}{(l_1-k_1)^2-m^2}\frac{i}{\sqrt{2}}(l_1+p)^\mu\frac{i}{\sqrt{2}}(p+l_2)^\nu \\ &= -4i\frac{\langle 2-|\not{l}_1|1-\rangle}{\sqrt{2}\langle 21\rangle}\frac{\langle 1-|\not{l}_2|2-\rangle}{\sqrt{2}\langle 12\rangle}\frac{1}{2}\frac{1}{-2l_1\cdot k_1} \\ &= -\frac{i}{2}\frac{4tr[w_-\not{k}_2\not{l}_2w_-\not{k}_1\not{l}_2]}{2\langle 21\rangle^2 2l_1\cdot k_1} \\ &= i\frac{2k_1\cdot k_2m^2 - 4k_1\cdot l_1k_2\cdot l_1}{\langle 21\rangle^2 2l_1\cdot k_1} \\ &= i\frac{\langle 21\rangle[12]m^2}{\langle 21\rangle^2 2l_1\cdot k_1} - i\frac{2k_2\cdot l_1}{\langle 21\rangle^2} \end{aligned} \tag{4.38}$$

where $w_- = \frac{1}{2}(1-\gamma^5)$. In the second equality we replaced $p^\mu = l_1^\mu - k_1^\mu$, with k_1^μ dropping out when contracted with the polarization vector. Similarly for p^ν. In the third equality we used that $\not{l}_1$ inside the polarization vector can be replaced by $\not{l}_2$ as a consequence of momentum conservation, since $\not{k}_i$ drops out when applied on the massless spinors.

Finally we can sum up the three amplitudes to obtain the complete tree amplitude for the process,

$$\begin{aligned} A_4^{tree}(-l_1, 1^+, 2^+, l_2) &= A^{(a)} + A^{(b)} + A^{(c)} \\ &= -i\frac{[21]}{\langle 21\rangle}\frac{m^2}{2l_1\cdot k_1} + i\frac{1}{\langle 21\rangle^2}(2k_1\cdot l_2 + k_1\cdot k_2 - k_1\cdot l_1 - k_1\cdot l_2) \\ &= -i\frac{[21]}{\langle 21\rangle}\frac{m^2}{2l_1\cdot k_1} \\ &= i\frac{[12]}{\langle 12\rangle}\frac{m^2}{(l_1-k_1)^2-m^2} \end{aligned} \tag{4.39}$$

where momentum conservation was used to cancel the second term in the second line.

4.3 On Shell Recursion Relations

The recently discovered BCF [19, 20] on-shell recursion relations provide a method of evaluating tree amplitudes in a somewhat analogous way to how unitarity is used to derive

loop amplitudes. The pole structure of tree amplitudes, namely singularities reached when internal particles go on-shell, allow one to construct larger tree amplitudes out of smaller more manageable pieces. In this section, we describe the general method and outline its mathematical derivation. A recalculation of the example from the previous chapter follows, demonstrating the capacity of this method to calculate tree amplitudes containing gluons as well as massive scalar particles [47]. [48, 49] extends the method to include both massive fermions and massive gauge bosons, and [50] discusses how dimensional regularization can be incorporated.

Consider a tree amplitude with all momenta incoming containing at least two massless external particles i and j with momenta k_i and k_j (see figure 4.5). [47] discusses the slightly more intricate cases of one or zero external massless particles. Instead of specifying a particle's momentum by its four vector, it is possible to look at its slashed momentum. The two representations are related by,

$$\not{k} = k_\mu \gamma^\mu = \begin{pmatrix} k^0 & 0 & k^3 & k^1 - ik^2 \\ 0 & k^0 & k^1 + ik^2 & -k^3 \\ -k^3 & -k^1 + ik^2 & -k^0 & 0 \\ -k^1 - ik^2 & k^3 & 0 & -k^0 \end{pmatrix} \tag{4.40}$$

where the Dirac representation of the gamma matrices (4.19) was used. We choose to shift the two massless momenta in the complex plane according to,

$$\begin{aligned} \not{k}_i &\to \hat{\not{k}}_i = \not{k}_i + z\not{\eta} \\ \not{k}_j &\to \hat{\not{k}}_j = \not{k}_j - z\not{\eta} \end{aligned} \tag{4.41}$$

where z is a complex variable and the momentum η is defined by,

$$\not{\eta} = u_+(k_j)\overline{u}_+(k_i) + u_-(k_i)\overline{u}_-(k_j) \tag{4.42}$$

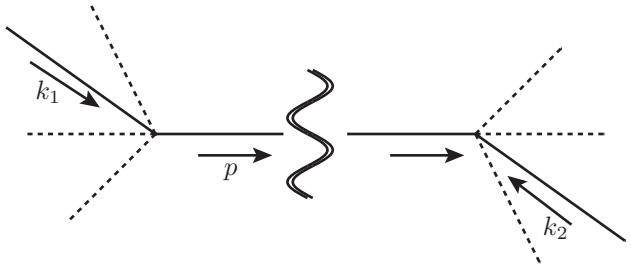

Figure 4.5: An amplitude is split into along every possible internal line separating two chosen particles i and j.

Such a shift in the slashed momenta implies an equivalent shift in the four-vector momenta. By inserting the spinor solutions (4.20) and (4.21) into the definition of η on can verify that η is a well defined complex momentum. Its components in the light-cone coordinates introduced in section 4.2 are,

$$\begin{aligned}
&\eta^+ = 2\sqrt{k_i^- k_j^-}\, e^{i(\psi_i - \psi_k)}, \qquad \eta^- = 2\sqrt{k_i^+ k_j^+} \\
&e^{i\psi_\eta} = -\left(\frac{k_i^+ k_j^-}{k_i^- k_j^+}\right)^{1/4} e^{\frac{i}{2}(\psi_i+\psi_j)}, \qquad e^{-i\psi_\eta} = -\left(\frac{k_i^- k_j^+}{k_i^+ k_j^-}\right)^{1/4} e^{-\frac{i}{2}(\psi_i+\psi_j)}
\end{aligned} \tag{4.43}$$

η has been chosen such that it is both massless and orthogonal to k_i and k_j, i.e. $\eta^2 = \eta \cdot k_i = \eta \cdot k_j = 0$. This implies that the shifted momenta, $\hat{k}_i$ and $\hat{k}_j$, are massless. Since (massless) momenta can be expressed in terms of spinors by the completeness relation, $\not{k} = \sum_\lambda u^\lambda(k)\overline{u}^\lambda(k)$, then the momenta shift implies a shift of the corresponding spinors,

$$\begin{aligned}
u_+(k_i) &\to u_+(\hat{k}_i) = u_+(k_i) + z u_+(k_j) \\
\overline{u}_-(k_i) &\to \overline{u}_-(\hat{k}_i) = \overline{u}_-(k_i) + z\overline{u}_-(k_j) \\
u_-(k_j) &\to u_-(\hat{k}_j) = u_-(k_j) - z u_-(k_i) \\
\overline{u}_+(k_j) &\to \overline{u}_+(\hat{k}_j) = \overline{u}_+(k_j) - z\overline{u}_+(k_i)
\end{aligned} \tag{4.44}$$

Let us now consider the consequences of such a shift on a tree amplitude. Since $\hat{k}_i + \hat{k}_j = k_i + k_j$, the overall momentum conservation remains intact. In a tree diagram, every internal line divides the diagram into two. We refer to these two parts as the left and right side. The momentum p flowing through an internal line is the sum of all external momenta on one side. If both particles i and j are located on one side of the internal line, its momentum remains untouched under the shift. If, on the other hand, the line separates the two particles, then p gets shifted by $z\eta$,

$$p = k_i + ... \to \hat{p}(z) = p + z\eta = k_i + z\eta + ... \tag{4.45}$$

The shifted internal momentum is a linear function of z and because η is massless, the shift in the inverse propagator is also linear in z,

$$\frac{1}{p^2 - m_p^2} \to \frac{1}{\hat{p}^2 - m_p^2} = \frac{1}{p^2 - m_p^2 + 2zp\cdot\eta} \tag{4.46}$$

This propagator contains a simple pole in z space at,

$$z = -\frac{p^2 - m_p^2}{2p\cdot\eta} \tag{4.47}$$

Consider all partitions of external particles of a given tree amplitude into a left group and

a right group, such that particle i is in the left group and j in the right group. If $\{i, j\}$ are gluons, then only the helicity configurations $\{\pm, \pm\}$ and $\{+, -\}$ are permitted, the fourth one can be obtained by replacing the positions of the particles. The tree amplitude is given by the following on-shell recursion formula,

$$A = \sum_{partitions} \sum_{s} A_L(\hat{k}_i, -\hat{p}) \frac{i}{p^2 - m_p^2} A_R(\hat{k}_j, \hat{p})\big|_{\hat{p}^2 = m_p^2} \tag{4.48}$$

Conforming to our choice of p flowing from left to right, $A_L(\hat{k}_i, -\hat{p})$ is the tree amplitude of all left side particles incoming and p outgoing (hence the minus sign), where both k_i and p are replaced by the corresponding shifted momenta with z fixed by the on-shell condition $\hat{p}^2 = m_p^2$. The value of z solving this condition is exactly the location of the pole (4.47). $A_R(\hat{k}_j, \hat{p})$ is the amplitude of all right side particles outgoing and p incoming. The sum over s is over all types of intermediary particles and all of their possible spin configurations.

The proof of this relation was first given in [20] (see also [47]). The main ingredient is a theorem of complex analysis stating that the sum over all residues of a rational function with only simple poles on the entire Riemann sphere is zero (see for example [51]). Having shifted two momenta in the amplitude A to obtain $\hat{A}(z)$, the theorem can be applied on $\hat{A}(z)/z$,

$$A = \hat{A}(0) = \text{Res}\left(\frac{\hat{A}(z)}{z}\right)_{z=0} = -\sum_{\alpha}\left(\frac{\hat{A}(z)}{z}\right)_{z=z_\alpha} - \left(\frac{\hat{A}(z)}{z}\right)_{z=\infty} \tag{4.49}$$

where $\{z_\alpha\}$ is the set of all finite simple poles of $\hat{A}(z)$. In the case of gluons, the above restrictions on the choice of helicities guarantees that the infinite term vanishes. For other types of particles it must be explicitly checked that this term is finite or preferably zero.

As discussed above, only the momentum of internal lines which separate the two hatted particles are shifted. The inverse propagator of such a line is linear in z and contributes a pole. In every partition, the flow of momentum through the dividing internal line is unique, making sure that only simple poles occur. The location of the pole $z_\alpha(p)$ is determined by equation (4.47). Inserting this value for z in (4.49) for every partition reproduces the on-shell recursion formula (4.48). This equation is consistent also in the case of internal fermion lines. In this case, the factor $\not{p} + m_p$ that appears in the numerator of the fermion propagator can be replaced by spinors using the completeness relation. These spinors correspond to the external fermions in the left and right tree amplitudes.

4.3.1 Example - $gg \to ss$ tree amplitude

Let us demonstrate this procedure by calculating again the color ordered amplitude of two scalars and two gluons of positive helicity [47]. Consider the same configuration as in

subsection 4.2.1. We have at our disposal exactly two massless particles which we will use as the hatted particles, $i = 1$ and $j = 2$. We shift their momentum accordingly by $z\not{\eta} = z\left(|2^+\rangle\langle 1^+| + |1^-\rangle\langle 2^-|\right)$,

$$\begin{aligned}\hat{\not{k}}_1 &= \not{k}_1 + z\not{\eta} \\ \hat{\not{k}}_2 &= \not{k}_1 - z\not{\eta}\end{aligned} \tag{4.50}$$

The shifted momenta remain massless and overall momentum conservation still applies. Shifting the momenta implies the following shifting of the spinors,

$$\begin{aligned}|\hat{1}^+\rangle &= |1^+\rangle + z|2^+\rangle \qquad & \langle\hat{1}^+| &= \langle 1^+| \\ \langle\hat{1}^-| &= \langle 1^-| + z\langle 2^-| \qquad & |\hat{1}^-\rangle &= |1^-\rangle \\ |\hat{2}^-\rangle &= |2^-\rangle - z|1^-\rangle \qquad & \langle\hat{2}^-| &= \langle 2^-| \\ \langle\hat{2}^+| &= \langle 2^+| - z\langle 1^+| \qquad & |\hat{2}^+\rangle &= |2^+\rangle\end{aligned} \tag{4.51}$$

We must now consider all possible partitions leaving particle 1 on the left side and particle 2 on the right side. Note that since both hatted particles are positive helicity gluons, we can safely neglect the residue of the amplitude at infinity as discussed above. Applying the Feynman rules for scalar particles (see appendix A), only one possible (color ordered) partition exists. This configuration is shown in figure 4.6. As opposed to the direct calculation, here only one diagram must be evaluated with the simplifying condition that the internal scalar is on shell, demonstrating the advantage of this method.

Following the prescription, we must calculate the diagrams on the left side and right side using the shifted values of the gluon momenta, and correspondingly of the internal momenta. These must be evaluated at the value of z given by (4.47). To calculate dot products involving η we use the fact that $\eta \cdot p = \frac{1}{4}tr[\not{\eta}\not{p}] = \frac{1}{2}\langle 1^+|\not{p}|2^+\rangle$.

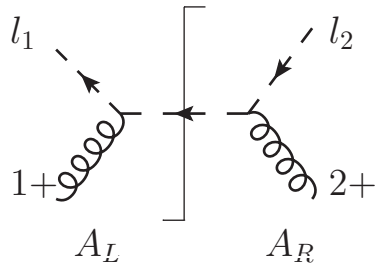

Figure 4.6: The possible partition of $A_4^{tree}(-l_1, 1^+, 2^+, l_2)$

$$z = -\frac{p^2 - m_p^2}{\langle 1^+|p|2^+\rangle} \tag{4.52}$$

where $p = l_1 - k_1 = l_2 + k_2$. The two reduced amplitudes are straightforward to calculate,

$$\begin{aligned} A_L &= \frac{\langle \hat{2}^-|\gamma^\mu|\hat{1}^-\rangle}{\sqrt{2}\langle \hat{2}\hat{1}\rangle}\frac{i}{\sqrt{2}}(l_1+p)_\mu = i\frac{\langle \hat{2}^-|\not{l}_1|\hat{1}^-\rangle}{\langle \hat{2}\hat{1}\rangle} \\ A_R &= \frac{\langle \hat{1}^-|\gamma^\mu|\hat{2}^-\rangle}{\sqrt{2}\langle \hat{1}\hat{2}\rangle}\frac{i}{\sqrt{2}}(p+l_2)_\mu = i\frac{\langle \hat{1}^-|\not{l}_2|\hat{2}^-\rangle}{\langle \hat{1}\hat{2}\rangle} \end{aligned} \tag{4.53}$$

where the polarization vectors were represented by spinor products as in (4.31), with the reference momentum of each gluon chosen to be the opposite gluon.

The denominators can be simply replaced by non shifted momenta, since,

$$\langle \hat{2}\hat{1}\rangle = \langle 2^-|\left(|1^+\rangle + z|2^+\rangle\right) = \langle 21\rangle = -\langle \hat{1}\hat{2}\rangle \tag{4.54}$$

Combining the two amplitudes and the propagator yields,

$$\begin{aligned} A_4^{tree} &= -\frac{\langle \hat{2}^-|\not{l}_1|\hat{1}^-\rangle}{\langle \hat{2}\hat{1}\rangle}\frac{i}{(l_1-k_1)^2-m^2}\frac{\langle \hat{1}^-|\not{l}_2|\hat{2}^-\rangle}{\langle \hat{1}\hat{2}\rangle} \\ &= i\frac{tr[w_-\not{\hat{k}}_2\not{l}_1\not{\hat{k}}_1\not{l}_1]}{\langle 21\rangle^2}\frac{1}{(l_1-k_1)^2-m^2} \\ &= i\frac{2(2\hat{k}_2\cdot l_1\hat{k}_1\cdot l_1 - \hat{k}_2\cdot\hat{k}_1 l_1^2)}{\langle 21\rangle^2}\frac{1}{(l_1-k_1)^2-m^2} \end{aligned} \tag{4.55}$$

Since the particle propagating through the partition is a scalar, there is no summation over helicities. We can use the following kinematic relations to simplify the expression,

$$\begin{aligned} \hat{p}^2 = m^2 = (l_1-\hat{k}_1)^2 = m^2 - 2\hat{k}_1\cdot l_1 \Rightarrow \hat{k}_1\cdot l_1 = 0 \\ 2k_1\cdot k_2 = (k_1+k_2)^2 = (\hat{k}_1+\hat{k}_2)^2 = 2\hat{k}_1\cdot\hat{k}_2 \end{aligned} \tag{4.56}$$

And the final result is,

$$A_4^{tree}(-l_1, 1^+, 2^+, l_2) = i\frac{[12]}{\langle 12\rangle}\frac{m^2}{(l_1-k_1)^2-m^2} \tag{4.57}$$

which agrees with (4.39).

4.4 Dimensional Regularization Revisited

In section 2.1, dimensional regularization was discussed as a method for regulating divergences in Feynman integrals. In this method, the dimension of space-time is extended to $4-2\epsilon$. In order to deal with four dimensional quantities such as polarization vectors for gauge bosons, the four-dimensional helicity scheme (FDH) was introduced. This scheme dictates that all quantities, except loop momenta, remain four dimensional. In this section, an elegant method for dealing with the extra dimensions will be discussed.

Consider a $(4-2\epsilon)$-dimensional vector P^λ (we follow the convention that large letters are $4-2\epsilon$ dimensional while small letters are four dimensional). This vector can be written as a sum of two vectors,

$$P^\lambda = p^\lambda + \mu^\lambda \tag{4.58}$$

where p^λ is effectively a four dimensional vector containing the first four components of P^λ, i.e. the projection of P^λ onto the four dimensional space. Similarly, μ^λ is a -2ϵ-vector, i.e. the projection of P^λ onto the remaining -2ϵ dimensions. Since these two vectors live in orthogonal sub-spaces, it follows that $p\cdot\mu = 0$, or in fact μ^λ is orthogonal to any four dimensional vector. This representation of a $4-2\epsilon$ vector was already discussed by 't Hooft and Veltman in their original paper [26]. Here we will follow the discussion in the appendix of [43].

In this extended space, the metric is extended to $4-2\epsilon$ dimensions such that it remains diagonal, with all extra dimensions having the signature of the spatial dimensions, $g^{\mu\nu} = \text{diag}(+,-,-,-,-,...)$. Since μ^λ lives in a Eucledian subspace, we use the unorthodox notation that $\mu^\lambda\mu_\lambda = -\mu^2$ where μ^2 is effectively a positive number (i.e. if 2ϵ is an integer, μ^2 is the sum of the squares of the components of μ^λ). The square of P is then,

$$P^2 = (p^\lambda + \mu^\lambda)(p_\lambda + \mu_\lambda) = p^2 - \mu^2 \tag{4.59}$$

Note that if P is a momentum with mass m, then $p^2 = m^2 + \mu^2$ and the extra dimensional part appears as an effective mass of the four dimensional momentum. In loop calculations, μ^2 will always appear in this combination. Remember, though, that this extra mass is later integrated out.

Let us now look at some special properties of μ^λ in the context of Dirac matrices. The usual algebra of the gamma matrices is extended to $4-2\epsilon$-dimensions following the normal definition, $\{\gamma^\lambda,\gamma^\rho\} = 2g^{\lambda\rho}$. From here it directly follows that for any four dimensional vector q^μ,

$$\{\not{q},\not{\mu}\} = 2q\cdot\mu = 0 \tag{4.60}$$

In QCD amplitudes, it is common to consider some fixed configuration of the external gluon helicities, in which case γ_5 matrices appear in the amplitude in the form of projection matrices $w^{\pm} = \frac{1}{2}(1 \pm \gamma_5)$. Using the arbitrary dimension definition for γ_5 (γ_5 is determined by the first four components of γ^λ, but it doesn't constrain the dimension of space-time or the number of components of γ^λ),

$$\gamma_5 = i\gamma^0\gamma^1\gamma^2\gamma^3 \tag{4.61}$$

it follows that any four dimensional vector contracted with γ^λ, anti-commutes with γ_5,

$$\{\not{q}, \gamma_5\} = \{q_0\gamma^0 + q_1\gamma^1 + q_2\gamma^2 + q_3\gamma^3, i\gamma^0\gamma^1\gamma^2\gamma^3\} = 0 \tag{4.62}$$

since every component of $\not{q}$ must be anti-commuted only three times. On the other hand, since $\not{\mu}$ does not contain any $0, 1, 2, 3$ components, then it must be anti-commuted through γ_5 four times, producing an overall *commutation* relation,

$$[\not{\mu}, \gamma_5] = 0 \tag{4.63}$$

This implies that in contrast to four dimensional vectors, which change the sign of the projection operators when commuting through them ($w_{\pm}\not{q} = \not{q}w_{\mp}$), $\not{\mu}$ simply commutes through them,

$$w_{\pm}\not{\mu} = \not{\mu}w_{\pm} \tag{4.64}$$

In unitarity calculations, where loop diagrams are cut and loop particles become external particles with on-shell momenta, we will often encounter fermionic spinors with $4 - 2\epsilon$ momenta. Consider such a fermion with momentum P^λ, and denote the spinor by $|P\rangle$ (we assume it is a fermion and not an anti-fermion, for anti-fermions $m \to -m$). By the Dirac equation,

$$\not{P}|P\rangle = m|P\rangle \Rightarrow \not{p}|P\rangle = (m - \not{\mu})|P\rangle \quad \text{and} \quad \langle P|\not{P} = \langle P|m \Rightarrow \langle P|\not{p} = \langle P|(m - \not{\mu}) \tag{4.65}$$

The completeness relation for such fermions, when summing over the two spin states, is,

$$\sum_{spins} |P\rangle\langle P| = \not{P} + m = \not{p} + \not{\mu} + m \tag{4.66}$$

Integral reduction

When evaluating a one-loop Feynman diagram using the FDH scheme, all propagators take on the form $((P + k_1 + ... + k_n)^2 - m^2)^{-1}$. Taking advantage of the fact that μ^λ is orthogonal to

four dimensional vectors, these factors simplify to $((p+k_1+...+k_n)^2-m^2-\mu^2)^{-1}$, noticing again that μ^2 appears as an additive term to the squared mass. Factors of μ^λ can also appear in the numerator. An odd number of such factors will cause the integral to vanish since all pairs will be eventually contracted against each other or against four dimensional quantities, leaving a single factor to be contracted against a four dimensional quantity. Alternatively, one can argue that the integrand will be odd and for that reason vanish. An even number of μ factors will be contracted against each other, or against four dimensional quantities, in which case they vanish. Finally, we will be left to deal only with factors of μ^2. A general integral expression is thus,

$$\int \frac{d^{4-2\epsilon}P}{(2\pi)^{4-2\epsilon}}(\mu^2)^m f(p^\lambda,\mu^2) \tag{4.67}$$

where m is some positive integer. We will now show that for any m, this integral can be reduced to a higher dimensional integral with $m=0$. To this end, we split the integral into a four dimensional measure and a (-2ϵ) measure, and transform the integral over μ^λ to spherical coordinates using (2.9),

$$\begin{aligned}\int \frac{d^{4-2\epsilon}P}{(2\pi)^{4-2\epsilon}}(\mu^2)^m f(p^\lambda,\mu^2) &= \int \frac{d^4p}{(2\pi)^4}\int \frac{d^{-2\epsilon}\mu}{(2\pi)^{-2\epsilon}}(\mu^2)^m f(p^\lambda,\mu^2)\\ &= \int \frac{d^4p}{(2\pi)^4}\int d\Omega^{-2\epsilon-1}\int_0^\infty \frac{d|\mu|}{(2\pi)^{-2\epsilon}}|\mu|^{-2\epsilon-1}(\mu^2)^m f(p^\lambda,\mu^2)\\ &= \int \frac{d^4p}{(2\pi)^4}\int d\Omega^{-2\epsilon-1}\int_0^\infty \frac{d\mu^2}{2(2\pi)^{-2\epsilon}}(\mu^2)^{-\epsilon-1+m} f(p^\lambda,\mu^2)\end{aligned} \tag{4.68}$$

where in the last step we used that $d\mu^2 = 2|\mu|d|\mu|$. Since the integrand does not depend on the angle of the vector μ^λ, the angular part can be performed using (2.14),

$$\int d\Omega^{-2\epsilon-1} = \frac{2\pi^{-\epsilon}}{\Gamma(-\epsilon)} \tag{4.69}$$

The integral still contains a factor of $(\mu^2)^{-\epsilon-1+m}$ which must be somehow absorbed in the integration measure. We perform the opposite step of transforming back from spherical coordinates to Euclidean coordinates, but this time around to $2m$ dimensions higher. In $-2\epsilon+2m$ dimensions, the μ^λ integral is,

$$\begin{aligned}\int \frac{d^{-2\epsilon+2m}\mu}{(2\pi)^{-2\epsilon+2m}} &= \int d\Omega^{-2\epsilon-1+2m}\int_0^\infty \frac{d|\mu|}{(2\pi)^{-2\epsilon+2m}}|\mu|^{-2\epsilon-1+2m}\\ &= \int d\Omega^{-2\epsilon-1+2m}\int_0^\infty \frac{d\mu^2}{2(2\pi)^{-2\epsilon+2m}}(\mu^2)^{-\epsilon-1+m}\\ &= \frac{2\pi^{-\epsilon+m}}{\Gamma(-\epsilon+m)}\int_0^\infty \frac{d\mu^2}{2(2\pi)^{-2\epsilon+2m}}(\mu^2)^{-\epsilon-1+m}\end{aligned} \tag{4.70}$$

Comparing this result with the above expression (4.68), the integral can be re-expressed in higher dimensions, and finally rewritten in terms of a higher dimensional vector P,

$$\begin{aligned}\int \frac{d^{4-2\epsilon}P}{(2\pi)^{4-2\epsilon}}(\mu^2)^m f(p^\lambda,\mu^2) &= (4\pi)^m \frac{\Gamma(-\epsilon+m)}{\Gamma(-\epsilon)} \int \frac{d^4p}{(2\pi)^4} \int \frac{d^{-2\epsilon+2m}\mu}{(2\pi)^{-2\epsilon+2m}} f(p^\lambda,\mu^2) \\ &= (4\pi)^m \frac{\Gamma(-\epsilon+m)}{\Gamma(-\epsilon)} \int \frac{d^{4+2m-2\epsilon}P}{(2\pi)^{4+2m-2\epsilon}} f(p^\lambda,\mu^2) \\ &= (4\pi)^m (-\epsilon+m-1)(-\epsilon+m-2)...(-\epsilon) \int \frac{d^{4+2m-2\epsilon}P}{(2\pi)^{4+2m-2\epsilon}} f(p^\lambda,\mu^2)\end{aligned} \tag{4.71}$$

where the relation (B.5) for Gamma functions was used in the last step.

We conclude that to reduce each power of μ^2 appearing in the numerator, two dimensions must be added to the integral. In general, higher dimension integrals are more prone to UV divergences, hence the appearance of factors of ϵ which reduce the degree of divergence to that of the original four dimensional integral.

In the case $m = 1$, a single power of μ^2 in the denominator, we have the following formula,

$$I_n^{d=4-2\epsilon}[\mu^2] = -4\pi\epsilon I_n^{d=6-2\epsilon} \tag{4.72}$$

where I_n^d is a scalar Feynman integral with n propagators and a d dimensional loop momentum.

The $6-2\epsilon$ dimension scalar integral can be calculated using the same techniques as discussed in section 2.1 (since the calculation was performed in arbitrary d-dimensions). Alternatively, recursive formulas exist to express higher dimensional scalar integrals in terms of lower dimensional scalar integrals with the same number of legs and with one leg contracted. Such a formula is presented in section 4.5.

4.4.1 Example - $gg \to q\bar{q}$ tree amplitude

To demonstrate the usefulness of the extra dimensional vector μ in calculating amplitudes in d-dimensions, we now calculate the color ordered tree amplitude for a process of two positive helicity gluons and two massive quarks. The amplitude of all outgoing particles, $A_4^{tree}(-L_1, 1^+, 2^+, L_2)$, together with the two contributing diagrams, is depicted in figure 4.7.

The quark momenta are evaluated in $d = 4-2\epsilon$. This tree amplitude can then be used to construct one loop amplitudes with a quark propagating in the loop using the unitarity method. The result of this tree calculation appears in [43, 52] where it is used to construct the $gggg$ and $gggH$ loop amplitudes. We will later make use of this result in evaluating the $ggHH$ one-loop amplitude.

Capital letter momenta will stand for d dimensional momenta and will be decomposed to $P^\alpha = p^\alpha + \mu^\alpha$. From overall momentum conservation, we know that $L_1 = L_2 + k_1 + k_2$, where $L_1 = l_1 + \mu$ and $L_2 = l_2 + \mu$ (both -2ϵ components of the two D-dim vectors are equal following from choosing μ to be orthogonal to all four dimensional vectors). For convenience, external fermions will appear using the bra-ket notation. An outgoing fermion will be denoted by $\langle L|$, while an incoming fermion by $|L\rangle$.

Using the color ordered Feynman rules appearing in appendix A, the amplitude of diagram 4.7(a) is:

$$A^{(a)} = \langle -L_1|\frac{-i}{\sqrt{2}}\gamma_\rho|-L_2\rangle\frac{-i}{P^2}\frac{i}{\sqrt{2}}(g^{\nu\mu}(k_2-k_1)^\rho + g^{\rho\nu}(p-k_2)^\mu + g^{\mu\rho}(k_1-p)^\nu)\epsilon^+_{1,\mu}(2)\epsilon^+_{2,\nu}(1) \quad (4.73)$$

where $\epsilon^+_{1,\mu}(2)$ refers to a polarization vector of an outgoing gluon with positive helicity, momentum k_1 and reference momentum k_2, and is represented in the spinor helicity formalism,

$$\epsilon^+_{1,\mu}(2) = \frac{\langle 2-|\gamma_\mu|1-\rangle}{\sqrt{2}\langle 21\rangle} \quad (4.74)$$

The last four terms in the 3-gluon vertex expression vanish following the relations,

$$\begin{aligned}\epsilon^+_{1,\mu}(2)\cdot k_1 = \epsilon^+_{1,\mu}(2)\cdot k_2 = 0\\ \epsilon^+_{2,\mu}(1)\cdot k_1 = \epsilon^+_{2,\mu}(1)\cdot k_2 = 0\end{aligned} \quad (4.75)$$

The first two terms are proportional to a metric that contracts the two polarization vectors:

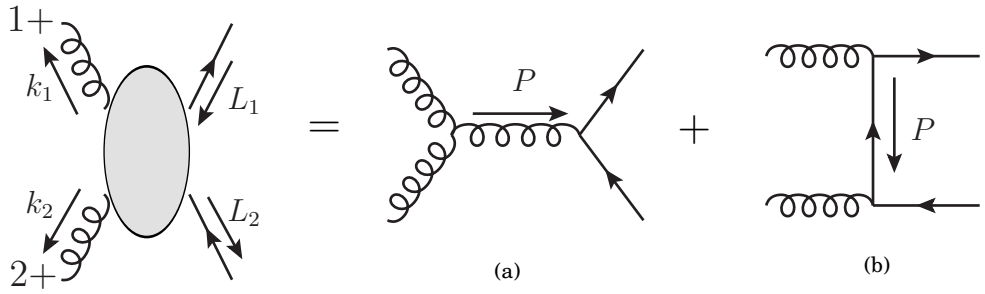

Figure 4.7: The $gg \to q\bar{q}$ color ordered tree amplitude

$$\epsilon^+_{1,\mu}(2)\cdot\epsilon_2^{+\mu}(1) = \frac{\langle 2-|\gamma_\mu|1-\rangle}{\sqrt{2}\langle 21\rangle}\frac{\langle 1-|\gamma^\mu|2-\rangle}{\sqrt{2}\langle 12\rangle}$$
$$= \frac{2\langle 21\rangle[21]}{\langle 21\rangle\langle 12\rangle} = \frac{2k_1\cdot k_2}{\langle 21\rangle^2} = \frac{P^2}{\langle 21\rangle^2} \tag{4.76}$$

where the Fierz identity was used in the second equality.

The amplitude for this diagram is,

$$A^{(a)} = \frac{-i}{2}\frac{1}{\langle 21\rangle^2}\langle -L_1|\not{k}_2-\not{k}_1|-L_2\rangle \tag{4.77}$$

The amplitude of diagram 4.7(b) is given by,

$$A^{(b)} = \langle -L_1|\frac{-i}{\sqrt{2}}\gamma_\mu\frac{i(-\not{P}+m)}{P^2-m^2}\frac{-i}{\sqrt{2}}\gamma_\nu|-L_2\rangle\epsilon_1^{+,\mu}(2)\epsilon_2^{+,\mu}(1)$$
$$= -\frac{i}{2}\langle -L_1|\not{\epsilon}_1^+(2)(-\not{P}+m)\not{\epsilon}_2^+(1)|-L_2\rangle\frac{1}{P^2-m^2} \tag{4.78}$$

Since $P = k_2 + L_2$, then $P^2 - m^2 = k_2^2 + L_2^2 + 2k_2\cdot L_2 - m^2 = 2k_2\cdot(l_2+\mu) = 2k_2\cdot l_2$, following our choice of μ being perpendicular to all four dimensional vectors. We also used the on-shellness of L_2. The expression so far is,

$$A^{(b)} = -\frac{i}{2}\langle -L_1|\not{\epsilon}_1^+(2)(-\not{k}_2-\not{l}_2-\not{\mu}+m)\not{\epsilon}_2^+(1)|-L_2\rangle\frac{1}{2k_2\cdot l_2} \tag{4.79}$$

To evaluate this expression, we use the property that $\{\not{l},\not{\mu}\} = 0$ for any four dimensional vector l^μ, to anticommute $\not{\epsilon}$ with $\not{\mu}$. We also use that,

$$\{\not{k}_2,\not{\epsilon}_2^+(1)\} = 2k_2\cdot\epsilon_2^+(1) = 0$$
$$\{\not{l}_2,\not{\epsilon}_2^+(1)\} = 2l_2\cdot\epsilon_2^+(1) \tag{4.80}$$

Using the Dirac equation in d dimensions, we can derive one more useful relation,

$$-\not{L}_2|-L_2\rangle = m|-L_2\rangle = (-\not{l}_2-\not{\mu})|-L_2\rangle \;\;\Rightarrow\;\; (\not{\mu}+m)|-L_2\rangle = -\not{l}_2|-L_2\rangle \tag{4.81}$$

Applying these relations to the amplitude, we obtain the expression,

$$A^{(b)} = \frac{-i}{2}\langle -L_1|\not{\epsilon}_1^+(2)\not{\epsilon}_2^+(1)(\not{k}_2+\not{l}_2+\not{\mu}+m) - \not{\epsilon}_1^+(2)2l_2\cdot\epsilon_2^+(1)|-L_2\rangle\frac{1}{2k_2\cdot l_2}$$
$$= \frac{-i}{2}\langle -L_1|\not{\epsilon}_1^+(2)\not{\epsilon}_2^+(1)\not{k}_2 - \not{\epsilon}_1^+(2)2l_2\cdot\epsilon_2^+(1)|-L_2\rangle\frac{1}{2k_2\cdot l_2} \tag{4.82}$$

where the term $\not{l}_2 + \not{\mu} + m$ cancels out by the Dirac equation when applied on $|-L_2\rangle$.

Consider now the expression between the d dimensional spinors. We can express the polarization vectors in terms of spinor products. This yields a trace which can be easily performed,

$$\begin{aligned}
&\not{\epsilon}_1^+(2)\not{\epsilon}_2^+(1)\not{k}_2 - \not{\epsilon}_1^+(2)2l_2\cdot\epsilon_2^+(1) \\
&= \gamma^\mu\gamma^\nu \frac{\langle 2-|\gamma_\mu|1-\rangle}{\sqrt{2}\langle 21\rangle}\frac{\langle 1-|\gamma_\nu|2-\rangle}{\sqrt{2}\langle 12\rangle}\not{k}_2 - \gamma^\mu \frac{\langle 2-|\gamma_\mu|1-\rangle}{\sqrt{2}\langle 21\rangle} 2\frac{\langle 1-|\not{l}_2|2-\rangle}{\sqrt{2}\langle 12\rangle} \\
&= \frac{1}{2}\frac{\langle 2-|\gamma_\mu|1-\rangle\langle 1-|\gamma_\nu|2-\rangle(\gamma^\mu\gamma^\nu\not{k}_2 - 2\gamma^\mu l_2^\nu)}{-\langle 21\rangle^2} \\
&= -\frac{1}{2}\frac{1}{\langle 21\rangle^2} tr[w_-\not{k}_2\gamma_\mu\not{k}_1\gamma_\nu](\gamma^\mu\gamma^\nu\not{k}_2 - 2\gamma^\mu l_2^\nu) \\
&= -\frac{1}{2}\frac{1}{\langle 21\rangle^2}(\gamma^\mu\gamma^\nu\not{k}_2 - 2\gamma^\mu l_2^\nu)2(-k_1\cdot k_2 g_{\mu\nu} + \{k_1,k_2\}_{\mu\nu} + i\epsilon_{\rho\sigma\mu\nu}k_1^\rho k_2^\sigma) \qquad (4.83) \\
&= -\frac{1}{\langle 21\rangle^2}\big[-4k_1\cdot k_2\not{k}_2 + 2k_1\cdot k_2\not{l}_2 + 2k_1\cdot k_2\not{k}_2 - 2k_2\cdot l_2\not{k}_1 - 2k_1\cdot l_2\not{k}_2 \\
&\quad + i\epsilon_{\rho\sigma\mu\nu}k_1^\rho k_2^\sigma(\gamma^\mu\gamma^\nu\not{k}_2 - 2\gamma^\mu l_2^\nu)\big]
\end{aligned}$$

where $w_- = \frac{1}{2}(1-\gamma^5)$. We can simplify the first five terms as follows,

$$\begin{aligned}
-2k_1\cdot k_2\not{k}_2 + 2k_1\cdot k_2\not{l}_2 - 2k_2\cdot l_2\not{k}_1 - 2k_1\cdot l_2\not{k}_2 &= 2k_1\cdot k_2\not{l}_2 + 2k_2\cdot(l_1-k_1)\not{k}_2 - 2k_2\cdot l_2\not{k}_1 \\
&= 2k_1\cdot k_2\not{l}_2 + 2k_2\cdot l_2(\not{k}_2 - \not{k}_1) \qquad (4.84)
\end{aligned}$$

The two terms proportional to the Levi-Civita tensor can can be re-expressed in terms of γ^5 using (C.13) and (C.14),

$$\begin{aligned}
\frac{i}{2}\epsilon_{\rho\sigma\mu\nu}(2\gamma^\mu l_2^\nu - \gamma^\mu\gamma^\nu\not{k}_2)k_1^\rho k_2^\sigma &= \frac{i}{2}\epsilon_{\rho\sigma\mu\nu}(\gamma^\mu\{\not{l}_2,\gamma^\nu\} - \gamma^\mu\gamma^\nu\not{k}_2)k_1^\rho k_2^\sigma \\
&= \frac{i}{2}\epsilon_{\rho\sigma\mu\nu}(\gamma^\mu\not{l}_2\gamma^\nu + \gamma^\mu\gamma^\nu(\not{l}_2 - \not{k}_2))k_1^\rho k_2^\sigma \\
&= \frac{1}{2}\left(\frac{1}{2}\gamma^5(\not{l}_2[\gamma_\rho,\gamma_\sigma] - [\gamma_\rho,\gamma_\sigma]\not{l}_2) + \gamma^5[\gamma_\rho,\gamma_\sigma](\not{l}_2 - \not{k}_2)\right)k_1^\rho k_2^\sigma
\end{aligned}$$

Using momentum conservation, we can replace $l_2 = l_1 - k_1 - k_2$ in the first term,

$$\begin{aligned}
&= \frac{1}{2}(\frac{1}{2}\gamma^5(\not{l}_1[\not{k}_1,\not{k}_2] - \not{k}_1[\not{k}_1,\not{k}_2] - \not{k}_2[\not{k}_1,\not{k}_2] - [\not{k}_1,\not{k}_2]\not{l}_2 + 2[\not{k}_1,\not{k}_2]\not{l}_2 - 2[\not{k}_1,\not{k}_2]\not{k}_2)) \qquad (4.85) \\
&= -\frac{1}{4}\{(-\not{l}_1)\gamma^5(-[\not{k}_1,\not{k}_2]) + \gamma^5[\not{k}_1,\not{k}_2](-\not{l}_2)\} - \frac{1}{4}\gamma^5\{\not{k}_1[\not{k}_1,\not{k}_2] + \not{k}_2[\not{k}_1,\not{k}_2] + 2[\not{k}_1,\not{k}_2]\not{k}_2\}
\end{aligned}$$

The first two terms cancel against each other when acted on by the two spinors on both sides in the full expression. $\langle -L_1|(-\not{l}_1) = \langle -L_1|(\not{\mu} + m)$ and $(-\not{l}_2)|-L_2\rangle = (\not{\mu}+m)|-L_2\rangle$.

The term $\not{\mu} + m$ can be freely commuted from one side to the other since it commutes with γ^5 and it commutes with the two four dimensional gamma matrices in $[\not{k}_1, \not{k}_2]$. Following these manipulations, the two first terms are identical with opposite signs and cancel each other.

When writing out the commutators explicitly, and using $\not{k}_i^2 = k_i^2 = 0$, the first three terms reduce to,

$$\begin{aligned}
&= -\frac{1}{4}\gamma^5\{-\not{k}_1\not{k}_2\not{k}_1 + \not{k}_2\not{k}_1\not{k}_2 - 2\not{k}_2\not{k}_1\not{k}_2\} \\
&= -\frac{1}{4}\gamma^5\{-\not{k}_1\not{k}_2\not{k}_1 - \not{k}_2\not{k}_1\not{k}_2\} \\
&= -\frac{1}{4}\gamma^5\{-2\not{k}_1 k_2 \cdot k_1 - 2\not{k}_2 k_1 \cdot k_2\} \\
&= -\frac{1}{4}\gamma^5(2k_1 \cdot k_2)(\not{l}_2 - \not{l}_1) \\
&= -\frac{1}{4}(2k_1 \cdot k_2)(\not{l}_1\gamma^5 + \gamma^5\not{l}_2) \\
&= \frac{1}{2}(2k_1 \cdot k_2)\gamma^5(\not{\mu} + m)
\end{aligned}$$

where in the last step we again applied $\not{l}_i$ on the spinors in the left and right hand side.

The final expression for this diagram is,

$$A^{(b)} = \frac{i}{2}\frac{1}{\langle 21\rangle^2}\left[\frac{-2k_1 \cdot k_2}{2k_2 \cdot l_2}\langle -L_1|(1+\gamma^5)(\not{\mu} + m)|-L_2\rangle + \langle -L_1|\not{k}_2 - \not{k}_1|-L_2\rangle\right] \tag{4.86}$$

The second term is equal to $-A^{(a)}$, and the final amplitude reduces to the simple expression,

$$\begin{aligned}
A_4^{tree}(-L_1, 1^+, 2^+, L_2) = A^{(a)} + A^{(b)} &= i\frac{[12]}{\langle 12\rangle}\frac{1}{2k_2 \cdot l_2}\langle -L_1|w_+(\not{\mu} + m)|-L_2\rangle \\
&= i\frac{[12]}{\langle 12\rangle}\frac{1}{(L_1 - k_1)^2 - m^2}\langle -L_1|w_+(\not{\mu} + m)|-L_2\rangle
\end{aligned} \tag{4.87}$$

4.5 Feynman Parameter Shift

A useful technique is introduced in [53], allowing one to reduce a tensor Feynman integral in a way other than the Passarino-Veltman reduction described in section 2.2. In loop calculations, one often encounters tensor integrals of the form,

$$I_n[p \cdot k_i] = \int \frac{d^d p}{(2\pi)^d}\frac{p \cdot k_i}{(p^2 - m^2)((p + k_1)^2 - m^2)...((p + k_1 + ... + k_{n-1})^2 - m^2)} \tag{4.88}$$

where $\{k_i\}$ is a set of outgoing external momenta. $p \cdot k_i$ can often be expressed as a difference of two inverse scalar propagators, in which case Passarino-Veltman can be straightforwardly applied to express $I_{n+1}[p \cdot k_i]$ in terms of n-point and $(n-1)$-point integrals. At other times, where this is not possible, the Feynman parameter shift method comes into use.

Let us define a general Feynman integral,

$$I_n[\mathcal{N}] = \int \frac{d^d p}{(2\pi)^d} \frac{\mathcal{N}}{(p^2 - m^2)((p+k_1)^2 - m^2)...((p+k_1+...+k_{n-1})^2 - m^2)} \tag{4.89}$$

and introduce the Feynman parameters according to the normal prescription,

$$\begin{aligned} I_n = &\int \frac{d^d p}{(2\pi)^d} \int_0^1 da_1 ... da_n \\ &\times \frac{(n-1)! \delta(1 - \sum_i a_i)}{[a_1(p^2 - m^2) + a_2((p+k_1)^2 - m^2) + ... + a_n((p+k_1+...+k_{n-1})^2 - m^2)]^n} \end{aligned} \tag{4.90}$$

Figure 4.8 depicts the case of a 4-point integral. After opening up the brackets in the denominator, the following variable redefinition must be performed to rid of all linear terms in the integration variable p,

$$p = l - (a_1(0) + a_2(k_1) + ... + a_n(k_1 + ... + k_{n-1})) \tag{4.91}$$

Let us now consider the case where $\mathcal{N}$ contains one power of p. After the parameter shift, the term linear in the new variable l will vanish (odd integral), and the remaining terms will

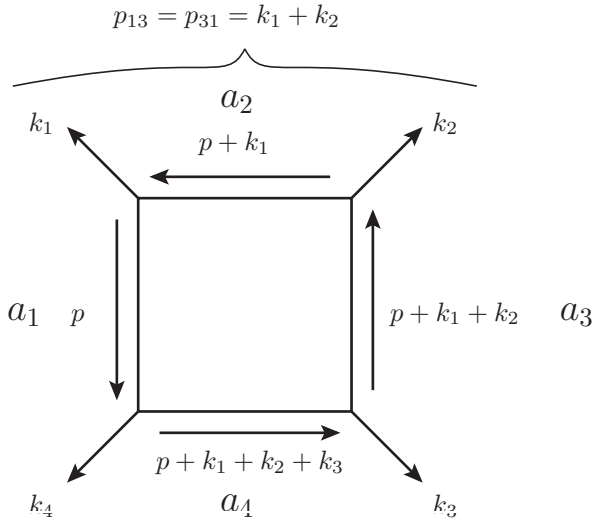

Figure 4.8: Example of a 4-point integral. All external momenta are outgoing. The Feynman parameter multiplying each leg is indicated. An example of a p_{ij} matrix element is given.

have one power of a_i in the numerator, i.e. will take the form $I_n[a_i]$.

We will now describe the formula, proven in [53], to express $I_n[a_i]$ in terms of scalar integrals $I_m[1]$, with $m = n$ or $m = n - 1$. First define a kinematical $n \times n$ matrix p_{ij}, s.t.,

$$p_{ij} = p_{ji} = k_i + k_{i+1} + ...k_{j-1}, \quad p_{ii} = 0 \tag{4.92}$$

Then define the S_{ij} matrix,

$$S_{ij} = m^2 - \frac{1}{2}(p_{ij})^2 \tag{4.93}$$

([53] treats the more general case where every leg has a different mass.)

Now one has to invert the matrix S_{ij}, and calculate the following quantities,

$$\begin{aligned} c_i &= \sum_{j=1}^{n} (S^{-1})_{ij} \\ c_0 &= \sum_{i=1}^{n} c_i \\ c_{ij} &= (S^{-1})_{ij} - \frac{c_i c_j}{c_0} \end{aligned} \tag{4.94}$$

Inverting this matrix can become quite messy and can be better calculated using a computer program such as Mathematica. In terms of these c quantities, the reduction formula is,

$$I_n[a_i] = -\frac{1}{2} \sum_{j=1}^{n} c_{ij} I_{n-1}^{(j)} + \frac{c_i}{c_0} I_n \tag{4.95}$$

where $I_{n-1}^{(j)}$ is a scalar integral with the leg multiplied by the parameter a_i eliminated. In [53, 35], a formula for $I_n[a_i a_j ... a_k]$ can be found in terms of derivatives of scalar integrals with respect to combinations of kinematical variables.

In chapter 6 we make use of this formula.

Higher dimensional integrals

In section 4.4, we saw that feynman integrals containing μ^2 in the numerator can be expressed as higher-dimensional integrals free of such factors. After introducing the S_{ij} matrix formalism, we can write out a recursive formula relating higher dimensional integrals to the familiar $4 - 2\epsilon$ dimensional integrals.

In [53, 35] such formulas are derived by solving n-point Feynman integrals with an inverse scalar propagator in the numerator in two ways. Once by simply cancelling the inverse

propagator in the numerator against the corresponding propagator, yielding an $(n-1)$-point scalar integrals. The second time, by introducing feynman parameters, yielding an n-point Feynman integral with a Feynman parameter in the numerator. Finally, summing over all possibilities of inverse propagators in the numerator, and using the fact that the sum over all Feynman parameters is one, one obtains the following recursive formula,

$$4\pi I_n^{d=6-2\epsilon} = \frac{1}{(n-5+2\epsilon)c_0}\left(2I_n^{d=4-2\epsilon} + \sum_{i=1}^{n} c_i I_{n-1}^{(i),d=4-2\epsilon}\right) \tag{4.96}$$

Similarly, for yet higher dimensions (useful for cases where $(\mu^2)^2$ appears in the denominator), the following holds,

$$4\pi I_n^{d=8-2\epsilon} = \frac{1}{(n-7+2\epsilon)c_0}\left(2I_n^{d=6-2\epsilon} + \sum_{i=1}^{n} c_i I_{n-1}^{(i),d=6-2\epsilon}\right) \tag{4.97}$$

CHAPTER 5

Mellin-Barnes Transformation

5.1 Mathematical Introduction

Feynman loop integrals gain in complexity as either the number of loops or the number of internal lines grows. Introducing masses to the internal lines removes infrared and collinear divergences, but at the same time complicates the integration over the Feynman parameters. The Mellin-Barnes transformation has been found useful in simplifying this part of the process, while introducing new integration variables that can be dealt with by contour integration methods. In essence, the Mellin-Barnes formula transforms sums of the type $(A+B)^{-a}$ into products of powers of A and B. This can be used in either transforming massive propagators to massless ones or in turning Feynman parameter integrals trivial. The mathematical technology dates back to work done by E.W. Barnes and H. Mellin in the turn of the 20th century and was first used in the context of loop integrals by Usyukina [21]. It is widely used today by various groups in tackling higher loop diagrams.

We begin with a mathematical introduction and a demonstration of the main tools [22]. As a pedagogical example, we will calculate a massive bubble diagram, demonstrating the main components of the method.

5.1.1 Hypergeometric series and function

The hypergeometric series is defined as a power series such that the ratio of successive coefficients is a rational function of n,

$$\sum_{n=0}^{\infty} a_n z^n \quad ; \quad \frac{a_{n+1}}{a_n} = \frac{A(n)}{B(n)} \tag{5.1}$$

where z is complex and $A(n)$ and $B(n)$ are polynomials in n. A finite polynomial can be in general factorized into linear pieces, $A(n) = (a_1 + n)(a_2 + n)...(a_N + n)$, where N is the polynomial degree. Any hypergeometric series can be accordingly brought to the form,

$$\begin{aligned} {}_pF_q(a_1, ..., a_p; b_1, ..., b_q; z) &= \sum_{n=0}^{\infty} \frac{(a_1)_n ... (a_p)_n}{(b_1)_n ... (b_q)_n} \frac{z^n}{n!} \\ &= \frac{\Gamma(b_1)...\Gamma(b_q)}{\Gamma(a_1)...\Gamma(a_p)} \sum_{n=0}^{\infty} \frac{\Gamma(a_1 + n)...\Gamma(a_p + n)}{\Gamma(b_1 + n)...\Gamma(b_q + n)} \frac{z^n}{n!} \end{aligned} \tag{5.2}$$

where $(a)_n = a(a+1)...(a+n-1)$ is the Pochhammer symbol and $(1)_n = n!$. In the context of the Mellin-Barnes transformation we will be interested in the following special case,

$$\frac{\Gamma(a)\Gamma(b)}{\Gamma(c)} F(a, b; c; z) = \sum_{n=0}^{\infty} \frac{\Gamma(a + n)\Gamma(b + n)}{\Gamma(c + n)} \frac{z^n}{n!} \tag{5.3}$$

which we simply denote by F. Note that F is convergent (and thus analytic) in the region $|z| < 1$.

Many known functions can be expressed as a hypergeometric series,

$$\begin{aligned} &\frac{\ln(1 - z)}{-z} = F(1, 1; 2; z) \\ &\frac{\arcsin z}{z} = F(\frac{1}{2}, \frac{1}{2}; \frac{3}{2}; z^2) \\ &\frac{1}{(1 - z)^a} = F(a, b; b; z) = \sum_{n=0}^{\infty} \frac{\Gamma(a + n)}{\Gamma(a)n!} z^n = 1 + az + \frac{a(a + 1)}{2!} z^2 + \frac{a(a + 1)(a + 2)}{3!} z^3 + ... \end{aligned} \tag{5.4}$$

We will specifically make use of the latter function. Note that while its series representation converges only in the region $|z| < 1$, the function itself converges in the entire region (connected) $z \neq 1$. The function, therefore, is an analytic continuation of the series in the region $z \neq 1$.

5.1.2 Barnes' contour integral for the hypergeometric function

We now seek an integral representation for (5.1). Begin with the following expression,

$$\frac{1}{2\pi i}\int_{-i\infty}^{i\infty}\frac{\Gamma(a+s)\Gamma(b+s)\Gamma(-s)}{\Gamma(c+s)}(-z)^s ds \tag{5.5}$$

The integrand has three sets of poles in s: $\{0,1,2,...\}$, $\{-a,-a-1,-a-2,...\}$ and $\{-b,-b-1,-b-2,...\}$, corresponding to the poles of $\Gamma(-s)$, $\Gamma(a+s)$ and $\Gamma(b+s)$, respectively. Assume that the integration path is such that the first set of poles is on the right side of the path while the other two sets are on the left side of the path.

To perform this integration using Cauchy's theorem, it is necessary to show that the integral over an arc of radius $N\to\infty$, on either the left side or the right side of the path, vanishes. To this end, it is necessary to assume for both cases that $|arg(-z)|<\pi$ (a branch cut along the positive real axis of z). Consider first the case of closing the contour by an arc on the right side of the path. It is shown in [22] that if $|z|<1$, the integral along the arc vanishes (by considering the asymptotic behaviour of the Γ functions). Then, by Cauchy's theorem, (5.5) is equal to the sum of all the residues of the poles of the integrand, which by assumption are just the poles of $\Gamma(-s)$,

$$\begin{aligned}\Gamma(-s) &= \frac{\Gamma(1-s)}{-s}=\frac{\Gamma(2-s)}{(-s)(-s+1)}=...=\frac{\Gamma(n+1-s)}{(-s)(-s+1)...(-s+n)}\\ &=(-1)^{n+1}\frac{\Gamma(n+1-2)}{s!}\frac{1}{s-n}\end{aligned} \tag{5.6}$$

In the last expression it is manifest that all poles are simple poles.

Picking up an extra minus sign because the contour is clockwise, the integral becomes,

$$\begin{aligned}(5.5) &= -\sum_{n=0}^{\infty}\frac{\Gamma(a+n)\Gamma(b+n)}{\Gamma(c+n)}(-1)^n z^n(-1)^{n+1}\frac{\Gamma(n+1-n)}{n!}\\ &=\sum_{n=0}^{\infty}\frac{\Gamma(a+n)\Gamma(b+n)}{\Gamma(c+n)}\frac{z^n}{n!}=\frac{\Gamma(a)\Gamma(b)}{\Gamma(c)}F(a,b;c;z)\end{aligned} \tag{5.7}$$

The integral (5.5) is analytic in a larger region than its series representation (5.7) which is analytic only in the region $|z|<1$. Let us find a representation in the remaining region. This is accomplished by closing the contour on the left side of the path. In this case we would have to assume that $|z|>1$ and that $a-b$ is non-integer (no overlapping poles). Similar to the previous case, it is shown in [22] that under these conditions the integral along the arc vanishes and (5.5) is the sum over all residues of poles of $\Gamma(a+n)$ and $\Gamma(b+n)$. In this region,

$$\begin{aligned}(5.5) &= \frac{\Gamma(a)\Gamma(a-b)}{\Gamma(a-c)}(-z)^a F(a,1-c+a;1-b+a;z^{-1})\\ &+\frac{\Gamma(b)\Gamma(b-a)}{\Gamma(b-c)}(-z)^b F(b,1-c+b;1-a+b;z^{-1})\end{aligned} \tag{5.8}$$

To summarize, we found that under the restriction that z is not real and positive, the hypergeometric series (5.1), analytic in the region $|z| < 1$, can be represented as the integral (5.5). In fact, this integral is analytic in a larger region and is thus an analytic continuation of the series. We additionaly found a representation for this series in the region $|z| > 1$ in terms of hypergeometric series that are functions of z^{-1}.

Special case for Feynman diagrams

For the evaluation of Feynman diagrams, we will be interested specifically in the last function in (5.4). We thus set $b = c$, and in the entire region $|arg(-z)| < \pi$ the following relation holds,

$$\frac{1}{(1-z)^a} = \frac{1}{2\pi i}\int_{-i\infty}^{i\infty} \frac{\Gamma(a+s)\Gamma(-s)}{\Gamma(a)}(-z)^s ds \tag{5.9}$$

Remember that the vertical integration path must cross the real access at $-a <$ Re $s < 0$, thus separating the poles of the two Gamma functions in the numerator.

5.1.3 Barnes' lemma

Barnes' lemma provides another useful formula in Mellin-Barnes calculations,

$$\frac{1}{2\pi i}\int_{-i\infty}^{i\infty} \Gamma(\alpha+s)\Gamma(\beta+s)\Gamma(\gamma-s)\Gamma(\delta-s)ds = \frac{\Gamma(\alpha+\gamma)+\Gamma(\alpha+\delta)+\Gamma(\beta+\gamma)+\Gamma(\beta+\delta)}{\Gamma(\alpha+\beta+\gamma+\delta)} \tag{5.10}$$

where in fact, as a corollary of this lemma, the integration path can be shifted left or right by any value. The proof appears in [22] and involves a straightforward contour integration and a summation over an infinite series of residues.

5.2 Massive Scalar Integrals

There are two different strategies to employ the Mellin-Barnes transformation in solving Feynman integrals. In the first, using (5.9), every massive propagator is rewritten as a massless propagator and an extra Mellin-Barnes integration,

$$\frac{1}{(q^2-m^2+i\epsilon)^a} = \frac{1}{\Gamma(a)}\frac{1}{2\pi i}\int_{-i\infty}^{i\infty} \frac{(-m^2)^s}{(q^2+i\epsilon)^{a+s}}\Gamma(a+s)\Gamma(-s)ds \tag{5.11}$$

After a straightforward evaluation of the simpler massless integral, the remaining Mellin-Barnes integrals are performed using either Barnes' lemma or a properly chosen contour

integration. The result can be expressed as a hypergeometric function which in simple cases can be translated into more familiar functions or in more complicated cases can be evaluated numerically. [23] applies this strategy in calculating massive bubble and triangle diagrams. In their calculation, the two propagators of the bubble or the three propagators of the triangle are raised to an arbitrary power. This can be useful, for example, for calculations in the analytic regularization scheme (see section 2.1) .

Equation (5.9) offers yet another alternative for tackling Feynman loop integrals. In chapter 2, we discussed the standard approach where first Feynman parameters are applied, followed by the momentum integration, leaving us with integrating out the Feynman parameters in the very end. The Feynman parameters were used as a tool intended to simplify the momentum integration by making the momentum dependence essentially spherical symmetric. Unfortunately, the number of parameters grows with the number of internal lines and these integrals become quite tedious.

In this strategy, the transformation is employed at a later stage, just before the Feynman parameter integrations. This scheme is neatly explained in [54]. Typically, in a dimensionally regularized one-loop integral, after introducing Feynman parameters and performing the momentum integration (see equation (B.11)) , one is left with the task of integrating a factor of $(M^2)^v$ with respect to all the Feynman parameters, where M^2 is a quadratic form in the Feynman parameters. Assume the quadratic form consists of N terms. We rewrite (5.9) in a more convenient form,

$$\frac{1}{(A+B)^v} = \frac{1}{2\pi i \Gamma(v)} \int_{-i\infty}^{i\infty} ds A^s B^{-s-v} \Gamma(v+s)\Gamma(-s) \tag{5.12}$$

Insert this identity $N-1$ times to reduce the sum of N terms in the denominator to a product of N factors. Then the Feynman parameter integration simplifies to the following beta-like function which can be expressed as a product of Gamma functions (the proof of which follows the same line as that of the beta function),

$$\int_0^1 \prod_{j=1}^{k} (dx_j x_j^{\alpha_j - 1}) \delta(1 - \sum x_i) = \frac{\Gamma(\alpha_1)...\Gamma(\alpha_k)}{\Gamma(\alpha_1 + ... + \alpha_k)} \tag{5.13}$$

Finally, we are left with the $N-1$ Mellin-Barnes integrations. At this point there is a subtlety concerning our dimensional regularization scheme. Having worked in $d = 4 - 2\epsilon$ dimensions, factors of ϵ will enter into the arguments of the various Gamma functions. If the original integral was UV or IR and collinear divergent, we expect this last integral to be so as well in the limit $\epsilon \to 0$. Tausk [24] developed a method in which we begin with ϵ in a region where the integral is manifestly finite. We then analytically continue the integral to cover the region around $\epsilon = 0$, on the way picking up residues of poles which will contain the expected divergences. The integral is then evaluated by contour integration or by Barnes'

lemma where possible.

To make this procedure clear, we perform an explicit calculation of the massive bubble integral.

Massive bubble integral

The massive bubble integral was calculated both straightforwardly and using the unitarity method in the context of the Vacuum polarization amplitude in earlier chapters. Since any tensor bubble integral can be reduced to scalar bubble (and tadpole) integrals, it will be sufficient to consider the scalar case,

$$\begin{aligned} B &= \int \frac{d^dk}{(2\pi)^d} \frac{1}{(k^2-m^2+i\epsilon)((k-p)^2-m^2+i\epsilon)} \\ &= \int \frac{d^dk}{(2\pi)^d} \int_0^1 da_1 da_2 \frac{\delta(1-a_1-a_2)}{[a_1(k^2-m^2)+a_2((k-p)^2-m^2)+i\epsilon]^2} \\ &= \int_0^1 da_1 da_2 \delta(1-a_1-a_2) \int \frac{d^dq}{(2\pi)^d} \frac{1}{[q^2-M^2+i\epsilon]^2} \end{aligned} \tag{5.14}$$

where the integration variable was shifted according to $q = k - a_2 p$, and,

$$M^2 = m^2 - a_1 a_2 s, \qquad s = p^2 \tag{5.15}$$

The momentum integration can be performed using (B.11),

$$B = \frac{i\Gamma(\epsilon)}{(4\pi)^2} \frac{1}{(4\pi)^{-\epsilon}} \int_0^1 da_1 da_2 \delta(1-a_1-a_2)(m^2-a_1a_2s)^{-\epsilon} \tag{5.16}$$

Apply (5.12) on the integrand,

$$\begin{aligned} B &= \frac{1}{2\pi i} \frac{i}{(4\pi)^2} \frac{1}{(4\pi)^{-\epsilon}} \int_0^1 da_1 da_2 \delta(1-a_1-a_2) \int_{-i\infty-k}^{i\infty-k} d\sigma (m^2)^\sigma (-s a_1 a_2)^{-\sigma-\epsilon} \Gamma_1(\sigma+\epsilon)\Gamma_2(-\sigma) \\ &= \frac{1}{2\pi i} \frac{i}{(4\pi)^2} \left(\frac{m^2}{4\pi}\right)^{-\epsilon} \int_{-i\infty-k}^{i\infty-k} d\sigma \left(\frac{m^2}{-\sigma}\right)^{\sigma+\epsilon} \Gamma_1(\sigma+\epsilon)\Gamma_2(-\sigma) \\ &\qquad \times \int_0^1 da_1 da_2 \delta(1-a_1-a_2) a_1^{-\sigma-\epsilon} a_2^{-\sigma-\epsilon} \end{aligned} \tag{5.17}$$

where we have numbered the Gamma functions for reference only. k must take some real value between $-\epsilon$ and 0 to separate the poles of Γ_1 and Γ_2. The Feynman parameters are in the desired form and the integrations can be performed using (5.12),

$$B = \frac{1}{2\pi i} \frac{i}{(4\pi)^2} \left(\frac{m^2}{4\pi}\right)^{-\epsilon} \int_{-i\infty-k}^{i\infty-k} d\sigma \left(\frac{m^2}{-\sigma}\right)^{\sigma+\epsilon} \frac{\Gamma_1(\sigma+\epsilon)\Gamma_2(-\sigma)\left(\Gamma_3(1-\sigma-\epsilon)\right)^2}{\Gamma(2-2\sigma-2\epsilon)} \tag{5.18}$$

The poles of the integrand are indicated in figure 5.1. For clarity reasons, the poles are drawn slightly off the real axis.

Note the following problem involving the dimensional regulator ϵ. The physical limit is reached when $\epsilon \to 0$. This limit cannot be taken, since the integration path crosses the real axis between $-\epsilon$ and 0. Let us assume that $k = \frac{1}{8}$ and $\epsilon = \frac{3}{8}$. In this case, the arguments of all the Gamma functions are positive, the integral does not cross any poles and is thus finite (the integrand is well behaved at $\sigma \to i\infty$ and $\sigma \to -i\infty$). This agrees with the fact that the original Feynman integral was well behaved at this value of ϵ, i.e. the divergence was regularized.

To reach the physical limit, we follow the method devised by Tausk [24]. Shift the integration path to the left past the first pole of Γ_1 at $-\epsilon$, for example to $k = \frac{1}{2}$. See figure 5.1. The contour around this pole contributes the residue of the integrand at $\sigma = -\epsilon$. This is easily calculated and contributes,

$$R = \frac{1}{2\pi i} \frac{i}{(4\pi)^2} \left(\frac{m^2}{4\pi} \right)^{-\epsilon} \Gamma(\epsilon) \tag{5.19}$$

The integral is at this point equal to,

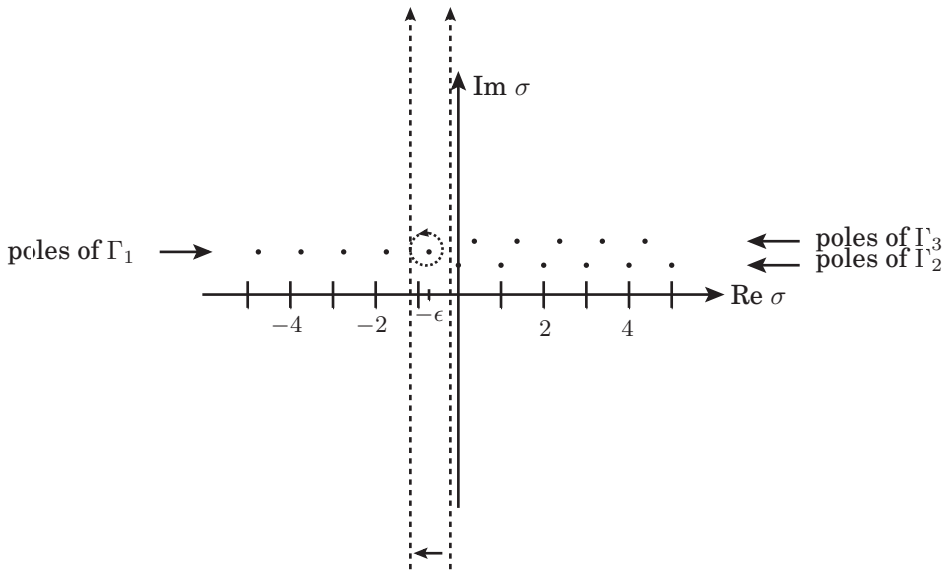

Figure 5.1: The pole structure of the Mellin-Barnes integral. All poles are on the real axis and are shifted upwards for clarity. The integration path spans from $(-i\infty - k)$ to $(i\infty - k)$, where k is real and takes some value between $-\epsilon$ and 0. When the integration path is shifted to the left of the first pole, $\sigma = -\epsilon$, the residue is picked by the loop surrounding the pole.

$$B = \frac{1}{2\pi i}\frac{i}{(4\pi)^2}\left(\frac{m^2}{4\pi}\right)^{-\epsilon}\int_{-i\infty-\frac{1}{2}}^{i\infty-\frac{1}{2}} d\sigma \left(\frac{m^2}{-\sigma}\right)^{\sigma+\epsilon}\frac{\Gamma_1(\sigma+\epsilon)\Gamma_2(-\sigma)\left(\Gamma_3(1-\sigma-\epsilon)\right)^2}{\Gamma(2-2\sigma-2\epsilon)} + R \quad (5.20)$$

The complete UV divergence now lies in the term R. We can now safely take the limit $\epsilon \to 0$ and evaluate the integral by closing the contour to the left and picking up the poles at all negative integer values of σ.

$$B = \frac{i}{(4\pi)^2}\left(\frac{m^2}{4\pi}\right)^{-\epsilon}\sum_{n=1}^{\infty}\left(\frac{m^2}{-s}\right)^{-n}\frac{(-1)^n}{n!}\frac{\Gamma(n)\Gamma(1+n)\Gamma(1+n)}{\Gamma(2+2n)} + R \quad (5.21)$$

where the residue of $\Gamma(\sigma)$ at $\sigma = -n$ is $\frac{(-1)^n}{n!}$. We use the formula $\Gamma(2z) = 2^{2z-1}\pi^{-1/2}\Gamma(z)\Gamma(z+1/2)$ to split the denominator. This gives,

$$\begin{aligned} B &= \frac{i}{(4\pi)^2}\left(\frac{m^2}{4\pi}\right)^{-\epsilon}\sum_{n=1}^{\infty}\left(\frac{s}{4m^2}\right)^n\frac{\sqrt{\pi}}{2}\frac{\Gamma(n)\Gamma(1+n)}{\Gamma(\frac{3}{2}+n)n!} + R \\ &= \frac{i}{(4\pi)^2}\left(\frac{m^2}{4\pi}\right)^{-\epsilon}\frac{\sqrt{\pi}}{2}\frac{s}{4m^2}\sum_{m=0}^{\infty}\left(\frac{s}{4m^2}\right)^m\frac{\Gamma(1+m)\Gamma(1+m)}{\Gamma(\frac{5}{2}+m)m!} + R \\ &= \frac{i}{(4\pi)^2}\left(\frac{m^2}{4\pi}\right)^{-\epsilon}\frac{\sqrt{\pi}}{2}\frac{s}{4m^2}\frac{1}{\Gamma(\frac{5}{2})}F(1,1;\frac{5}{2};\frac{s}{4m^2}) + R \end{aligned} \quad (5.22)$$

where $(1+m)\Gamma(1+m) = \Gamma(2+m)$. The hypergeometric function can be found in mathematical handbooks (such as [55]) or evaluated using Mathematica. The result is,

$$\begin{aligned} B &= \frac{i}{(4\pi)^2}\left(\frac{m^2}{4\pi}\right)^{-\epsilon}\left(\Gamma(\epsilon) + 2 - 2\sqrt{\frac{1}{r}-1}\sin^{-1}\sqrt{r}\right) \\ &= \frac{i}{(4\pi)^2}\left(\frac{1}{\epsilon} - \gamma_E - \ln 4\pi - \ln m^2 + 2 - 2\sqrt{\frac{1}{r}-1}\sin^{-1}\sqrt{r}\right) + \mathcal{O}(\epsilon) \end{aligned} \quad (5.23)$$

where $r = \frac{s}{4m^2}$. This result agrees with a calculation using the methods of section 2.1.3. In contrast to a direct calculation, this calculation evades any complicated integrals. In this case, it was simple to express the hypergeometric functions as known functions. In the general case, it is not possible and the result can be left as a hypergeometric representation, which can be evaluated numerically to obtain cross sections.

CHAPTER 6

Higgs Pair Production, $gg \to HH$

As a final example demonstrating the methods introduced throughout this thesis, we calculate the leading order contribution to the process of double Higgs production through gluon fusion. This process is of potential interest in the upcoming LHC proton collider experiment and future experiments, since it provides a possible channel for measuring the Higgs self coupling vertex of the Standard Model. Various studies have been carried out on this topic [56, 57, 58].

The Yukawa coupling terms, which following spontaneous symmetry breaking give mass to the fermions, couples the Higgs scalar particle to fermions through a three-vertex. The coupling strength is proportional to $\frac{m_q}{v}$, the quark mass divided by the Higgs vacuum expectation value. The Higgs potential, which is responsible for the symmetry breaking and thus

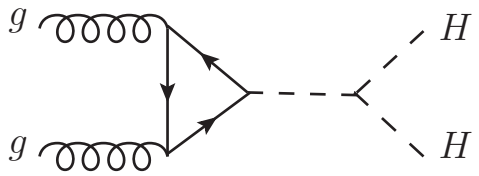

Figure 6.1: Leading order diagram, containing a Higgs self-coupling vertex, of the double Higgs production through gluon fusion process. Reversing the flow of charge yields a second diagram.

invaluable to the electroweak model, generates a self interaction of three Higgs particles proportional to λv, where λ is the coupling constant of the Higgs scalar doublet field before symmetry breaking. These two vertices, together with the normal QCD vertices, give rise to the leading order diagram shown in figure 6.1. This diagram carries an overall constant factor of $g_s^2 \lambda m_q$, where g_s is the strong coupling constant.

An important background to this process is the production of two Higgs particles through a fermionic box diagram. The contributions of these diagrams to the cross section must be subtracted from the overall signal if one was to measure the Higgs self coupling constant. The Six possible diagrams, all of order $g_s^2 \frac{m_q^2}{v^2}$, are depicted in figure 6.2. Two extra diagrams, containing a triangle quark loop connected to a three gluon vertex, vanish as a result of a trace over a single color matrix.

In this chapter we will calculate the contribution of these box diagrams to the amplitude. All six diagrams contain a color factor of $tr[T^a T^b]$ which we leave out for the moment. Since we are dealing with two external Higgs particles that do not carry color charge, the partial amplitude is not color ordered and we must consider all orderings of external legs. The amplitude will be derived by taking advantage of the unitarity method, i.e. taking various cuts of the amplitude and fixing the coefficients of an expansion in base integrals, as discussed in section 3.4. We will carry a complete calculation of the case where both gluons have positive helicity, $A_4^{1-loop}(1+, 2+, 3_H, 4_H)$. For brevity, we omit the particle specification and refer to the amplitude as A_4^{1-loop}.

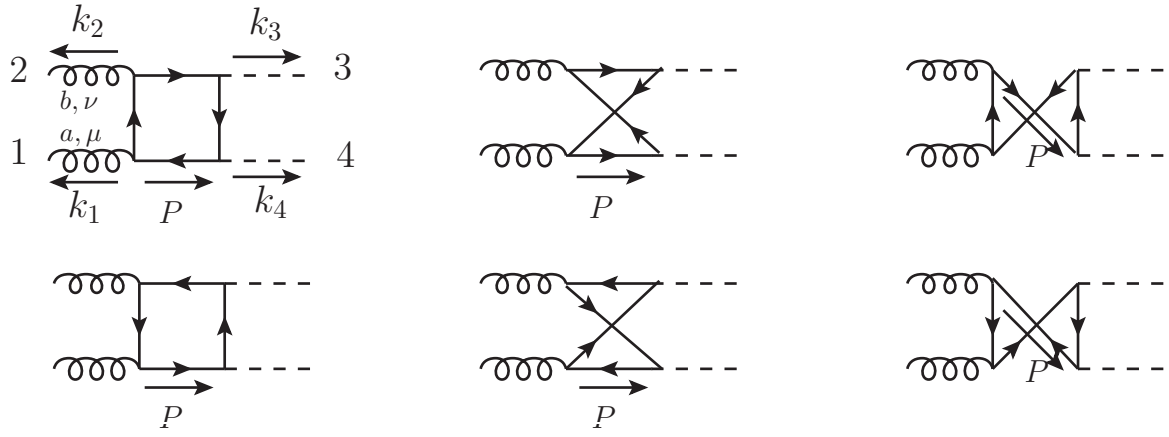

Figure 6.2: Leading order box diagrams to the double Higgs production process.

6.1 Integral Basis

From the diagrams in figure 6.2, and following a convenient choice of the loop momentum P, we deduce that there are six different scalar propagators appearing in the six diagrams. By this we mean that following Passarino-Veltman reduction, scalar Feynman integrals containing only these propagators will appear. The possible denominators are,

$$\begin{aligned} d_1 &= P^2 - m^2 \\ d_2 &= (P + k_1)^2 - m^2 \\ d_3 &= (P + k_2)^2 - m^2 \\ d_4 &= (P + k_1 + k_2)^2 - m^2 \\ d_5 &= (P + k_1 + k_3)^2 - m^2 \\ d_6 &= (P + k_1 + k_2 + k_3)^2 - m^2 \end{aligned} \tag{6.1}$$

The final amplitude we obtain should not be UV divergent, since this is the leading order contribution and no counter terms exist that could potentially cancel the divergences. We also don't expect any IR or collinear divergences, since all internal legs are massive. Nevertheless, it would be wise to work in dimensional regularization in case any intermediate divergences appear. We choose the FDH scheme, as introduced in section 4.4. The loop momentum P is a $4 - 2\epsilon$ vector, while all external vectors are four dimensional.

We denote the integrals constructed from the above six propagators by $I_{i..k}$, where the subscript refers to the propagators present, e.g.,

$$I_{1256} = \frac{1}{d_1 d_2 d_5 d_6} \tag{6.2}$$

where for convenience we suppress the integral.

From figure 6.2, it is apparent that only three possible box scalar integrals can appear, these correspond to "non-reduced" integrals. A single Passarino-Veltman reduction can remove one of the propagators, resulting in a triangle diagram. Excluding multiplicities, 12 such triangles can occur. The 15 possible box and triangle diagrams are explicitly listed in figure 6.3. Similarly, one further PV reduction leaves us with 12 possible bubble diagrams, and a final reduction step can potentially generate 6 different tad-poles, corresponding to the 6 different propagators. All the tadpole integrals are equal, since they are related by a momentum shift. They depend only on the squared mass of the quark, m^2.

Let us take for a moment a closer look at the triangle diagrams. Note that in figure 6.3 there are two different triangle integrals with external legs 1 and 4 contracted. These diagrams seem to be identical up to a reflection, yet one of them contains propagators 2, 4

and 6, while the other contains propagators 2, 5 and 6. Written out, these integrals are,

$$I_{246} = \frac{1}{[(P+k_1)^2 - m^2][(P+k_1+k_2)^2 - m^2][(P+k_1+k_2+k_3)^2 - m^2]}$$
$$I_{256} = \frac{1}{[(P+k_1)^2 - m^2][(P+k_1+k_3)^2 - m^2][(P+k_1+k_2+k_3)^2 - m^2]} \tag{6.3}$$

Now notice that under the substitution $P + k_1 \to -P - k_1 - k_2 - k_3$, the first integral is transformed into the second integral. Such pairs containing the same set of contracted legs are thus identical.

Now let us choose the following two triangle integrals: one with external legs 2 and 3

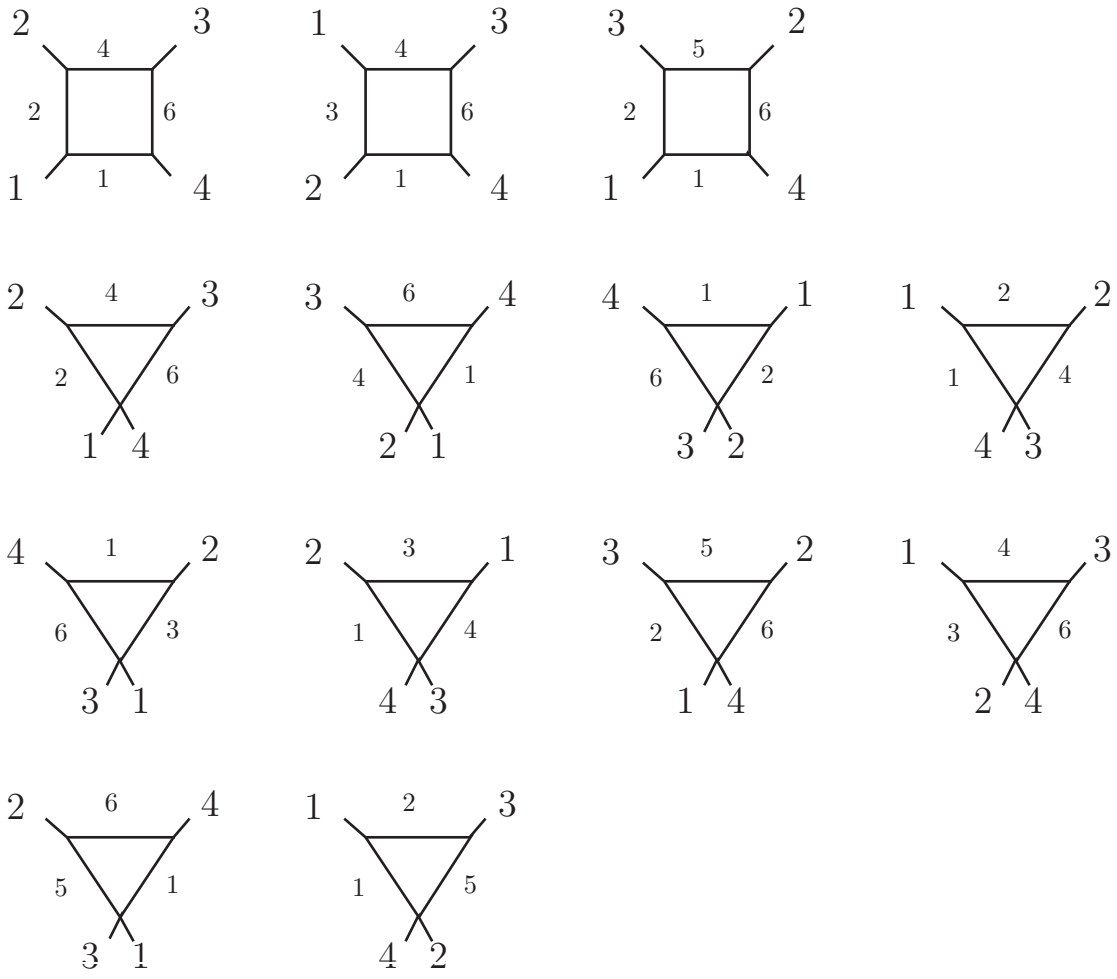

Figure 6.3: List of all possible box and triangle scalar integrals that can appear after PV reduction. The larger numbers refers to the numbering of the external legs, while the smaller numbers refer to the propagator number.

contracted and one with external legs 1 and 4 contracted. For example,

$$I_{126} = \frac{1}{[P^2 - m^2][(P + k_1)^2 - m^2][(P - k_4)^2 - m^2]}$$
$$I_{246} = \frac{1}{[(P + k_1)^2 - m^2][(P + k_1 + k_2)^2 - m^2][(P + k_1 + k_2 + k_3)^2 - m^2]} \tag{6.4}$$

where $k_4 = -k_1 - k_2 - k_3$. Notice that if we perform the substitution $P + k_1 + k_2 \to -P$, we get,

$$I_{126} = \frac{1}{[P^2 - m^2][(P + k_1)^2 - m^2][(P - k_4)^2 - m^2]}$$
$$I_{246} = \frac{1}{[P^2 - m^2][(P + k_2)^2 - m^2][(P - k_3)^2 - m^2]} \tag{6.5}$$

Both integrals are Lorentz scalars. The first integral, for example, can only depend on k_1^2, k_4^2, $k_1 \cdot k_4$ and m^2. Since $k_1^2 = k_2^2$, $k_4^2 = k_3^2$ and $k_1 \cdot k_4 = k_2 \cdot k_3$, then the integrals must be identical.

Using these identifications of integrals, we can reduce the 12 triangle integrals to 4. Following the notation of [56], we denote these integrals by the letter C and by the momenta of the two non-contracted legs, i.e.,

$$C(k_1, k_2) = \frac{1}{[P^2 - m^2][(P + k_1)^2 - m^2][(P + k_1 + k_2)^2 - m^2]} \tag{6.6}$$

In this notation, the four independent integrals are,

$$C(k_1, k_2) \quad C(k_3, k_4) \quad C(k_1, k_3) \quad C(k_2, k_3) \tag{6.7}$$

The box integrals will be denoted by the letter D and the three external legs following the propagator d_1, i.e.,

$$D(k_1, k_2, k_3) = \frac{1}{[P^2 - m^2][(P + k_1)^2 - m^2][(P + k_1 + k_2)^2 - m^2][(P + k_1 + k_2 + k_3)^2 - m^2]} \tag{6.8}$$

The three possible boxes are,

$$D(k_1, k_2, k_3) \quad D(k_2, k_1, k_3) \quad D(k_1, k_3, k_2) \tag{6.9}$$

We denote the bubble integrals by the letter B, and let them be a function of the squared momentum of one of the external legs,

$$B(k_1^2) = \frac{1}{[P^2 - m^2][(P + k_1)^2 - m^2]} \tag{6.10}$$

The 12 different bubble integrals are thus reduced to the following 5,

$$B(s) \quad B(t) \quad B(u) \quad B(0) \quad B(M_H^2) \tag{6.11}$$

The single tadpole will be denoted by the letter A.

Having set up the basis, we are now ready to calculate the coefficients of the 13 basis integrals.

6.2 Unitarity

In chapter 3 we have seen that by taking advantage of the unitarity condition on the S-matrix, expression (3.7) can be derived, relating the imaginary part of an amplitude with respect to some cut to the gluing of two tree amplitudes along that cut. By cut, it is meant that some subset of the external particles are taken to be incoming (and the others outgoing). When the invariant formed by the incoming momenta becomes large enough, the amplitude will typically develop an imaginary part. For example, in a $2 \to 2$ process, possible cuts are s, t and u, or a decay of any one of the particles.

For each cut, we slice the amplitude such that the incoming particles are on the left side and the outgoing on the right, thus obtaining two new amplitudes. The particles in the loop, which are now flowing through the cut, are placed on shell. These particles become outgoing external particles of a tree level amplitude to the left of the cut and incoming external particles of a tree amplitude to the right of the cut. We will see that the on-shellness of the loop particles is a powerful feature, significantly simplifying expressions at intermediate stages. The product of the two tree amplitudes is integrated over all of phase space (since the particles are one shell), and summed over all possible spins or helicities (also color and flavor where relevant).

The procedure will become clearer as we use it to calculate the amplitude of the present process. As discussed in section 3.4, since we have already expanded the amplitude in a base of integrals, we can use this procedure to fix the coefficients of the expansion, thus obtaining the full amplitude and not merely its imaginary part. Let us begin with the s-cut. We follow a similar path to that taken in [52], where the $gg \to gH$ amplitude was calculated.

s-cut

The s-cut corresponds to taking particles 1 and 2 to be incoming and particles 3 and 4 to be outgoing. The relevant Mandelstam variable is $s = (k_1 + k_2)^2$, the squared sum of the incoming momenta. If we consider this process in the center of mass frame of reference of

the two incoming particles, then $s = 4E^2$, where E is the energy of one of the incoming gluons. For this physical process, therefore, s is always positive. When s is large enough, we expect the amplitude to develop an imaginary part.

This cut is portrayed in figure 6.4. In fact, we must consider all possible amplitudes where two gluons scatter into n particles and then the same n particles scatter into 2 Higgs particles. Since we are only interested in the one loop contribution to this process, i.e. the $g_s^2 \frac{m_q^2}{v^2}$ order, then only the tree amplitudes presented in the figure are relevant. For higher orders, we should also consider larger tree and loop amplitudes on each side of the cut.

Our task is to calculate the two tree amplitudes on both sides of the cut and then plug them into (3.46). We will simplify the expression obtained by removing all loop momenta from the numerator. This will allow us to identify the scalar integrals and their coefficients.

Three different diagrams contribute to the left tree amplitude in figure 6.4, these appear in figure 6.5. Diagram 6.5(c) does not contribute since it contains a color matrix that will later be contracted with a Kronecker delta in color space coming from the amplitude to the right of the cut. This will result in a vanishing trace over a single color matrix. Diagram 6.5(a) was previously calculated, up to a factor 2, and its contribution is given by equation (4.86). The factor 2 results from the fact that (4.86) was calculated using color ordered Feynman rules, whereas here we use the usual Feynman rules. The relevant Feynman rules are identical up to a factor of $-\frac{1}{\sqrt{2}}$ appearing in each vertex. Diagram 6.5(b) can be obtained from diagram 6.5(a) by the substitution $1 \leftrightarrow 2$. The resulting amplitude is,

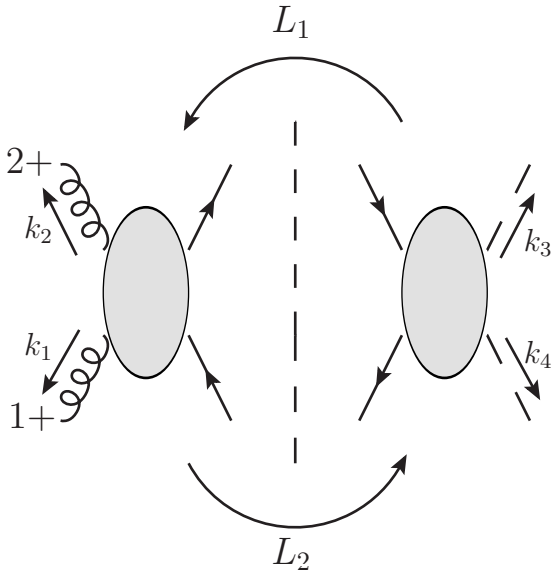

Figure 6.4: s-cut of the $gg \to HH$ amplitude.

$$A^{left} = 2ig_s^2 \frac{[12]}{\langle 12\rangle}\left[\frac{1}{(L_1-k_1)^2-m^2}+\frac{1}{(L_1-k_2)^2-m^2}\right]\langle -L_1|w_+(\not{\mu}+m)|-L_2\rangle \tag{6.12}$$

We recall that the spinor helicity representation of the polarization vectors was used for this calculation,

$$\epsilon^+_{1,\mu}(2) = \frac{\langle 2-|\gamma_\mu|1-\rangle}{\sqrt{2}\langle 21\rangle}, \qquad \epsilon^+_{2,\mu}(1) = \frac{\langle 1-|\gamma_\mu|2-\rangle}{\sqrt{2}\langle 12\rangle} \tag{6.13}$$

where k_2 was chosen as the reference momentum for the polarization vector $\epsilon^+_{1,\mu}$ of particle $1+$, and k_1 was chosen as the polarization vector for $2+$. Each tree amplitude we calculate in this chapter is independently gauge invariant, and we are free to choose different reference momenta in each case. In practice, this choice is suitable in all cases. For brevity, we will write ϵ_i to denote the polarization vector of particle i, recalling that it has positive helicity and the aforementioned reference momentum.

Two diagrams contribute to the amplitude to the right side of the cut, these are shown in figure 6.6. These can be easily calculated, yielding the amplitude,

$$\begin{aligned} A^{right} &= \left(-i\frac{m}{v}\right)^2 \langle -L_2|\frac{i(-\not{L}_1-\not{k}_3+m)}{(L_1+k_3)^2-m^2}+\frac{i(-\not{L}_1-\not{k}_4+m)}{(L_1+k_4)^2-m^2}|-L_1\rangle \\ &= i\frac{m^2}{v^2}\langle -L_2|\frac{\not{k}_3-2m}{(L_1+k_3)^2-m^2}+\frac{\not{k}_4-2m}{(L_1+k_4)^2-m^2}|-L_1\rangle \end{aligned} \tag{6.14}$$

We may now plug the two tree amplitude into (3.49), allowing us to identify the coefficients of all base integrals containing an s-cut,

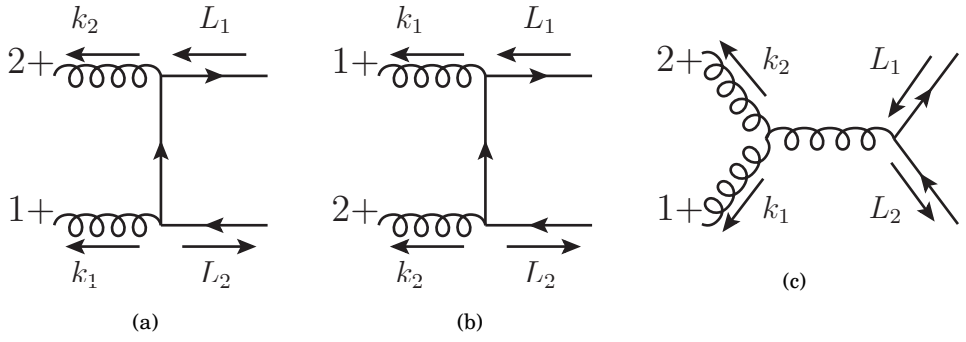

Figure 6.5: Diagram contributing to the tree amplitude to the left of the s-cut.

$$
\begin{aligned}
&A_4^{1-loop}\big|_{s-cut} \\
&= \frac{2g_s^2 m^2}{v^2}\frac{[12]}{\langle 12\rangle}\sum_{helicity}\int\frac{d^dL_1}{(2\pi)^d}\frac{1}{(L_2^2-m^2)(L_1^2-m^2)}\left(\frac{1}{(L_1-k_1)^2-m^2}+\frac{1}{(L_1-k_2)^2-m^2}\right) \\
&\times\langle -L_1|w_+(\not{\mu}+m)|-L_2\rangle\langle -L_2|\frac{\not{k}_3-2m}{(L_1+k_3)^2-m^2}+\frac{\not{k}_4-2m}{(L_1+k_4)^2-m^2}|-L_1\rangle\big|_{s-cut}
\end{aligned}
\tag{6.15}
$$

After summing over helicities, four different traces are obtained, each with a different set of propagators,

$$
\begin{aligned}
&A_4^{1-loop}\big|_{s-cut} \\
&= \frac{2g_s^2 m^2}{v^2}\frac{[12]}{\langle 12\rangle}\int\frac{d^dL_1}{(2\pi)^d}\Big\{\frac{tr[w_+(\not{\mu}+m)(-\not{L}_2+m)(\not{k}_3-2m)(-\not{L}_1+m)]}{(L_2^2-m^2)(L_1^2-m^2)((L_1-k_1)^2-m^2)((L_1+k_3)^2-m^2)} \\
&+\frac{tr[w_+(\not{\mu}+m)(-\not{L}_2+m)(\not{k}_4-2m)(-\not{L}_1+m)]}{(L_2^2-m^2)(L_1^2-m^2)((L_1-k_1)^2-m^2)((L_1+k_4)^2-m^2)} \\
&+\frac{tr[w_+(\not{\mu}+m)(-\not{L}_2+m)(\not{k}_3-2m)(-\not{L}_1+m)]}{(L_2^2-m^2)(L_1^2-m^2)((L_1-k_2)^2-m^2)((L_1+k_3)^2-m^2)} \\
&+\frac{tr[w_+(\not{\mu}+m)(-\not{L}_2+m)(\not{k}_4-2m)(-\not{L}_1+m)]}{(L_2^2-m^2)(L_1^2-m^2)((L_1-k_2)^2-m^2)((L_1+k_4)^2-m^2)}\Big\}\big|_{s-cut}
\end{aligned}
\tag{6.16}
$$

We would now like to identify the denominator of each term with the denominator of one of our three basis box integrals. To this end, we are allowed to shift or reflect our loop momenta. In the case of reflection, we must take care to only reflect the four dimensional part, in which case the Jacobian is trivial. Recall that $L_1 = l_1 + \mu$ and $l_1 = l_2 + k_1 + k_2$. If in the first term we perform the shift $l_1 = p + k_1 + k_2$, then the denominator take the form,

$$
(P^2-m^2)((P+k_1+k_2)^2-m^2)((P+k_2)^2-m^2)((P+k_1+k_2+k_3)^2-m^2) \tag{6.17}
$$

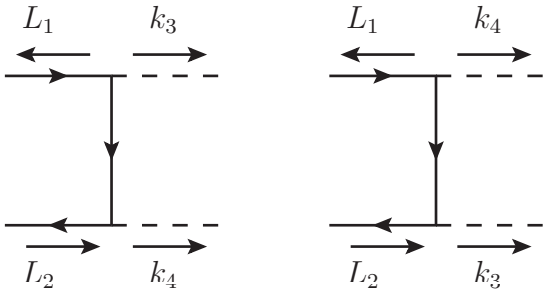

Figure 6.6: Diagram contributing to the tree amplitude to the right of the s-cut.

which is simply the denominator of the basis integral I_{1346}. The same shift can be performed on the third term, while the second and fourth term get reflected according to $l_1 = -p$. In each case, the numerators have to be shifted accordingly, yielding,

$$\begin{aligned}
&A_4^{1-loop}\big|_{s-cut} \\
&= \frac{2g_s^2 m^2}{v^2}\frac{[12]}{\langle 12\rangle}\{I_{1346}[tr_+((\not{\mu}+m)(-\not{p}-\not{\mu}+m)(\not{k}_3-2m)(-\not{p}-\not{\mu}-\not{k}_1-\not{k}_2+m))] \\
&+I_{1246}[tr_+((\not{\mu}+m)(\not{p}-\not{\mu}+\not{k}_1+\not{k}_2+m)(\not{k}_4-2m)(\not{p}-\not{\mu}+m))] \\
&+I_{1246}[tr_+((\not{\mu}+m)(-\not{p}-\not{\mu}+m)(\not{k}_3-2m)(-\not{p}-\not{\mu}-\not{k}_1-\not{k}_2+m))] \\
&+I_{1346}[tr_+((\not{\mu}+m)(\not{p}-\not{\mu}+\not{k}_1+\not{k}_2+m)(\not{k}_4-2m)(\not{p}-\not{\mu}+m))]\}\big|_{s-cut}
\end{aligned} \tag{6.18}$$

where the notation $I_{1246}[\mathcal{N}]$ stands for scalar integral I_{1246} with the 1 in the numerator replaced by the expression $\mathcal{N}$ in the square brackets. tr_+ stands for $tr[w_+...]$.

Let us now take a closer look at one of these traces. Using the fact that $\not{\mu}$ anticommutes with any gamma matrix contracted with a four dimensional vector, we can bring all $\not{\mu}$'s to be adjacent. Then we can apply $\not{\mu}\not{\mu} = -\mu^2$, and drop any term containing a single non-contracted μ factor, since the integrand would be odd in μ. Consider the first trace,

$$\begin{aligned}
&tr_+[(\not{\mu}+m)(-\not{p}-\not{\mu}+m)(\not{k}_3-2m)(-\not{p}-\not{\mu}-\not{k}_1-\not{k}_2+m)] \\
&= tr_+[\not{\mu}(-\not{\mu})(\not{k}_3-2m)(-\not{p}-\not{k}_1-\not{k}_2+m)+\not{\mu}(-\not{p}+m)(\not{k}_3-2m)(-\not{\mu}) \\
&\quad +m(-\not{\mu})(\not{k}_3-2m)(-\not{\mu})+m(-\not{p}+m)(\not{k}_3-2m)(-\not{p}-\not{k}_1-\not{k}_2+m)] \\
&= (m^2+\mu^2)tr_+[-\not{k}_3\not{p}-\not{p}\not{k}_3-\not{k}_3\not{k}_1-\not{k}_3\not{k}_2-2m^2]-2m^2 tr_+[\not{p}\not{p}+\not{p}\not{k}_1+\not{p}\not{k}_2]
\end{aligned} \tag{6.19}$$

In the last step, all odd occurrences of gamma matrices were dropped. Finally, we can perform the trace. All terms containing a γ_5 cancel, since there is a maximum of two gamma matrices,

$$tr_+(...) = -2(m^2+\mu^2)(2p\cdot k3 + k_3\cdot k_1 + k_3\cdot k_2 + 2m^2) - 4m^2(p\cdot p + p\cdot k_1 + p\cdot k_2) \tag{6.20}$$

We can use Passarino-Veltman reduction to remove p's from the denominator. Since we are dealing with the first term in (6.18), the propagators $(d_1 d_3 d_4 d_6)$ are available for the reduction,

$$\begin{aligned}
p\cdot p &= d_1 + m^2 + \mu^2 \\
2p\cdot k_1 &= d_4 - d_3 - 2k_1\cdot k_2 \\
2p\cdot k_2 &= d_3 - d_1 \\
2p\cdot k_3 &= d_6 - d_4 - 2k_1\cdot k_3 - 2k_2\cdot k_3 - M_H^2
\end{aligned} \tag{6.21}$$

We also apply the kinematic relations,

$$2k_3 \cdot k_1 = u - M_H^2$$
$$2k_3 \cdot k_2 = t - M_H^2 \tag{6.22}$$

Putting it all together, the first term in (6.18) reduces to,

$$I_{1346}[tr_+(...)] = I_{1346}[(m^2+\mu^2)(-s+2M_H^2-8m^2)+2m^2 s] - 2I_{134}[m^2+\mu^2] + 2I_{136}[\mu^2] - 2I_{346}[m^2] \tag{6.23}$$

Following the same steps for the three other terms, (6.18) becomes,

$$\begin{aligned} A_4^{1-loop}\big|_{s-cut} = \frac{2g_s^2 m^2}{v^2}\frac{[12]}{\langle 12\rangle}\Big\{ & I_{1246}[(m^2+\mu^2)(-2s+4M_H^2-16m^2)+4m^2 s] \\ & + I_{1346}[(m^2+\mu^2)(-2s+4M_H^2-16m^2)+4m^2 s] \\ & - 4I_{124}[m^2+\mu^2] - 4I_{134}[m^2+\mu^2] + 2I_{246}[\mu^2-m^2] \\ & + 2I_{346}[\mu^2-m^2] + 2I_{126}[\mu^2-m^2] + 2I_{136}[\mu^2-m^2]\Big\}\big|_{s-cut} \end{aligned} \tag{6.24}$$

The s-cut on the right hand side of the equation amounts to cancelling all scalar integrals that cannot be cut such that particles 1 and 2 would remain on one side of the cut. This originates from the fact that in the cut, we placed the two quarks on shell (see (3.46)), causing occurrences of d_1 and d_4 in the numerator to vanish. If we would have performed this step in (6.20), integrals I_{246}, I_{346}, I_{126} and I_{136} would have not appeared. Alternatively, we took the path of ignoring this "on-shellness" and applying the cut in this last step.

At this point, since all integrals are scalar integrals, we can identify them with our basis integrals. As explained in the beginning of this chapter, integrals I_{124} and I_{134} are equal to each other and can be both identified with basis integral $C(k_1,k_2)$. We thus get,

$$\begin{aligned} A_4^{1-loop}\big|_{s-cut} = \frac{g_s^2 m^2}{v^2}\frac{[12]}{\langle 12\rangle}\Big\{ & D(k_1,k_2,k_3)[(m^2+\mu^2)(-4s+8M_H^2-32m^2)+8m^2 s] \\ & + D(k_2,k_1,k_3)[(m^2+\mu^2)(-4s+8M_H^2-32m^2)+8m^2 s] - 16C(k_1,k_2)[m^2+\mu^2]\Big\} \end{aligned} \tag{6.25}$$

We have managed fixed all the coefficients of integrals which contain an s-cut. This includes the integrals $C(k3,k4)$ and $B(s)$ which do not appear in our expression and thus have a vanishing coefficient. We are still left with the integration over the μ^2 terms in the numerator. We will tackle this problem in the end.

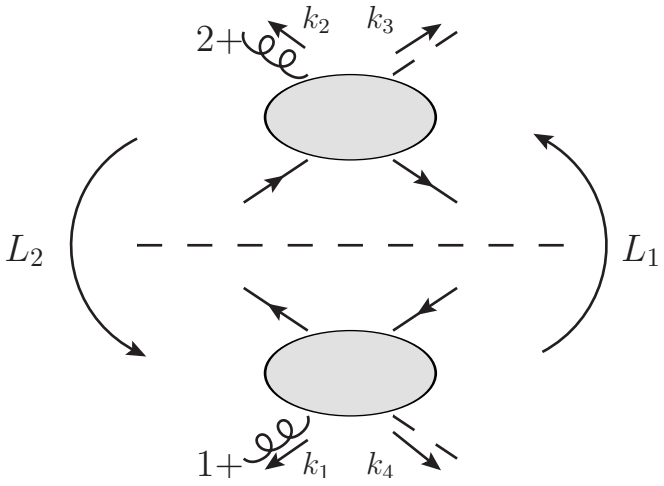

Figure 6.7: t-cut of the $gg \to HH$ amplitude.

t-cut

The t-cut is slightly more complicated and will require applying some more of the tools introduced earlier. The main cause for the extra intricacy is the fact that the external gluon lines lie on opposite sides of the cut. This prevents us from simplifying the tree level expressions, leaving the simplification to be done only after the gluing.

The diagrams contributing to the tree level amplitude located above the cut appear in figure 6.8. These are easily evaluated, yielding,

$$\begin{aligned} A^{top} &= \langle -L_1|(-i\frac{m}{v})\frac{i(\not{k}_4 - \not{L}_1 + m)}{(L_1-k_4)^2-m^2}(ig_s\not{\epsilon}_1) + (ig_s\not{\epsilon}_1)\frac{i(-\not{k}_4 - \not{L}_2 + m)}{(L_1-k_1)^2-m^2}(-i\frac{m}{v})| - L_2\rangle \\ &= \frac{ig_s m}{v}\langle -L_1|\frac{(\not{k}_4 + 2m)\not{\epsilon}_1}{(L_1-k_4)^2-m^2} + \frac{\not{\epsilon}_1(-\not{k}_4 + 2m)}{(L_1-k_1)^2-m^2}| - L_2\rangle \end{aligned} \tag{6.26}$$

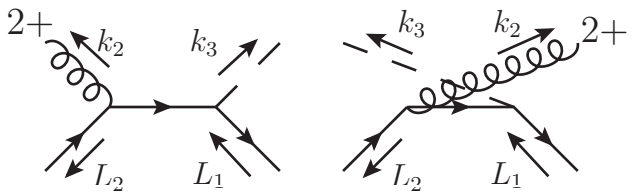

Figure 6.8: Diagram contributing to the tree amplitude above the t-cut.

where in the second step $-\not{L}_1$ and $-\not{L}_2$ were applied on the spinors to the left and to the right, respectively.

The amplitude on the bottom can be obtained from the top amplitude by replacing $L_1 \leftrightarrow L_2$, $\epsilon_1 \rightarrow \epsilon_2$ and $k_4 \rightarrow k_3$, and using the momentum conservation of the tree amplitude $L_2 = L_1 + k_2 + k_3$,

$$A^{bottom} = \frac{ig_s m}{v}\langle -L_2|\frac{(\not{k}_3 + 2m)\not{\epsilon}_2}{(L_1+k_2)^2 - m^2} + \frac{\not{\epsilon}_1(-\not{k}_3 + 2m)}{(L_1+k_3)^2 - m^2}| - L_1\rangle \tag{6.27}$$

In the same way as in the case of the s-cut, we obtain the t-cut of the loop amplitude,

$$\begin{aligned}
&A_4^{1-loop}\big|_{t-cut} \\
&= -\frac{g_s^2 m^2}{v^2}\int \frac{d^d L_1}{(2\pi)^d}\{\frac{tr[(-\not{L}_1 + m)(\not{k}_4 + 2m)\not{\epsilon}_1(-\not{L}_2 + m)(\not{k}_3 + 2m)\not{\epsilon}_2]}{(L_1^2 - m^2)((L_1+k_2+k_3)^2 - m^2)((L_1 - k_4)^2 - m^2)((L_1+k_2)^2 - m^2)} \\
&+\frac{tr[(-\not{L}_1 + m)\not{\epsilon}_1(-\not{k}_4 + 2m)(-\not{L}_2 + m)(\not{k}_3 + 2m)\not{\epsilon}_2]}{(L_1^2 - m^2)((L_1+k_2+k_3)^2 - m^2)((L_1 - k_1)^2 - m^2)((L_1+k_2)^2 - m^2)} \\
&+\frac{tr[(-\not{L}_1 + m)(\not{k}_4 + 2m)\not{\epsilon}_1(-\not{L}_2 + m)\not{\epsilon}_1(-\not{k}_3 + 2m)]}{(L_1^2 - m^2)((L_1+k_2+k_3)^2 - m^2)((L_1 - k_4)^2 - m^2)((L_1+k_3)^2 - m^2)} \\
&+\frac{tr[(-\not{L}_1 + m)\not{\epsilon}_1(-\not{k}_4 + 2m)(-\not{L}_2 + m)\not{\epsilon}_1(-\not{k}_3 + 2m)]}{(L_1^2 - m^2)((L_1+k_2+k_3)^2 - m^2)((L_1 - k_1)^2 - m^2)((L_1+k_3)^2 - m^2)}\}\big|_{t-cut}
\end{aligned} \tag{6.28}$$

In contrast to the s-cut, it is better to perform the kinematical and Passarino-Veltman reductions before shifting the momentum. The fact that vectors L_1 and L_2 are on shell will come into great use, as any appearance of L_i^2 can be immediately replaced by the mass m^2.

We will now outline the set of reductions applied to this expression. These have been implemented using Form. After replacing $L_2 = L_1 + k_2 + k_3$ and performing the trace, we are left with various contractions of the different vectors appearing in the numerator. Recall that as in the case of the s-cut, performing the trace we leave us with four dimensional vectors only and factors of μ^2.

We will first deal with the combination $l_1 \cdot \epsilon_1 l_1 \cdot \epsilon_2$. Choosing again the reference momenta of ϵ_1 and ϵ_2 to be k_2 and k_1, respectively, and using the spinor helicity representation, we obtain,

$$\begin{aligned} l_1 \cdot \epsilon_1 l_1 \cdot \epsilon_2 &= \frac{\langle 2 - |\not{l}_1| 1 - \rangle \langle 1 - |\not{l}_1| 2 - \rangle}{2\langle 21 \rangle \langle 12 \rangle} \\ &= -\frac{tr_-[\not{k}_2 \not{l}_1 \not{k}_1 \not{l}_1]}{\langle 12 \rangle^2} \\ &= \frac{k_2 \cdot k_1 l_1^2 - 2k_2 \cdot l_1 k_1 \cdot l_1}{\langle 12 \rangle^2} \\ &= \frac{k_2 \cdot k_1 (m^2 + \mu^2) - 2k_2 \cdot l_1 k_1 \cdot l_1}{\langle 12 \rangle^2} \end{aligned} \tag{6.29}$$

where again $tr_-[...]$ refers to having the projection matrix w_- as the leading factor. Note that in the last step we used the fact that L_1 is on shell, which means that l_1 has the effective mass $m^2+\mu^2$. The terms containing γ_5 vanish, since a trace with γ_5 must contain four independent vectors, which is not the case here. On the other hand, in the combination $l_1 \cdot \epsilon_1 k_3 \cdot \epsilon_2$, there are four independent vectors, and thus the trace will also result in terms with the Levi-Civita tensor contracted with the four vectors. To avoid such terms, we will instead evaluate the following sum in the same way as above,

$$l_1 \cdot \epsilon_1 k_3 \cdot \epsilon_2 + k_3 \cdot \epsilon_1 l_1 \cdot \epsilon_2 = 2\frac{k_1 \cdot k_2 l_1 \cdot k_3 - k_2 \cdot l_1 k_1 \cdot k_3 - k_2 \cdot k_3 k_1 \cdot l_1}{\langle 12 \rangle^2} \tag{6.30}$$

For the cases where only one of the two terms appear, we will use a different method to be described below.

The next step will be to perform Passarino-Veltman type reductions. Here, the on-shellness of L_1 also greatly simplifies the process. For example,

$$\frac{2l_1 \cdot k_3}{(L_1 + k_3)^2 - m^2} = \frac{((L_1 + k_3)^2 - m^2) - k_3^2}{(L_1 + k_3)^2 - m^2} = 1 - \frac{M_H^2}{(L_1 + k_3)^2 - m^2} \tag{6.31}$$

or if this propagator is not present, two propagators must be used,

$$\begin{aligned} &\frac{2l_1 \cdot k_3}{((L_1 + k_2 + k_3)^2 - m^2)((L_1 + k_3)^2 - m^2)} \\ &\quad = \frac{((L_1 + k_2 + k_3)^2 - m^2) - ((L_1 + k_3)^2 - m^2) - 2k_2 \cdot k_3}{((L_1 + k_2 + k_3)^2 - m^2)((L_1 + k_3)^2 - m^2)} \\ &\quad = \frac{1}{(L_1 + k_3)^2 - m^2} - \frac{1}{(L_1 + k_2 + k_3)^2 - m^2} - \frac{t - M_H^2}{((L_1 + k_2 + k_3)^2 - m^2)((L_1 + k_3)^2 - m^2)} \end{aligned} \tag{6.32}$$

thus reducing an n-point integral to two $(n-1)$-point integrals and one n-point integral, all with one power of l_1 less. In a similar fashion, other combinations of l_1 contracted with an external vector can be reduced. In some cases, two reductions can be done, and an $(n-2)$-point integral is obtained.

At some point, no more reductions can be performed, because no more suited denominators are at our disposal. In addition, we are still left with terms containing $l_1 \cdot \epsilon_1 k_3 \cdot \epsilon_2$, which

we were not able to reduce above because we wanted to avoid Levi-Civita tensors. At this stage, after the above reductions are performed, a maximum of one power of l_1 appears in the numerator.

We will first perform a shift of the variable, as was done for the s-cut, to transform all of our integrals to integrals having the form of one of the basis integrals. Each of the four terms in (6.29), or any term derived from it by reduction, can be shifted independently. Terms coming from the first or third line will be shifted according to $l_1 = p + k_1$, while terms coming from the second or fourth line will be shifted according to $l_1 = -p - k_1 - k_2 - k_3$. The first and fourth line will be transformed to integrals of the form I_{1256} (or contractions of this box integral), while the second and third will be transformed to I_{1246}. This was expected, since only these two integrals contain a t-cut. In fact, it can be easily seen from figure 6.3 that only integrals containing the propagators d_2 and d_6 contain a t-cut. As explained above, any integrals not containing these propagators that arise from the reduction of the two box integrals can be immediately cancelled because of the t-cut appearing on the right hand side of (6.29). This will greatly reduce the algebra at all points of the calculation, and is one of the advantages of the unitarity method.

We will now deal with any remaining factors of the integration variable p appearing in the numerator. In this case, only the following term remains,

$$I_{1256}[p \cdot \epsilon_2] \tag{6.33}$$

We will use the Feynman parameter shift method (described in detail in section 4.5) to express this integral in terms of scalar integrals. This integral is illustrated in figure 6.9. We first introduce Feynman parameters, naming the parameters according to the leg number they are multiplied against, e.g. a_5 will multiply $d_5 = ((p + k_1 + k_3)^2 - \mu^2 - m^2)$. To remove all linear terms in p, we perform the following variable shift,

$$p = q - (a_2 k_1 + a_5(k_1 + k_3) + a_6(k_1 + k_2 + k_3)) \tag{6.34}$$

Since p is contracted with ϵ_2 according to our choice of reference momentum, $k_1 \cdot \epsilon_2$ as well as $k_2 \cdot \epsilon_2$ will vanish. In addition, the term linear in q vanishes since the integrand is odd in q. We are thus left with evaluating,

$$k_3 \cdot \epsilon_2 (I_{1256}[a_5] + I_{1256}[a_6]) \tag{6.35}$$

According to the prescription in section 4.5, we must first calculate the kinematical $(p_{ij})^2$ matrix (note that every element is squared separately) and then derive the S_{ij} matrix. Using Mathematica, these are found to be,

$$(p_{ij})^2 = \begin{bmatrix} 0 & 0 & u & M_H^2 \\ 0 & 0 & M_H^2 & t \\ u & M_H^2 & 0 & 0 \\ M_H^2 & t & 0 & 0 \end{bmatrix} \qquad S_{ij} = m^2 \begin{bmatrix} 1 & 1 & 1-\frac{u}{2m^2} & 1-\frac{M_H^2}{2m^2} \\ 1 & 1 & 1-\frac{M_H^2}{2m^2} & 1-\frac{t}{2m^2} \\ 1-\frac{u}{2m^2} & 1-\frac{M_H^2}{2m^2} & 1 & 1 \\ 1-\frac{M_H^2}{2m^2} & 1-\frac{t}{2m^2} & 1 & 1 \end{bmatrix} \tag{6.36}$$

The S_{ij} matrix can be inverted and the quantities c_i, c_0 and c_{ij} calculated. These are inserted into (4.95), and the following simple relation is found after removing integrals that do not contain a t-cut,

$$I_{1256}[a_5] + I_{1256}[a_6] = \frac{1}{2} I_{1256}[1] \tag{6.37}$$

Following this long series of reductions and simplifications, we finally reach a compact expression for the t-cut of the amplitude,

$$\begin{aligned} A_4^{1-loop}\big|_{t-cut} = \frac{g_s^2 m^2}{v^2} \frac{[12]}{\langle 12 \rangle} \Big\{ & D(k_1,k_2,k_3)[(m^2+\mu^2)(-4s+8M_H^2-32m^2)+8m^2 s] \\ & + D(k_1,k_3,k_2)[(m^2+\mu^2)(-4s+8M_H^2-32m^2)+8m^2 s \\ & + \frac{4}{s}(M_H^4-ut)(4m^2-M_H^2)] + C(k_2,k_3)[\frac{8}{s}(M_H^2-t)(M_H^2-4m^2)] \Big\} \end{aligned} \tag{6.38}$$

In this cut, we have managed to fix the coefficients of the integrals $D(k_1,k_2,k_3)$, $D(k_1,k_3,k_2)$ and $C(k_2,k_3)$, and $B(t)$ which is zero since it does not appear in the cut. Since the integral $D(k_1,k_2,k_3)$ contains both s- and t-cuts, it appears in both equations (6.38) and (6.26) with

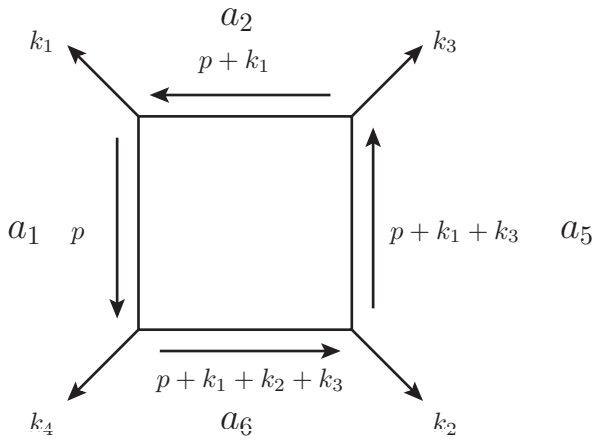

Figure 6.9: Reduction of $I_{1256}[p \cdot \epsilon_2]$ using the Feynman parameter shift method. This figure depicts the integral, including the Feynman parameters.

an identical coefficient, as expected. Similarly, we expect $D(k_1, k_3, k_2)$ to also appear in the u-cut with an identical coefficient.

u-cut

The u-cut is depicted in figure 6.10. We notice that it only defers from the t-cut by the exchange $k_3 \leftrightarrow k_4$. If we take a look at (6.38), we see that such a transformation implies the following transformations: $t \leftrightarrow u$, $C(k_2, k_3) \rightarrow C(k_2, k_4) = C(k_1, k_3)$, $D(k_1, k_2, k_3) \rightarrow D(k_1, k_2, k_4) = D(k_2, k_1, k_3)$ and $D(k_1, k_3, k_2) \rightarrow D(k_1, k_4, k_2) = D(k_1, k_3, k_2)$. The transformations of the scalar integrals can be simply deduced by writing out the integrals, applying the transformation and reordering the legs.

The result of this cut is then,

$$\begin{aligned} A_4^{1-loop}\big|_{u-cut} = \frac{g_s^2 m^2}{v^2}\frac{[12]}{\langle 12\rangle}\Big\{ & D(k_2,k_1,k_3)[(m^2+\mu^2)(-4s+8M_H^2-32m^2)+8m^2 s] \\ & + D(k_1,k_3,k_2)[(m^2+\mu^2)(-4s+8M_H^2-32m^2)+8m^2 s \\ & + \frac{4}{s}(M_H^4-ut)(4m^2-M_H^2)] + C(k_1,k_3)[\frac{8}{s}(M_H^2-u)(M_H^2-4m^2)]\Big\} \end{aligned} \quad (6.39)$$

Reduction of μ^2

After fixing all possible cuts, we are still left with task of simplifying the integrals containing μ^2 in the numerator. The box integrals of the form $D(k_1, k_2, k_3)$ are UV finite by simple power

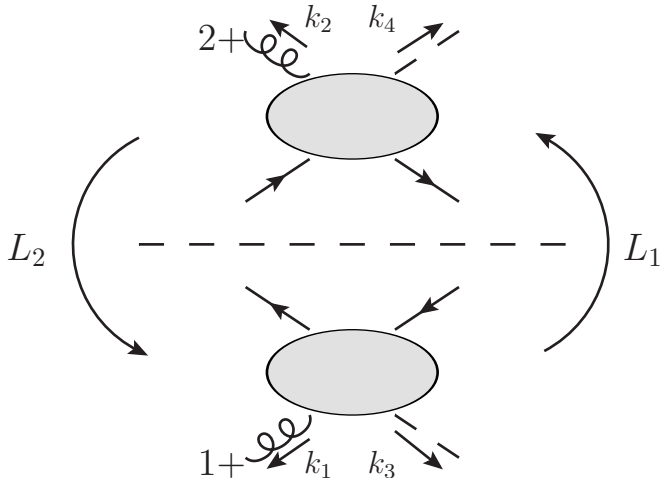

Figure 6.10: u-cut of the $gg \rightarrow HH$ amplitude.

counting, both for the case of four and six dimensions. Since all legs are massive, they are also free of IR or collinear divergences. Hence, such box integrals are free of any $\frac{1}{\epsilon}$ terms. Applying (4.72) to all box integrals containing a factor of μ^2, we see that,

$$D^{d=4-2\epsilon}(k_2, k_1, k_3)[\mu^2] = -4\pi\epsilon D^{d=6-2\epsilon}(k_2, k_1, k_3) \xrightarrow[\epsilon \to 0]{} 0 \tag{6.40}$$

In the s-cut only, (6.26), we observe that there is one triangle diagram containing μ^2 which can be expressed as a higher dimensional integral,

$$C^{d=4-2\epsilon}(k_1, k_2)[\mu^2] = -4\pi\epsilon C^{d=6-2\epsilon}(k_1, k_2) \tag{6.41}$$

This integral can be in turn reduced using the method described in section 4.5. We must first write down the p_{ij} matrix, and then derive the scalar c_0 and the vector $\frac{c_i}{c_0}$. Using Mathematica, these are,

$$(p_{ij})^2 = \begin{bmatrix} 0 & 0 & s \\ 0 & 0 & 0 \\ 0 & 0 & 0 \end{bmatrix}, \qquad c_0 = \frac{1}{m^2}, \qquad \frac{c_i}{c_0} = \begin{bmatrix} 0 \\ 1 \\ 0 \end{bmatrix} \tag{6.42}$$

Applying (4.96), the triangle diagram reduces to,

$$C^{d=4-2\epsilon}(k_1, k_2)[\mu^2] = \frac{\epsilon}{2-2\epsilon}(2m^2 C^{d=4-2\epsilon}(k_1, k_2) + B^{d=4-2\epsilon}(s)) \tag{6.43}$$

As in the box integral case, since C is UV finite in four dimensions and IR and collinear finite when the internal legs are massive, the first term vanishes when ϵ is taken to zero. Bubble integrals, on the other hand, do contain UV divergences, and could yield a finite contribution when multiplied by ϵ. [34] lists all divergent one loop scalar integrals up to four legs ([31] is another good source containing a compilation of full expressions for scalar integrals). The divergent part of the bubble integral is,

$$B(s) = \frac{1}{\epsilon} + \mathcal{O}(0) \tag{6.44}$$

And the triangle diagram with one factor of μ^2 becomes,

$$C^{d=4-2\epsilon}(k_1, k_2)[\mu^2] = \frac{1}{2} \tag{6.45}$$

This is a surprising result. Our s-cut seems to have fixed a constant term which appears to contain no cuts, and we could be tempted to throw this term away as we did other terms

that arose in the "wrong" cuts. But this term in fact originates from a $C(k_1, k_2)$ integral in six dimensions, or alternatively from a $B(s)$ integral in four dimensions. Both integrals do contain s-cuts.

When performing a straightforward calculation of a one-loop amplitude, following the traditional Passarino-Veltman reduction scheme, we reduce all tensor integrals to scalar integrals with some kinematical coefficients. When working in dimensional regularization, these coefficients could contain factors of ϵ as a result of taking traces over $4-2\epsilon$-dimensional Kronecker delta functions. As we saw here, a product of such a coefficient with a divergent integral could result in a rational term (i.e. term without cuts), since the divergent terms in scalar integrals are often rational functions that do not contain imaginary parts.

To avoid such ambiguities of rational terms, we chose to work with the μ scheme described in section 4.4. Under this scheme, coefficients of basis integrals do not contain powers of ϵ, at the expense of having to deal with an enlarged basis of integrals, one containing also higher dimensional integrals. These integrals all contain kinematical cuts as long as their four dimensional counterparts do as well. After we extract the coefficients of these integrals from the various cuts, we can reduce them using 4.96, this way successfully reproducing terms which would otherwise be rational and "cut-less".

Remaining integrals

Out of the 13 basis integrals enumerated in the beginning of the chapter, we managed to fix 10 using three different cuts. The integral $B(M_H^2)$ has still not been fixed, but can also be fixed if we imagine M_H^2 to be a kinematical variable (corresponding to one of the external Higgs particles being off shell). In this case, we could choose M_H^2 to take on values such that the integral will develop imaginary parts. Such integrals could be isolated by taking cuts along the pairs $\{1,6\}$, $\{4,6\}$ or $\{5,6\}$. An explicit calculation shows that this cut vanishes and the coefficient of this integral is zero.

The remaining integrals, i.e. $B(0)$ and the tadpole A, do not contain cuts in any kinematical variable. If the internal legs were massless, these integrals would vanish and we would have by now fixed the full amplitude. In the massive case they do not vanish. [43] describes a method of calculating the remaining coefficients by using known UV or IR behaviors of these amplitudes. We could apply this method in the current case since we know that our amplitude must be UV finite. This follows from the fact that our theory is renormalizable and there are no possible counter terms to absorb infinities if those should show up.

Tadpole integrals are characterized by a quadratic UV divergence, which appears as $\Gamma(-1+\epsilon)$ when solved to all orders in ϵ. Bubble diagrams, on the other hand, contain only a logarithmic divergence, characterized by $\Gamma(\epsilon)$. Since these two types of divergences cannot cancel each other at all orders, yet the amplitude should not contain any such Γ functions

at any order of ϵ, then we can conclude that the coefficients of these integrals should vanish independently. Note that to order $\frac{1}{\epsilon}$ only, linear combinations of these two integrals which are non-divergent but non-zero could appear, but to all orders in ϵ such cases could be ruled out.

6.3 Final Result

Having fixed the coefficients for all basis integrals, the full amplitude with the color factors is,

$$\begin{aligned}
&A_4^{1-loop}(1+,2+,3_H,4_H) \\
&= \frac{g_s^2 m^2}{v^2} tr[T^a T^b] \frac{[12]}{\langle 12\rangle} \Big\{ 4m^2(s+2M_H^2-8m^2)(D(k_1,k_2,k_3)+D(k_2,k_1,k_3)+D(k_1,k_3,k_2)) \\
&+\frac{4}{s}(M_H^4-ut)(4m^2-M_H^2)D(k_1,k_3,k_2) - 16m^2 C(k_1,k_2) - 8 \\
&+\frac{8}{s}(M_H^2-t)(M_H^2-4m^2)C(k_2,k_3) + \frac{8}{s}(M_H^2-u)(M_H^2-4m^2)C(k_1,k_3) \Big\}
\end{aligned} \tag{6.46}$$

This result agrees with [56]. Following the same procedure, but choosing one of the polarization vectors to be negative helicity, the remaining helicity amplitudes can be calculated. (see [56] for the full expressions).

CHAPTER 7

Conclusion

As in many realms of physics, a deeper understanding and an extensive ”box of tricks” can render a seemingly unsolvable problem doable. In this thesis we demonstrated how a ubiquitous property in quantum field theory, branch cuts of the amplitude, can be manipulated to extract information in clever ways. The unitarity method (chapter 3), which is generalized by the Cutkosky rules, was long known as a way of obtaining discontinuities along these branch cuts by gluing smaller pieces. Only recently, though, it was discovered that if it is used for fixing coefficients of an expansion, instead of a direct calculational tool, problems concerning rational functions and messy integrals can be circumvented. The unitarity method alone was not enough for this task, and to completely reduce the ambiguity, dimensional regularization (chapter 4), a seemingly unrelated tool, together with the UV properties of the amplitude were employed. In chapter 6, we demonstrated how these set of ”tricks” are sufficient to calculate an amplitude containing gluon, scalar and massive fermion particles.

Various other methods were employed in this final $gg \to HH$ calculation and other calculations throughout the thesis. These include: the spinor helicity method for representing external vector particles; color decomposition for decomposing a QCD amplitude into smaller color-ordered partial amplitudes; on-shell recursive relations for recursively constructing higher point tree amplitudes; and the Mellin-Barnes transformation, a powerful mathematical tool for calculating loop integrals.

But even having this set of tools at hand, large algebraic expressions must still be dealt

with, and at some level of complexity become unmanageable to perform manually. Even in the case of the calculation performed in chapter 6, it was found necessary to employ a combination of FORM, for algebraic manipulations, and Wolfram's Mathematica, for matrix operations. Automatizing calculation of amplitudes is by no doubt the future of Standard Model and Beyond the Standard Model phenomenology. Many powerful tools exist for the evaluation of tree level and one-loop level contributions (see [59] for a recent review). Most one-loop level programs perform the necessary reductions using the traditional Passarino-Veltman reduction scheme, or similar reduction techniques, to turn raw Feynman diagram expressions into the final analytical functions, which are in turn integrated over using, for example, Monte Carlo techniques. To obtain a complete result for QCD processes, these tools must also perform the factorization and hadronization, thus accounting for initial hadronic states and outgoing jets.

Recently, the unitarity method has been put into code by the `Blackhat` collaboration [60, 61], `Rocket` [62] and by Ellis [63] et al. Ossola, Papadopoulos, Pittau have proposed an alternative method, resembling unitarity in that coefficients of a scalar integral expansion are fixed by an approach resembling generalized unitarity, i.e. multiple cuts. In their method, the manipulations are performed at the integrand level, and the coefficients are determined by equating the integrand to a scalar integral expansion at specific, properly chosen, values of the loop momentum. This method could prove to be superior for numerical evaluation, and was already implemented by the same group in the program `CutTools` [64].

As a final remark personal remark, this thesis work was my first plunge into this fascinating world of particle physics, in a period which could be either the beginning of a new era in physics or a strong confirmation that we are on the right path, all depending on the results collected from the LHC experiment. If you have reached this point (without skipping), I hope this thesis proved helpful to you in one way or another.

APPENDIX A

Feynman Rules

An assortment of Standard Model Feynman rules relevant for calculations performed in this thesis is presented. These are borrowed from [8] and [31]. We first present the relevant Lagrangian parts. The QED Lagrangian is,

$$\mathcal{L}_{QED} = \sum_i (\bar{f}_i(i\partial\!\!\!/ - m_i)f_i - e\bar{f}_i\gamma^\mu f A_\mu) - \frac{1}{4}(F_{\mu\nu})^2 \tag{A.1}$$

where f_i are the various fermion fields, m_i their mass, and A_μ the photon gauge field. The QCD Lagrangian is,

$$\begin{aligned}\mathcal{L}_{QCD} = & \sum_i (\bar{f}_i(i\partial\!\!\!/ - m_i)f_i + g_s G^a_\mu \bar{f}_i\gamma^\mu T^a f_i) - \frac{1}{4}(\partial_\mu G^a_\nu - \partial_\nu G^a_\mu)^2 \\ & -g_s f^{abc}(\partial_\mu G^a_\nu)G^{\mu b}G^{\nu c} - \frac{1}{4}g_s^2(f^{eab}G^a_\mu G^b_\nu)(f^{ecd}G^c_\mu G^d_\nu)\end{aligned} \tag{A.2}$$

where G^a_μ is the gluon gauge field, carrying a $SU(3)$ (color) index $a = 1...8$. f^{abc} is the $SU(3)$ group structure constant. The sum is over quarks, the fermion particles that transform under the $SU(3)$ fundamental representation. The Yukawa term, coupling the Higgs particle to the fermions, is,

$$\mathcal{L}_Y = -\sum_i m_i \bar{f}_i f_i \left(1 + \frac{H}{v}\right) \tag{A.3}$$

H is the offset of the Higgs scalar field from its vacuum expectation value v. The $SU(2)$ gauge freedom of the original Higgs doublet field has been fixed to the unitary gauge, leaving one degree of freedom. The Higgs self coupling terms are,

$$\mathcal{L}_H = -\frac{1}{2}M_H^2 H^2 - \frac{M_H^2}{v}H^3 - \frac{1}{2}\frac{M_H^2}{v^2}H^4 \tag{A.4}$$

where M_H is the Higgs field mass.

We also present a non-Standard Model Lagrangian term of a scalar field transforming under a non-Abelian gauge theory,

$$\mathcal{L}_\phi = |(\not{\partial} + ig_s \not{G}^a T^a)\phi|^2 - m_\phi^2|\phi|^2 \tag{A.5}$$

Propagators

The gauge boson propagator is given in the 't Hooft-Feynman gauge (fixing the residual gauge remaining after the choice of the Lorentz gauge). Note that all propagators must be multiplied by a unit matrix in the space corresponding to the representations under which they transform. Quark propagators are multiplied by δ^i_j, where i and j are indices of the fundamental representation of $SU(3)$, whereas gluons transform under the adjoint representation of $SU(3)$.

gauge boson	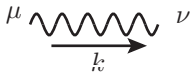	$\frac{-i}{k^2 + i\epsilon}g^{\mu\nu}$
fermion	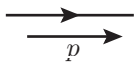	$\frac{i(\not{p} + m)}{p^2 - m^2 + i\epsilon}$
Higgs (or other scalar particle)	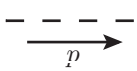	$\frac{i}{p^2 - M_H^2 + i\epsilon}$

Vertices

In the vertices, all momenta are taken to be incoming. Q is the charge of the fermion, $Q = -1$ for an electron.

QED 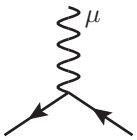

$iQe\gamma^\mu$

QCD 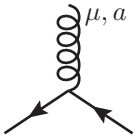

$ig\gamma^\mu T^a$

3 gluon 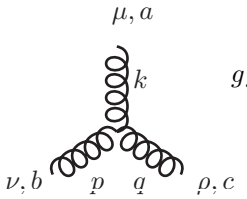

$gf^{abc}[g^{\mu\nu}(k-p)^\rho + g^{\nu\rho}(p-q)^\mu + g^{\rho\mu}(q-k)^\nu]$

4 gluon 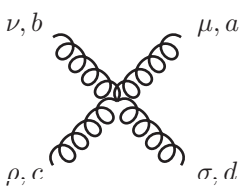

$$-ig^2[\ f^{abe}f^{cde}(g^{\mu\rho}g^{\nu\sigma} - g^{\mu\sigma}g^{\nu\rho}) + f^{ace}f^{bde}(g^{\mu\nu}g^{\rho\sigma} - g^{\mu\sigma}g^{\nu\rho}) + f^{ade}f^{bce}(g^{\mu\nu}g^{\rho\sigma} - g^{\mu\rho}g^{\nu\sigma})]$$

Yukawa coupling 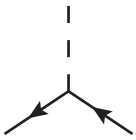
$-i\frac{m_i}{v}$

3 Higgs coupling 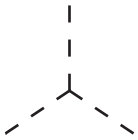
$-i\frac{3M_H^2}{v}$

4 Higgs coupling  $-i\frac{3M_H^2}{v^2}$

Color Ordered Feynman Rules

We list here the color ordered Feynman rules used in this text [6, 47]. The propagators are identical to the normal Feynman rules, with the color matrix stripped off the gluon propagator. As before, all momenta are taken to be incoming in the vertices. Coupling constants are also stripped off (and absorbed in the color factor of the color decomposition).

3 gluon coupling 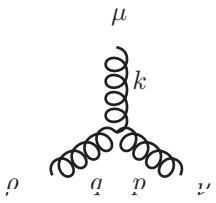

$\frac{i}{\sqrt{2}}(g^{\mu\nu}(k-p)^\rho + g^{\rho\mu}(q-k)^\nu + g^{\nu\rho}(p-q)^\mu)$

QCD 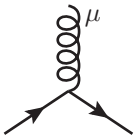

$-\frac{i}{\sqrt{2}}\gamma_\mu$

QCD 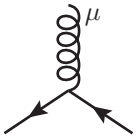

$\frac{i}{\sqrt{2}}\gamma_\mu$

scalar theory 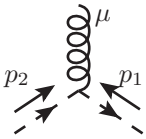

$\frac{i}{\sqrt{2}}(p_1-p_2)^\mu$

scalar theory 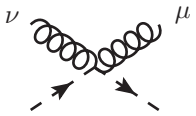

$\frac{i}{2}g^{\mu\nu}$

External fermions

incoming fermion 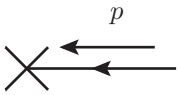

$u^s(p)$

outgoing fermion 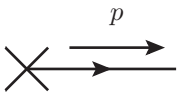

$\bar{u}^s(p)$

incoming anti-fermion 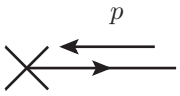

$\bar{v}^s(p)$

outgoing anti-fermion 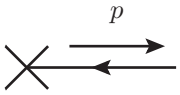

$v^s(p)$

$u^s(p)$ and $v^s(p)$ are spinors satisfying the Dirac equation,

$$\begin{aligned}(\not{p}-m)u^s(p) &= \bar{u}^s(p)(\not{p}-m) = 0 \\ (\not{p}+m)v^s(p) &= \bar{v}^s(p)(\not{p}+m) = 0\end{aligned} \tag{A.6}$$

where s is an index numbering the two spin degrees of freedom of the spinor. The spinors satisfy the completeness relation,

$$\sum_s u^s(p)\bar{u}^s(p) = \not{p}+m \qquad \sum_s v^s(p)\bar{v}^s(p) = \not{p}-m \tag{A.7}$$

APPENDIX B

Dimensional Regularization

Gamma function The definition and the properties of the Gamma function:

$$\Gamma(z) = \int_0^\infty t^{z-1} e^{-t} dt \tag{B.1}$$

$$\Gamma(n) = (n-1)! \quad (n \in \mathbb{Z}) \tag{B.2}$$

$$\Gamma(1) = 1 \tag{B.3}$$

$$\Gamma(1/2) = \sqrt{\pi} \tag{B.4}$$

$$\Gamma(z+1) = z\Gamma(z) \tag{B.5}$$

$$\Gamma'(1) = -\gamma_E \quad (\gamma_E \text{ is the Euler constant}) \tag{B.6}$$

$$\Gamma'(1) = \gamma_E^2 + \frac{\pi^2}{6} \tag{B.7}$$

$$\Gamma(1+\epsilon) = 1 - \epsilon\gamma_E + O(\epsilon^2) \quad (\epsilon \ll 1) \tag{B.8}$$

Beta function The definition of the Beta function and its representation in terms of Gamma functions:

$$\beta(x,y) = \int_0^1 t^{x-1}(1-t)^{y-1} dt = \frac{\Gamma(x)\Gamma(y)}{\Gamma(x+y)} \tag{B.9}$$

Dirac matrices Section 2.1.2 discusses contraction of Dirac matrices in d dimensions. Following is a list of useful formulae:

$$\begin{aligned}
&g^{\mu\nu}g_{\mu\nu} = d \\
&\gamma^\mu\gamma_\mu = d \\
&\gamma^\mu\gamma^\nu\gamma_\mu = (2-d)\gamma^\nu \\
&\gamma^\mu\gamma^\nu\gamma^\rho\gamma_\mu = 4g^{\nu\rho} - (4-d)\gamma^\nu\gamma^\rho \\
&\gamma^\mu\gamma^\nu\gamma^\rho\gamma^\sigma\gamma_\mu = -2\gamma^\sigma\gamma^\rho\gamma^\nu + (4-d)\gamma^\nu\gamma^\rho\gamma^\sigma
\end{aligned} \tag{B.10}$$

Loop integrals In section 2.1, a scalar integral was solved for the case of no loop momenta in the numerator. Following the same steps, integrals containing powers of the loop momentum invariant q^2 in the numerator can be calculated. If the integral contains an odd number of q^μ factors, then the integrand is odd and the integral vanishes. If the integral contains a factor of $q^\mu q^\nu$ in the numerator, then one first notes that the result must be proportional to the metric $g^{\mu\nu}$, since there are no other tensorial quantities in the integral. Then, contracting the integral with the metric, one can determine the proportionality factor and replace $q^\mu q^\nu \to \frac{1}{d}q^2 g^{\mu\nu}$. Following is a list of integrals (for more, see [8]):

$$\int \frac{d^dq}{(2\pi)^d}\frac{1}{[q^2-M^2]^s} = \frac{(-1)^s i}{(4\pi)^{\frac{d}{2}}}\frac{\Gamma(s-\frac{d}{2})}{\Gamma(s)}(M^2)^{\frac{d}{2}-s} \tag{B.11}$$

$$\int \frac{d^dq}{(2\pi)^d}\frac{q^2}{[q^2-M^2]^s} = \frac{(-1)^{s-1} i}{(4\pi)^{\frac{d}{2}}}\frac{d}{2}\frac{\Gamma(s-\frac{d}{2}-1)}{\Gamma(s)}(M^2)^{\frac{d}{2}-s+1} \tag{B.12}$$

$$\int \frac{d^dq}{(2\pi)^d}\frac{q^\mu q^\nu}{[q^2-M^2]^s} = \frac{(-1)^{s-1} i}{(4\pi)^{\frac{d}{2}}}\frac{g^{\mu\nu}}{2}\frac{\Gamma(s-\frac{d}{2}-1)}{\Gamma(s)}(M^2)^{\frac{d}{2}-s+1} \tag{B.13}$$

APPENDIX C

Dirac Matrices

The metric convention used throughout this thesis is:

$$g_{\mu\nu} = (1, -1, -1, -1) \tag{C.1}$$

The Dirac matrices are defined by the following anti-commutator:

$$\{\gamma^\mu, \gamma^\nu\} = \gamma^\mu\gamma^\nu + \gamma^\nu\gamma^\mu = 2g^{\mu\nu} \tag{C.2}$$

Some traces over the Dirac matrices are:

$$tr[\mathbb{1}] = 1 \tag{C.3}$$

$$tr[\gamma^\mu\gamma^\nu] = 4g^{\mu\nu} \tag{C.4}$$

$$tr[\gamma^\mu\gamma^\nu\gamma^\rho\gamma^\sigma] = 4(g^{\mu\nu}g^{\rho\sigma} - g^{\mu\rho}g^{\nu\sigma} + g^{\mu\sigma}g^{\nu\rho}) \tag{C.5}$$

$$tr[\text{odd number of Dirac matrices}] = 0 \tag{C.6}$$

The chirality matrix is defined to be:

$$\gamma^5 = \gamma_5 = i\gamma^0\gamma^1\gamma^2\gamma^3 = -\frac{i}{4!}\epsilon_{\mu\nu\sigma\rho}\gamma^\mu\gamma^\nu\gamma^\sigma\gamma^\rho \tag{C.7}$$

It obeys the properties:

$$\gamma_5^2 = 1 \tag{C.8}$$

$$\{\gamma_5, \gamma^\mu\} = 0 \tag{C.9}$$

Traces involving the chirality matrix yield:

$$tr[\gamma^5] = 0 \tag{C.10}$$

$$tr[\gamma^\mu\gamma^\nu\gamma^5] = 0 \tag{C.11}$$

$$tr[\gamma^\mu\gamma^\nu\gamma^\rho\gamma^\sigma\gamma^5] = -4i\epsilon^{\mu\nu\rho\sigma} \tag{C.12}$$

Two useful identities relating γ^5 with the Levi-Civita tensor are:

$$\gamma^5[\gamma_\mu, \gamma_\nu] = i\epsilon_{\mu\nu\sigma\rho}\gamma^\sigma\gamma^\rho \tag{C.13}$$

$$\frac{1}{2}\gamma^5[\gamma^\tau, [\gamma_\mu, \gamma_\nu]] = i\epsilon_{\mu\nu\sigma\rho}\gamma^\sigma\gamma^\tau\gamma^\rho \tag{C.14}$$

where $\epsilon^{0123} = -\epsilon_{0123} = 1$.

Proof of (C.14): We note that for the case $\mu = \nu$ both sides are zero from anti-symmetry. In the case $\mu \neq \nu \neq \tau$ the left side is zero since γ^τ commutes in this case with $[\gamma^\mu, \gamma^\nu]$. The right hand side is zero since the index τ must have the same value of either ρ or σ (otherwise the ϵ tensor is zero), in which case:

$$\epsilon_{\mu\nu\sigma\rho}\gamma^\sigma\gamma^\tau\gamma^\rho = \frac{1}{2}\epsilon_{\mu\nu\sigma\rho}(\gamma^\sigma\gamma^\tau\gamma^\rho - \gamma^\rho\gamma^\tau\gamma^\sigma) = 0$$

So the only non-zero case is when $\mu \neq \nu$ and $\tau = \mu$ or $\tau = \nu$. Consider the case $\tau = \mu$. Then:

$$\begin{aligned} i\epsilon_{\mu\nu\sigma\rho}\gamma^\sigma\gamma^\tau\gamma^\rho = -i\epsilon_{\mu\nu\sigma\rho}\gamma^\sigma\gamma^\rho\gamma^\tau = -\gamma^5[\gamma_\mu, \gamma_\nu]\gamma^\tau = -\frac{1}{2}\gamma^5([\gamma_\mu, \gamma_\nu]\gamma^\tau + [\gamma_\mu, \gamma_\nu]\gamma^\tau) \\ = \frac{1}{2}\gamma^5(\gamma^\tau[\gamma_\mu, \gamma_\nu] - [\gamma_\mu, \gamma_\nu]\gamma^\tau) = \frac{1}{2}\gamma^5[\gamma^\tau, [\gamma_\mu, \gamma_\nu]] \end{aligned}$$

where in the second equality (C.13) was used. In the last equality, the indices μ and τ can be interchanged, and thus γ^τ can be brought to the other side of the commutator with an added minus sign. The case $\tau = \nu$ follows from the antisymmetry between μ and ν.

APPENDIX D

Spinor Helicity

In chapter 4.2, the spinor helicity method was introduced. We list here a list of identities involving spinor products and the spinor representation for polarization vectors. Useful references are [7, 6].

Spinor products

Massless spinors, solutions of the massless Dirac equation, are denoted by the bra-ket notation,

$$|i^{\pm}\rangle \equiv |k_i^{\pm}\rangle \equiv u_{\pm}(k_i) = v_{\mp}(k_i), \qquad \langle i^{\pm}| \equiv \langle k_i^{\pm}| \equiv \overline{u_{\pm}(k_i)} = \overline{v_{\mp}(k_i)} \tag{D.1}$$

Positive (negative) helicity fermions are proportional to negative (positive) helicity antifermions, and can be chosen to be equal. Spinor products can be constructed as follows,

$$\langle ij\rangle \equiv \langle i^-|j^+\rangle = \overline{u_-(k_i)}u_+(k_j), \qquad [ij] \equiv \langle i^+|j^-\rangle = \overline{u_+(k_i)}u_-(k_j) \tag{D.2}$$

Like helicity products vanish since opposite helicities are eigenvectors of opposite projection matrices. Spinor products are antisymmetric,

$$\langle i^+|j^+\rangle = 0, \qquad \langle i^-|j^-\rangle = 0, \qquad \langle ij\rangle = -\langle ji\rangle, \qquad [ij] = -[ji], \qquad \langle ii\rangle = [ii] = 0 \tag{D.3}$$

The projection operator,

$$|i^{\pm}\rangle\langle i^{\pm}| = \frac{1}{2}(1 \pm \gamma_5)\not{k}_i \tag{D.4}$$

allows us to derive a connection to the more common kinematic notation, either through pairs of opposite products,

$$\langle ij\rangle[ji] = 2k_i \cdot k_j \equiv s_{ij} \tag{D.5}$$

or through larger traces over Dirac matrices such as,

$$\langle ij\rangle[jl]\langle lm\rangle[mi] = Tr[\frac{1}{2}(1-\gamma_5)\not{k}_i\not{k}_j\not{k}_l\not{k}_m] = \frac{1}{2}(s_{ij}s_{lm} - s_{il}s_{jm} + s_{im}s_{jl} - 4i\epsilon_{ijlm}) \tag{D.6}$$

where $\epsilon_{ijlm} \equiv k_i^{\mu}k_j^{\nu}k_l^{\rho}k_m^{\sigma}\epsilon_{\mu\nu\rho\sigma}$. When calculating cross sections, we will need the complex conjugate of spinor products,

$$\langle ij\rangle^* = [ji], \qquad \langle i^{\pm}|\gamma_{\mu}|j^{\pm}\rangle^* = \langle j^{\pm}|\gamma_{\mu}|i^{\pm}\rangle \tag{D.7}$$

Other useful identities are the Gordon identity and charge conjugation,

$$\langle i^{\pm}|\gamma^{\mu}|i^{\pm}\rangle = 2k_i^{\mu}, \qquad \langle i^{+}|\gamma^{\mu}|j^{+}\rangle = \langle j^{-}|\gamma^{\mu}|i^{-}\rangle \tag{D.8}$$

Fierz rearrangements,

$$\begin{aligned}
\langle i^{+}|\gamma^{\mu}|j^{+}\rangle\langle k^{+}|\gamma_{\mu}|l^{+}\rangle &= 2[ik]\langle lj\rangle \\
\langle i^{-}|\gamma^{\mu}|j^{-}\rangle\langle k^{-}|\gamma_{\mu}|l^{-}\rangle &= 2\langle ik\rangle[lj] \\
\langle i^{+}|\gamma^{\mu}|j^{+}\rangle\langle k^{-}|\gamma_{\mu}|l^{-}\rangle &= 2[il]\langle kj\rangle
\end{aligned} \tag{D.9}$$

Schouten identity,

$$\langle ij\rangle\langle kl\rangle = \langle ik\rangle\langle jl\rangle + \langle il\rangle\langle kj\rangle \tag{D.10}$$

If a set of momenta is conserved, $\sum_{i=1}^{n} k_i^{\mu} = 0$, then the following holds,

$$\sum_{\substack{i=1 \\ i\neq j,k}}^{n} [ji]\langle ij\rangle = 0 \tag{D.11}$$

Polarization vectors

Positive and negative helicity polarization vectors of massless gauge bosons (photons, gluons, etc.) can be represented in terms of spinor products as follows,

$$\epsilon_\mu^+(k;q) = \frac{\langle q^-|\gamma_\mu|k^-\rangle}{\sqrt{2}\langle qk\rangle}, \qquad \epsilon_\mu^-(k;q) = -\frac{\langle q^+|\gamma_\mu|k^+\rangle}{\sqrt{2}[qk]} \tag{D.12}$$

with the following normalization and orthogonality conditions,

$$\epsilon^+(k;q)\cdot\epsilon^-(k;q) = -1, \qquad \epsilon^+(k;q)\cdot\epsilon^+(k;q) = \epsilon^-(k;q)\cdot\epsilon^-(k;q) = -1 \tag{D.13}$$

Complex conjugation relates opposite helicities,

$$(\epsilon^+(k;q))^* = \epsilon^-(k;q) \tag{D.14}$$

q is a massless reference momenta reflecting gauge invariance. It can be chosen arbitrarily per polarization vector. The choice must be consistent within each gauge invariant quantity such as a fixed helicity amplitude, and can be changed when calculating a new gauge invariant quantity.

A list of useful identities used to simplify expressions by a judicious choice of reference momenta is,

$$\begin{aligned}
\epsilon^\pm(k;q)\cdot k &= 0\\
\epsilon^\pm(k;q)\cdot q &= 0\\
\epsilon^\pm(k_i;q)\cdot\epsilon^\pm(k_j;q) &= 0\\
\epsilon^\pm(k_i;k_j)\cdot\epsilon^\mp(k_j;q) &= 0\\
\not{\epsilon}^\pm(k_i;k_j)|k_j^\pm\rangle &= 0\\
\langle k_j^\pm|\not{\epsilon}^\mp(k_i;k_j) &= 0
\end{aligned} \tag{D.15}$$

Polarization vectors contracted with the Dirac matrices can be represented in the following way,

$$\not{\epsilon}^\pm(k;q) = \pm\frac{\sqrt{2}}{\langle q^\mp|k^\pm\rangle}(|q^\pm\rangle\langle k^\pm| + |k^\mp\rangle\langle q^\mp|) \tag{D.16}$$

When working in dimensional regularization, one must take note that this representation is only valid if this matrix is multiplied on one side by a four dimensional quantity.

Bibliography

[1] J. Kublbeck, M. Bohm, and A. Denner, "FEYN ARTS: COMPUTER ALGEBRAIC GENERATION OF FEYNMAN GRAPHS AND AMPLITUDES," *Comput. Phys. Commun.* **60** (1990) 165–180.

[2] H. M. Georgi, S. L. Glashow, M. E. Machacek, and D. V. Nanopoulos, "Higgs Bosons from Two Gluon Annihilation in Proton Proton Collisions," *Phys. Rev. Lett.* **40** (1978) 692.

[3] S. Dawson, "Radiative corrections to Higgs boson production," *Nucl. Phys.* **B359** (1991) 283–300.

[4] A. Djouadi, M. Spira, and P. M. Zerwas, "Production of Higgs bosons in proton colliders: QCD corrections," *Phys. Lett.* **B264** (1991) 440–446.

[5] M. Spira, A. Djouadi, D. Graudenz, and P. M. Zerwas, "Higgs boson production at the LHC," *Nucl. Phys.* **B453** (1995) 17–82, `arXiv:hep-ph/9504378`.

[6] L. J. Dixon, "Calculating Scattering Amplitudes Efficiently," `arXiv:hep-ph/9601359`.

[7] M. L. Mangano and S. J. Parke, "Multi-Parton Amplitudes in Gauge Theories," *Phys. Rept.* **200** (1991) 301–367, `arXiv:hep-th/0509223`.

[8] M. Peskin and D. Schroeder, *An Introduction to Quantum Field Theory*. Addison-Wesley, 1995.

[9] R. E. Cutkosky, "Singularities and Discontinuities of Feynman Amplitudes," *J. Math. Phys.* **1** (1960) 429–433.

[10] L. D. Landau, "On Analytic Properties of Vertex Parts in Quantum Field Theory," *Nucl. Phys.* **13** (1959) 181–192.

[11] Z. Bern, L. J. Dixon, D. C. Dunbar, and D. A. Kosower, "One-Loop n-Point Gauge Theory Amplitudes, Unitarity and Collinear Limits," *Nucl. Phys.* **B425** (1994) 217–260, arXiv:hep-ph/9403226.

[12] Z. Bern, L. J. Dixon, D. C. Dunbar, and D. A. Kosower, "Fusing gauge theory tree amplitudes into loop amplitudes," *Nucl. Phys.* **B435** (1995) 59–101, arXiv:hep-ph/9409265.

[13] Z. Bern, L. J. Dixon, and D. A. Kosower, "On-Shell Methods in Perturbative QCD," *Annals Phys.* **322** (2007) 1587–1634, arXiv:0704.2798 [hep-ph].

[14] Z. Bern, L. J. Dixon, and D. A. Kosower, "One loop corrections to five gluon amplitudes," *Phys. Rev. Lett.* **70** (1993) 2677–2680, arXiv:hep-ph/9302280.

[15] Z. Bern, L. J. Dixon, and D. A. Kosower, "One loop corrections to two quark three gluon amplitudes," *Nucl. Phys.* **B437** (1995) 259–304, arXiv:hep-ph/9409393.

[16] Z. Kunszt, A. Signer, and Z. Trocsanyi, "One loop radiative corrections to the helicity amplitudes of QCD processes involving four quarks and one gluon," *Phys. Lett.* **B336** (1994) 529–536, arXiv:hep-ph/9405386.

[17] G. Ossola, C. G. Papadopoulos, and R. Pittau, "Reducing full one-loop amplitudes to scalar integrals at the integrand level," *Nucl. Phys.* **B763** (2007) 147–169, arXiv:hep-ph/0609007.

[18] E. Witten, "Perturbative gauge theory as a string theory in twistor space," *Commun. Math. Phys.* **252** (2004) 189–258, arXiv:hep-th/0312171.

[19] R. Britto, F. Cachazo, and B. Feng, "New Recursion Relations for Tree Amplitudes of Gluons," *Nucl. Phys.* **B715** (2005) 499–522, arXiv:hep-th/0412308.

[20] R. Britto, F. Cachazo, B. Feng, and E. Witten, "Direct Proof Of Tree-Level Recursion Relation In Yang- Mills Theory," *Phys. Rev. Lett.* **94** (2005) 181602, arXiv:hep-th/0501052.

[21] N. I. Usyukina, "On a Representation for Three Point Function," *Teor. Mat. Fiz.* **22** (1975) 300–306.

[22] E. Whittaker and G. Watson, *A Course of Modern Analysis*. Cambridge University Press, 1946.

[23] E. E. Boos and A. I. Davydychev, "A Method of Evaluating Massive Feynman Integrals," *Theor. Math. Phys.* **89** (1991) 1052–1063.

[24] J. B. Tausk, "Non-planar massless two-loop Feynman diagrams with four on-shell legs," *Phys. Lett.* **B469** (1999) 225–234, arXiv:hep-ph/9909506.

[25] B. de Wit and J. Smith, *Field Theory in Particle Physics Vol. 1*. Elsevier Science Publishers B.V., 1986.

[26] G. 't Hooft and M. J. G. Veltman, "Regularization and Renormalization of Gauge Fields," *Nucl. Phys.* **B44** (1972) 189–213.

[27] G. Passarino and M. J. G. Veltman, "One Loop Corrections for e+ e- Annihilation Into mu+ mu- in the Weinberg Model," *Nucl. Phys.* **B160** (1979) 151.

[28] Z. Bern and D. A. Kosower, "The Computation of Loop Amplitudes in Gauge Theories," *Nucl. Phys.* **B379** (1992) 451–561.

[29] J. Vermaseren, "Symbolic manipulation with form, version 3.3." Computer algebra nederland, amsterdam (1991), available for download at http://www.nikhef.nl/~form/.

[30] S. Weinberg, *The Quantum Theory of Fields Vol. 1*. Cambridge University Press, 1995.

[31] A. Denner, "Techniques for Calculation of Electroweak Radiative Corrections at the One Loop Level and Results for W Physics at LEP-200," *Fortschr. Phys.* **41** (1993) 307–420, arXiv:0709.1075 [hep-ph].

[32] D. Ross, "Modern methods in perturbative qcd (pg)." http://www.hep.phys.soton.ac.uk/hepwww/staff/D.Ross/mhv/.

[33] G. 't Hooft and M. J. G. Veltman, "Scalar One Loop Integrals," *Nucl. Phys.* **B153** (1979) 365–401.

[34] R. K. Ellis and G. Zanderighi, "Scalar One-Loop Integrals for QCD," *JHEP* **02** (2008) 002, arXiv:0712.1851 [hep-ph].

[35] Z. Bern, L. J. Dixon, and D. A. Kosower, "Dimensionally Regulated Pentagon Integrals," *Nucl. Phys.* **B412** (1994) 751–816, arXiv:hep-ph/9306240.

[36] S. D. Drell and T.-M. Yan, "Massive Lepton Pair Production in Hadron-Hadron Collisions at High-Energies," *Phys. Rev. Lett.* **25** (1970) 316–320.

[37] B. Potter, "Calculational techniques in perturbative qcd: The drell-yan process." Talk given at the colloquium of the gradiuertenkolleg "theoretische elementarteilchenphysik", hamburg university, 1997.

[38] T. Muta, *Foundations of Quantum Chromodynamics*. World Scientific, 1998.

[39] J. Bjorken and S. Drell, *Relativistic Quantum Fields*. McGraw-Hill Book Company, 1965.

[40] B. A. Kniehl, "Dispersion Relations in Loop Calculations," *Acta Phys. Polon.* **B27** (1996) 3631–3644, arXiv:hep-ph/9607255.

[41] M. Abramowitz and I. Stegun, *Handbook of Mathematical Functions*. National Bureau of Standards, 1972.

[42] J. Marsden, *Basic Complex Analysis*. W.H. Freeman and Company, 1973.

[43] Z. Bern and A. G. Morgan, "Massive Loop Amplitudes from Unitarity," *Nucl. Phys.* **B467** (1996) 479–509, arXiv:hep-ph/9511336.

[44] Z. Bern, L. J. Dixon, and D. A. Kosower, "Progress in One-Loop QCD Computations," *Ann. Rev. Nucl. Part. Sci.* **46** (1996) 109–148, arXiv:hep-ph/9602280.

[45] Z. Bern and D. A. Kosower, "Color Decomposition of One Loop Amplitudes in Gauge Theories," *Nucl. Phys.* **B362** (1991) 389–448.

[46] Z. Xu, D.-H. Zhang, and L. Chang, "Helicity Amplitudes for Multiple Bremsstrahlung in Massless Nonabelian Gauge Theories," *Nucl. Phys.* **B291** (1987) 392.

[47] S. D. Badger, E. W. N. Glover, V. V. Khoze, and P. Svrcek, "Recursion Relations for Gauge Theory Amplitudes with Massive Particles," *JHEP* **07** (2005) 025, arXiv:hep-th/0504159.

[48] S. D. Badger, E. W. N. Glover, and V. V. Khoze, "Recursion Relations for Gauge Theory Amplitudes with Massive Vector Bosons and Fermions," *JHEP* **01** (2006) 066, arXiv:hep-th/0507161.

[49] K. J. Ozeren and W. J. Stirling, "Scattering amplitudes with massive fermions using BCFW recursion," *Eur. Phys. J.* **C48** (2006) 159–168, arXiv:hep-ph/0603071.

[50] C. Quigley and M. Rozali, "Recursion relations, helicity amplitudes and dimensional regularization," *JHEP* **03** (2006) 004, arXiv:hep-ph/0510148.

[51] P. G. G.M. Khenkin, A.G. Vitushkin and J. King, *Several Complex Variables II (Encyclopedia of Mathematical Sciences)*. Springer-Verlag, 1994.

[52] J. S. Rozowsky, "Feynman Diagrams and Cutting Rules," arXiv:hep-ph/9709423.

[53] Z. Bern, L. J. Dixon, and D. A. Kosower, "Dimensionally Regulated One-Loop Integrals," *Phys. Lett.* **B302** (1993) 299–308, arXiv:hep-ph/9212308.

[54] T. Riemann, "Feynman integrals mellin-barnes representations sums." http://www-zeuthen.desy.de/~riemann/Talks/riemann-capp-09.pdf. Talk given at The DESY CAPP School March-April 2009.

[55] I. Gradshteyn and I. Ryzhik, *Table of Integrals, Series and Products*. Academic Press, 2007.

[56] E. W. N. Glover and J. J. van der Bij, "Higgs Boson Pair Production via Gluon Fusion," *Nucl. Phys.* **B309** (1988) 282.

[57] U. Baur, T. Plehn, and D. L. Rainwater, "Measuring the Higgs Boson Self Coupling at the LHC and Finite Top Mass Matrix Elements," *Phys. Rev. Lett.* **89** (2002) 151801, arXiv:hep-ph/0206024.

[58] T. Plehn, M. Spira, and P. M. Zerwas, "Pair Production of Neutral Higgs Particles in Gluon–Gluon Collisions," *Nucl. Phys.* **B479** (1996) 46–64, arXiv:hep-ph/9603205.

[59] T. Binoth, "LHC phenomenology at next-to-leading order QCD: theoretical progress and new results," arXiv:0903.1876 [hep-ph].

[60] C. F. Berger *et al.*, "An Automated Implementation of On-Shell Methods for One- Loop Amplitudes," *Phys. Rev.* **D78** (2008) 036003, arXiv:0803.4180 [hep-ph].

[61] C. F. Berger *et al.*, "One-Loop Calculations with BlackHat," *Nucl. Phys. Proc. Suppl.* **183** (2008) 313–319, arXiv:0807.3705 [hep-ph].

[62] W. T. Giele and G. Zanderighi, "On the Numerical Evaluation of One-Loop Amplitudes: The Gluonic Case," *JHEP* **06** (2008) 038, arXiv:0805.2152 [hep-ph].

[63] R. K. Ellis, W. T. Giele, and Z. Kunszt, "A Numerical Unitarity Formalism for Evaluating One-Loop Amplitudes," *JHEP* **03** (2008) 003, arXiv:0708.2398 [hep-ph].

[64] G. Ossola, C. G. Papadopoulos, and R. Pittau, "CutTools: a program implementing the OPP reduction method to compute one-loop amplitudes," *JHEP* **03** (2008) 042, arXiv:0711.3596 [hep-ph].